THESIS

Quantum Monte Carlo Study

on

Low-Dimensional Spin Systems

December, 1992

Department of Physics, University of Tokyo

Naomichi Hatano

Acknowledgments

First of all I would like to express my sincere gratitude to Professor Masuo Suzuki for his continual encouragement, for his helpful comments and discussions, and for the collaboration. I am very happy to start my scientific career under his guidance. I am also grateful to the members of the Suzuki group and to Dr. A. Terai for their useful comments.

I thank the Japan Society for the Promotion of Science and Nihon-Sekiyu-Kagaku for the fellowships.

The simulations reported in Chapter 2 were performed on HITAC S820/80 at the Computer Centre, University of Tokyo, and on HITAC S820/80 at the Hokkaido University Computing Center. The program for the simulations was prepared on VAX6440 at the Meson Science Laboratory, Faculty of Science, University of Tokyo. The usage of the random-number generator RNDTIK coded by N. Ito and Y. Kanada is gratefully acknowledged. The study was supported partly by Grant-in-Aid for Scientific Research from the Ministry of Education, Science and Culture, and partly by Grant-in-Aid for Scientific Research on Priority Area "Computational Physics as a New Frontier in Condensed Matter Research" from the Ministry of Education, Science and Culture.

I am grateful to Dr. N. Kawashima for his valuable comment on the study in Chapter 3. The program for the simulations reported in Chapter 3 was prepared on VAX6440 at the Meson Science Laboratory, Faculty of Science, University of Tokyo. The study was supported by Grant-in-Aid for Scientific Research on Priority Area "Computational Physics as a New Frontier in Condensed Matter Research" from the Ministry of Education, Science and Culture.

The collaboration with Prof. H. Nishimori and Mr. T. Nakamura on the subject of Chapter 4 is gratefully acknowledged. I am also grateful to Dr. M. Takasu, Dr. N. Ito, and Mr. N. Furukawa for stimulating discussions. The calculations reported in Chapter 4 were performed, partly on the HITAC M680 of the Computer Centre, University of Tokyo, partly on the VAX6440 of the Meson Science Laboratory, Faculty of Science, University of Tokyo.

List of Papers Submitted for the Requirement of the Degree

1. N. Hatano and M. Suzuki, Correlation length of the $S = 2$ antiferromagnetic Heisenberg chain, J. Phys. Soc. Jpn **62** (1993) 1346-1353.

2. N. Hatano and M. Suzuki, Ground-state quantum Monte Carlo method applied to alternating-bond spin chains, J. Phys. Soc. Jpn **62** (1993) 847-850.

3. N. Hatano and M. Suzuki, Representation basis in quantum Monte Carlo calculations and the negative-sign problem, Phys. Lett. A **163** (1992) 246-249.

4. N. Hatano and M. Suzuki, Quantum Monte Carlo and related methods — Recent developments —, to be published in *Quantum Monte Carlo Methods in Condensed Matter Physics*, ed. by M. Suzuki (World Scientific, Singapore).

5. N. Hatano and M. Suzuki, Transfer-matrix calculations of the spin 1/2 antiferromagnetic XXZ model on the 4×2 triangular lattice using the fractal decomposition, Prog. Theor. Phys. **85** (1991) 481-491.

6. N. Hatano and M. Suzuki, Correction-term theorem concerning decompositions of exponential operators, Phys. Lett. A **153** (1991) 191-194.

List of Papers Added in Reference

1. T. Nakamura, N. Hatano and H. Nishimori, Reweighting method for quantum Monte Carlo simulations with the negative-sign problem, J. Phys. Soc. Jpn. **61** (1992) 3494-3502.

2. T. Nakamura, N. Hatano and H. Nishimori, Negative-sign problem in quantum Monte Carlo and the reweighting method, in *Computer Aided Innovation of New Materials II*, ed. by M. Doyama, J. Kihara, M. Tanaka and R. Yamamoto (Elsevier, Amsterdam, 1993) 379-382.

3. N. Hatano and M. Suzuki, Effective-field theory of spin glasses and the coherent-anomaly method. I, J. Stat. Phys. **63** (1991) 25-46.

4. N. Hatano and M. Suzuki, Effective-field theory of spin glasses and the coherent-anomaly method. II. Double-cluster approximation, J. Stat. Phys. **66** (1992) 897-911.

5. N. Kawashima, N. Hatano and M. Suzuki, Critical behavior of the two-dimensional EA model with a Gaussian bond distribution, J. Phys. A: Math. Gen. **25** (1992) 4985-5003.

6. M. Suzuki, N. Hatano and Y. Nonomura, Canonicality of the double-cluster approximation in the CAM theory, J. Phys. Soc. Jpn. **60** (1991) 3990-3992.

7. M. Suzuki, N. Hatano and Y. Nonomura, Numerical CAM analysis of critical phenomena in spin systems, in *Computational Approaches in Condensed-Matter Physics*, ed. by S. Miyashita, M. Imada and H. Takayama (Springer-Verlag, Berlin, 1992) 187-192.

Contents

Chapter 1

Introduction

In this century, two branches of physics have been greatly developed; namely the quantum mechanics and the statistical physics. While the quantum mechanics was, at first, mainly applied to the elementary-particle and nuclear physics, the main subject of the statistical mechanics has been to study macroscopic many-body systems. Our knowledge on critical phenomena, in particular, has progressed remarkably in the second half of this century.

A strong backbone which has supported the recent development of the statistical physics is the computational physics. Considering the rapid progress of the computer technology, we can expect that the importance of the computational physics will increase still more. In actual fact, many important numerical calculations have been performed in these ten years. They have yielded great insights into physical systems, for example, spin glasses and quantum systems.

In the quantum-mechanical statistical physics, one of the most interesting aspects is the macroscopic manifestation of a quantum-mechanical effect; the superconductivity was the first and striking example. It was recently understood that the macroscopic quantum effect may appear more easily in low-dimensional systems. The low-dimensionality is probably essential to the appearance of the quantum Hall effect and the high-$T_{\rm c}$ superconductivity.

The Haldane problem, which is the main subject of Chapter 2 and Chapter 3, is also one of the phenomena in which the quantum mechanics affects the system strongly. Haldane [Haldane 83a, Haldane 83b] conjectured in 1983 that the low-temperature behavior of one-dimensional Heisenberg antiferromagnet depends on whether the magnitude of the spins is half-integral or integral; while the half-integer model is critical in the ground state, the integer model is disordered. It should be remarked that the first confirmation of the Haldane conjecture was a numerical investigation [Kolb 83]; there the $S = 1/2$ and $S = 3/2$ cases were distinguished from the $S = 1$ case. Even later on, numerical works have played an important role in the progress of the study on the Haldane problem.

In the numerical calculation reported in Chapter 2, we treated the $S = 2$ model. We there confirmed that the Haldane conjecture is correct even quantitatively. We can thereby presume the behavior of the higher-spin models rather precisely, using a formula given by Haldane.

In Chapter 3, we deal with another aspect of the Haldane problem, that is, ground-state transitions which take place when we change a parameter of the model. The transitions have been investigated numerically. Incidentally, recent numerical observation

by Hida [Hida 92a, Hida 92b] has given a simple interpretation of the Haldane effect. According to his observation, the $S = 1$ antiferromagnetic chain can be described by the $S = 1/2$ alternating-bond spin chain, and the phase transitions of the models are expected to be of the same character.

Bearing this observation in mind, we investigate, in Chapter 3, the phase transitions of the $S = 1/2$ alternating-bond model. We propose an application of the quantum Monte Carlo method based on the Suzuki-Trotter transformation to studies on ground-state transitions. The efficiency of the method is confirmed in the investigation of the model.

The Haldane problem is an example of a phenomenon in which the system is disordered owing to quantum-mechanical fluctuation. Another possible example is the two-dimensional frustrated spin system. It is expected that such a disordered state, so-called spin liquid, may be a precursor of the high-T_c superconductivity.

Unfortunately, when we investigate frustrated systems by means of the quantum Monte Carlo method, the statistics of the simulation seriously deteriorates at low temperatures; this problem is called the negative-sign problem. This methodological problem has been the main obstacle to the numerical investigation on frustrated systems. A solution of the negative-sign problem is one of the pressing needs in the computational physics.

In Chapter 4 the origin of the negative-sign problem is explored. We present an argument by which we can estimate the statistical error before we perform actual Monte Carlo simulations. On the basis of the argument, we ascribe the problem to the violation of the spirit of the importance sampling. An application of the reweighting method to the quantum Monte Carlo simulation is proposed towards the solution of the negative-sign problem.

In Chapter 5 we review some of the quantum Monte Carlo methods proposed so far.

Chapter 2

Correlation of One-Dimensional Heisenberg Antiferromagnets*

Temperature dependence of the correlation length of the one-dimensional $S = 2$ Heisenberg antiferromagnet is investigated numerically, to compare with those of the $S = 1/2$, 1, $3/2$ models. The correlation length of the $S = 2$ model is found to be saturated to a value $\xi^{-1} \simeq 0.012(2)$ as $T \to 0$, which confirms the Haldane conjecture. Combined with the estimate $\xi^{-1} \simeq 0.16$ of the $S = 1$ model by other authors, the present estimate is well explained by $\xi^{-1} \sim S \exp(-\pi S)$.

2.1 Introduction

The Heisenberg antiferromagnetic chains described by the dimensionless Hamiltonian

$$\mathcal{H} = \sum_{i=1}^{N} \boldsymbol{S}_i \cdot \boldsymbol{S}_{i+1}, \tag{2.1}$$

have interested many researchers greatly since Haldane conjectured [Haldane 83a, Haldane 83b] that, *only* for integer-spin chains, (i) an energy gap opens above the ground state, and (ii) the spin correlation in the ground state decays exponentially:

$$\langle S_0^\alpha S_r^\alpha \rangle \sim \exp(-r/\xi_\alpha) \quad \text{as} \quad r \to \infty, \qquad (\alpha = x, y, z). \tag{2.2}$$

(In the isotropic case we have $\xi_x = \xi_y = \xi_z$.) This conjecture surprised at first many solid-state physicists, who had known the celebrated Bethe-ansatz solution [Bethe 31] of the $S = 1/2$ Heisenberg chain. The Bethe-ansatz solution gives the continuous spectrum above the ground state and the power-law decay of the spin correlation:

$$\langle S_0^\alpha S_r^\alpha \rangle \sim r^{-\eta} \quad \text{as} \quad r \to \infty. \tag{2.3}$$

Numerical calculations combined with the finite-size scaling analysis distinguished [Kolb 83] the $S = 1$ case from the $S = 1/2$, $3/2$ cases, and confirmed the Haldane conjecture in the $S = 1$ case. Experimental evidences [Buyers 86] and rigorous arguments

*The content of this chapter will be published in [Hatano 93a].

Reference	ΔE	ξ^{-1}
[Nightingale 86]	0.41	
[Takada 87]		0.12
[Takahashi 88]	0.36	$(5.5 \pm 2)^{-1}$
[Takahashi 89]	0.41	
[Nomura 89a]	0.425	0.160
[Liang 90]		6.2^{-1}
[Sakai 90a]	0.411 ± 0.001	$(5.2 \pm 0.3)^{-1}$
[Kubo 92]	0.40	0.15

Table 2.1 The magnitude of the energy gap and the correlation length of the $S = 1$ Heisenberg antiferromagnet estimated so far.

[Affleck 88] appeared later. In this sense numerical works have played an important role in the progress of the study on the Haldane problem. (See [Affleck 89] for a review.)

Further investigation has been done to estimate the magnitude of the energy gap and the correlation length of the $S = 1$ model. The estimates obtained so far are listed in Table 2.1. The values $\Delta E \simeq 0.41$ and $\xi^{-1} \simeq 0.16$ now seem to be widely accepted.

There are very few studies of extending the numerical calculations to the $S = 2$ chain, because it is rather difficult to study it owing to a larger number of spin degrees of freedom and owing to a smaller magnitude of the gap in the $S = 2$ case. Hatsugai [Hatsugai 92] recently performed numerical diagonalization of finite $S = 2$ chains of size up to $N = 10$. However, he has not reached any quantitative conclusions on the magnitude of the energy gap. No estimates of the correlation length have been available.

Here we report a numerical calculation of the correlation length ξ of the $S = 2$ Heisenberg chain. We adopted the Monte Carlo power method proposed by Koma [Koma 93] to overcome the difficulty of many degrees of freedom (Section 2.2). We observed that the correlation length is saturated to a finite value $\xi^{-1} \simeq 0.012(2)$ as $T \to 0$ (Section 2.3).

Haldane [Haldane 83a, Haldane 83b] derived the following approximate formulae for the magnitude of the energy gap and the ground-state correlation length:

$$\Delta E \propto S^2 \mathrm{e}^{-\pi S} \tag{2.4}$$

and

$$\xi^{-1} \propto S \mathrm{e}^{-\pi S} \qquad \text{as} \quad S \to \infty, \tag{2.5}$$

respectively. (For more precise evaluation, S may be replaced by $\sqrt{S(S+1)}$.) Haldane argued that a Heisenberg chain with large-S spins is approximately mapped to a $(1+1)$-dimensional $O(3)$ nonlinear sigma model with a coupling constant $g = 2/S$ (or $g = 2/\sqrt{S(S+1)}$). A renormalization-group argument suggests that the system is disordered in the length scale greater than $g^{-1}\exp(2\pi/g)$, which gives (2.5). Though the expression (2.5) is justified in the large-S limit, a naive application of it to the $S = 1$ and $S = 2$ cases explains the present estimate well; when we use the value $\xi^{-1}(S = 1) = 0.16$, the formula (2.5) gives $\xi^{-1}(S = 2) = 0.011$, which agrees well with the present estimate. (We have used $\sqrt{S(S+1)}$ instead of S.) Incidentally, the formula (2.4) combined with the estimate $\Delta E(S = 1) = 0.41$ yields $\Delta E(S = 2) = 0.048$.

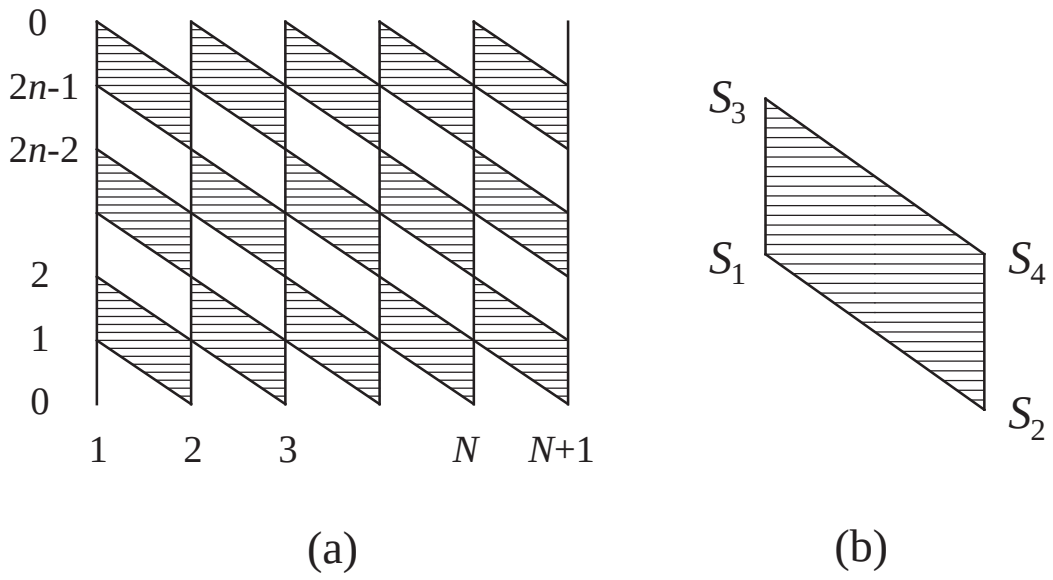

Figure 2.1 (a) The classical system is defined on a strip of width $2n$. Periodic boundary condition is required across the strip. The hatched quadrangle denotes a four-body interaction. (b) The four-body interaction conserves the magnetization in the Trotter direction.

2.2 Method of numerical calculation

In the present section we describe the formulation of the method used here. We combine the virtual-space transfer-matrix method with the Monte Carlo power method.

In order to make explicit the positivity of transfer matrices (explained below), we use the Hamiltonian in the form

$$\mathcal{H} = \sum_i \mathcal{H}_i \qquad \text{with} \qquad \mathcal{H}_i \equiv -S_i^x S_{i+1}^x - S_i^y S_{i+1}^y + S_i^z S_{i+1}^z, \tag{2.6}$$

which is equivalent to (2.1) via a unitary transformation.

The Suzuki-Trotter decomposition [Suzuki 76a, Suzuki 76b] has become a standard method of treating quantum systems. It has been applied to quantum Monte Carlo simulations [Suzuki 77b, Suzuki 87b], to transfer-matrix calculations [Suzuki 85a, Betsuyaku 85], and to analytic arguments [Suzuki 87c].

There are many alternative ways of the decomposition. Here we adopted the "real-space decomposition" [Suzuki 76b], that is,

$$\mathrm{e}^{-\beta\mathcal{H}} = \lim_{n\to\infty} \left(\mathrm{e}^{-\beta\mathcal{H}_1/n}\mathrm{e}^{-\beta\mathcal{H}_2/n}\mathrm{e}^{-\beta\mathcal{H}_3/n}\cdots\mathrm{e}^{-\beta\mathcal{H}_N/n}\right)^n. \tag{2.7}$$

The real-space decomposition is more convergent than the checkerboard decomposition is in an $S = 1/2$ spin chain [Betsuyaku 85]. We insert into (2.7) the resolution of the unit operator $\hat{1}$ with respect to a complete set of bases diagonalizing every S_i^z. We thus obtain a two-dimensional spin-S Ising system [Suzuki 76b], as shown in Fig. 2.1 (a). The size of this transformed system is $(N+1)$ by $2n$. It has four-body interactions defined by the Boltzmann factor

$$w(S_1, S_2, S_3, S_4) \equiv \left\langle S_1, S_2 \left| \mathrm{e}^{-\beta\mathcal{H}_i/n} \right| S_3, S_4 \right\rangle, \tag{2.8}$$

as shown in Fig. 2.1 (b). Note that the Boltzmann factor is positive when the relation

$$S_1 + S_2 = S_3 + S_4, \tag{2.9}$$

is satisfied, and otherwise it vanishes; every four-body interaction conserves the magnetization in the Trotter direction.

The partition function of the transformed classical system is, as it is, written in terms of transfer matrices which transfer spin states in the Trotter direction. We rewrite the partition function in terms of the virtual-space transfer matrix [Suzuki 85a, Betsuyaku 85]. Requiring the periodic-boundary condition $\sigma_1 = \sigma_{N+1}$, we have

$$Z_{\rm q} = \lim_{n\to\infty} Z_n, \qquad \text{with} \qquad Z_n(N) = \mathrm{Tr}\ \mathcal{T}_n^N. \tag{2.10}$$

Here the matrix $\mathcal{T}_n$ transfers the spin states on the i-th column to those of the $(i+1)$-th one, namely, in the real-space direction; in other words, $\mathcal{T}_n$ represents interactions on a *column*. The size of the matrix is $(2S+1)^{2n}$ by $(2S+1)^{2n}$.

A merit of the form (2.10) is the tractability of the infinite-size limit $N \to \infty$. The interchangeability of the two limits $n \to \infty$ and $N \to \infty$ was proved [Suzuki 85a, Suzuki 87c]; hence we have

$$f \equiv -\lim_{N\to\infty} \frac{1}{N\beta} \log Z_{\rm q} = -\lim_{n\to\infty}\lim_{N\to\infty} \frac{1}{N\beta} \log \mathrm{Tr}\, \mathcal{T}_n^N = -\lim_{n\to\infty} \frac{1}{\beta} \log \Lambda_1, \tag{2.11}$$

where Λ_1 is the largest eigenvalue of the transfer matrix $\mathcal{T}_n$. Only this eigenvalue thereby gives an approximant of the free energy of the quantum system of infinite size. The convergence of f in the limit $n \to \infty$ is well known as the $1/n^2$ law [Suzuki 85d].

Besides, a correlation length is given, without any finite-size correction, by the ratio between the relevant eigenvalue and the maximum one:

$$\begin{aligned} \xi_\alpha^{-1} &\equiv -\lim_{r\to\infty} \frac{1}{r} \log \left\langle S_i^\alpha S_{i+r}^\alpha \right\rangle = -\lim_{n\to\infty}\lim_{r\to\infty}\lim_{N\to\infty} \frac{1}{r} \log \frac{\mathrm{Tr}\, \mathcal{T}_n^i S^\alpha \mathcal{T}_n^r S^\alpha \mathcal{T}_n^{N-(i+r)}}{\mathrm{Tr}\, \mathcal{T}_n^N} \\ &= \lim_{n\to\infty} \log \frac{\Lambda_1}{\Lambda_\nu}. \end{aligned} \tag{2.12}$$

Here the eigenvalue Λ_ν is the largest one whose eigenvector $|\phi_\nu\rangle$ satisfies

$$|\langle \phi_1 | S^\alpha | \phi_\nu \rangle| \neq 0. \tag{2.13}$$

This approach has been further developed to analytic treatments [Suzuki 87c, Inoue 88] and numerically rigorous treatments [Koma 87, Koma 89] of one-dimensional quantum models.

The transfer matrix $\mathcal{T}_n$ is explicitly block-diagonalized. Because of the conservation rule (2.9), the four-body interaction conserves the staggered magnetization in the real-space direction, namely

$$S_1 - S_3 = -S_2 + S_4. \tag{2.14}$$

The transfer matrix thus conserves the *column* staggered magnetization,

$$M_{\rm stag} \equiv \sum_{j=1}^{2n} (-1)^j S_j. \tag{2.15}$$

Hence the matrix is diagonalized into blocks each of which is labeled with the value of $M_{\rm stag}$.

We can prove the following two propositions: (i) The maximum eigenvalue of the matrix $\mathcal{T}_n$ exists in the $M_{\rm stag}=0$ block. (ii) The correlation length ξ_z is controlled by the second maximum eigenvalue in the $M_{\rm stag}=0$ block, while ξ_x is controlled by the maximum eigenvalue in the $M_{\rm stag}=\pm 1$ block. (For the isotropic Heisenberg model these two eigenvalues are degenerate, hence $\xi_z=\xi_x$.) Proofs of the propositions are briefly given in Appendix 2.A.

Here we concentrate on evaluation of the correlation length ξ_x, which is given by the largest eigenvalues of the blocks $M_{\rm stag}=0$ and 1.

The simplest method of evaluating the maximum eigenvalue of an asymmetric matrix is the power method: the Rayleigh quotient with a trial vector $|\psi\rangle$,

$$\lambda(N) \equiv \frac{\langle\psi|\mathcal{T}_n^{N+1}|\psi\rangle}{\langle\psi|\mathcal{T}_n^{N}|\psi\rangle}, \qquad (N=0,1,2,\cdots), \tag{2.16}$$

converges to the maximum eigenvalue rapidly as $N\to\infty$:

$$\Lambda_1 = \lim_{N\to\infty}\lambda(N). \tag{2.17}$$

Components of the other eigenvectors in the trial vector $|\psi\rangle$ disappear exponentially fast. The quotient of length N greater than ξ is enough to isolate the maximum eigenvalue. (If the trial vector is orthogonal to the eigenvector of the second-largest eigenvalue, the convergence is more rapid.) Repeated matrix multiplications give the desired result. Several authors have employed this approach to investigate the $S=1$ model [Kubo 86, Delica 91, Kubo 92].

In the $S=2$ case, however, the size of the trial vector is of the order of 5^{2n}. As the Trotter number n is increased, it becomes practically impossible to perform the matrix multiplication. This difficulty prevents us from the calculation at low temperatures; when β is large, we have to calculate up to a large value of n in order to keep small the correction in (2.7), $O(\beta^3/n^2)$.

The cluster-transfer-matrix method [Tsuzuki 85, Tsuzuki 86, Betsuyaku 86a] solves the problem partially. In this method we decompose the total Hamiltonian into many-spin clusters instead of the two-spin clusters of (2.7). We may obtain enough convergence with comparatively small n, because the coefficient of the correction $O(\beta^3/n^2)$ becomes small. We used this method to supplement the present Monte Carlo calculation. However, we could not reach very low temperatures by this method; the larger the cluster is, the more time the matrix multiplication takes, and the more difficult the diagonalization of the cluster Hamiltonian is.

Recently Koma [Koma 93] proposed a Monte Carlo method of evaluating the quotient (2.16) itself. His idea is as follows; choose as the trial vector $|\psi\rangle$ a vector every component of which is unity, that is, a superposition of all the bases of an orthonormal set:

$$|\psi\rangle \equiv \sum_{\{S\}} |S_1, S_2, \ldots, S_{2n}\rangle\,. \tag{2.18}$$

Then we can interpret the Rayleigh quotient (2.16) as a measurable quantity of a classical system. The classical system here differs from the system defined below (2.7) only by

a boundary condition. Since we expand the trial vector $|\psi\rangle$ of (2.16) as in (2.18), any spin configuration can appear on the left and right ends of the system; in other words the classical system in Fig. 2.1 (a) is under the free-boundary condition. When we concentrate on eigenvalues of a block of the transfer matrix, we have to restrict the summation in (2.18) only to the bases of that block.

The trial vector (2.18) is never orthogonal to the eigenvector $|\phi_1\rangle$ of the largest eigenvalue. The Perron-Frobenius theorem ensures that all the components of the eigenvector $|\phi_1\rangle$ is non-negative. Therefore $|\phi_1\rangle$ and the vector of (2.18) have an overlap.

2.3 Results

We present the data for the $S = 2$ chain, and compare them with the data for the $S = 1/2$, 1, $3/2$ cases, which we also calculated by the same approach.

We obtained the data points $\beta \leq 5$ by the cluster-transfer-matrix method, while the data points $\beta \geq 10$ by the Monte Carlo power method.

In the former calculation we used decompositions up to four-spin clusters. We adopted the data as far as the extrapolated estimate does not deviate as we change the cluster size.

In the latter calculation we observed that both initial-relaxation time and autocorrelation time of the Monte Carlo dynamics are considerably short. We also noticed that the quantity $\lambda(N)$ averaged over Monte Carlo steps does not follow a Gaussian distribution but the logarithm of it, $\log\lambda$, does. Hence we estimated the statistical error of the Monte Carlo data as follows: We partitioned off the whole $M(> 10^7)$ steps into $m(\simeq 10)$ sections excluding initial $M_{\rm init}(\simeq 10^4)$ steps. We averaged the quantity λ over $(M - M_{\rm init})/m$ steps in each section. Then we calculated the average and the deviation of $\log\lambda$ over the sections.

We thus evaluated $\log\lambda$ in the blocks $M_{\rm stag} = 0$ and 1 with the system size fixed. We calculated up to $N = 100$ and $n = 100$. The data obtained, $\{\log\lambda(n, N, M_{\rm stag}) \pm \sigma(M_{\rm stag})\}$, were further analyzed as follows: First we calculated $\xi_x^{-1}(n, N)$, following the formula

$$\xi_x^{-1}(n, N) = \log\lambda(n, N, 0) - \log\lambda(n, N, 1). \tag{2.19}$$

We obtained the statistical error of this as follows:

$$\sigma_\xi^2 = \sigma(0)^2 + \sigma(1)^2. \tag{2.20}$$

Next we extrapolated the data to the limit $N \to \infty$:

$$\xi_x^{-1}(n, \infty) = \xi_x^{-1}(n, N) + O\left(\mathrm{e}^{-cN}\right). \tag{2.21}$$

In the actual analyses, however, the correction term was buried in the statistical errors of the data. Thus we tried to make the decision of the convergence by eye. Finally we extrapolated the data to the limit $n \to \infty$:

$$\xi_x^{-1}(\infty, \infty) = \xi_x^{-1}(n, \infty) + O\left(n^{-2}\right). \tag{2.22}$$

This correction term was fitted by the least-squares method.

We plotted the final estimates in Fig. 2.2. In the region $T \geq 0.2$ the inverse of

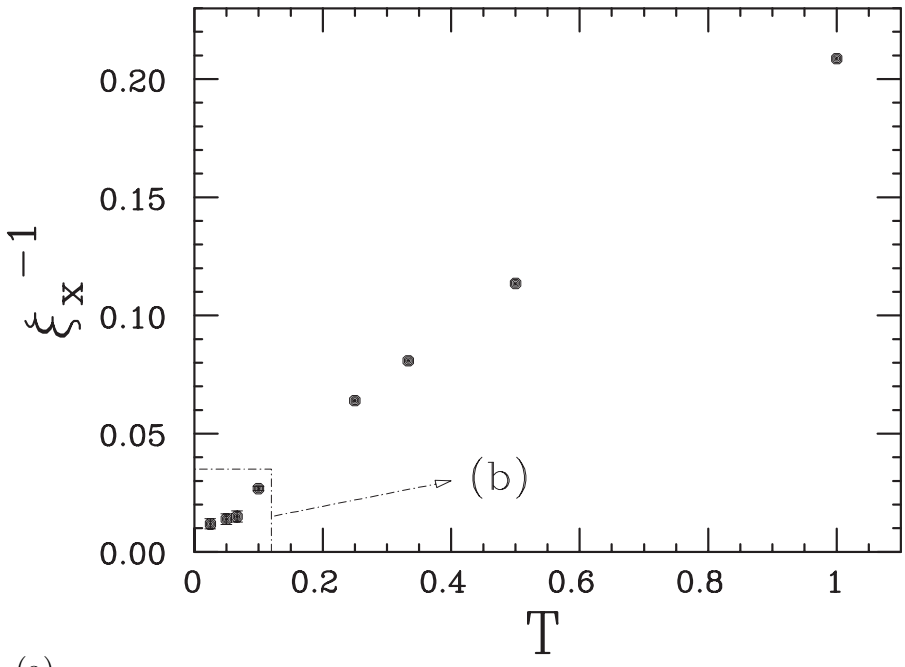

(a)

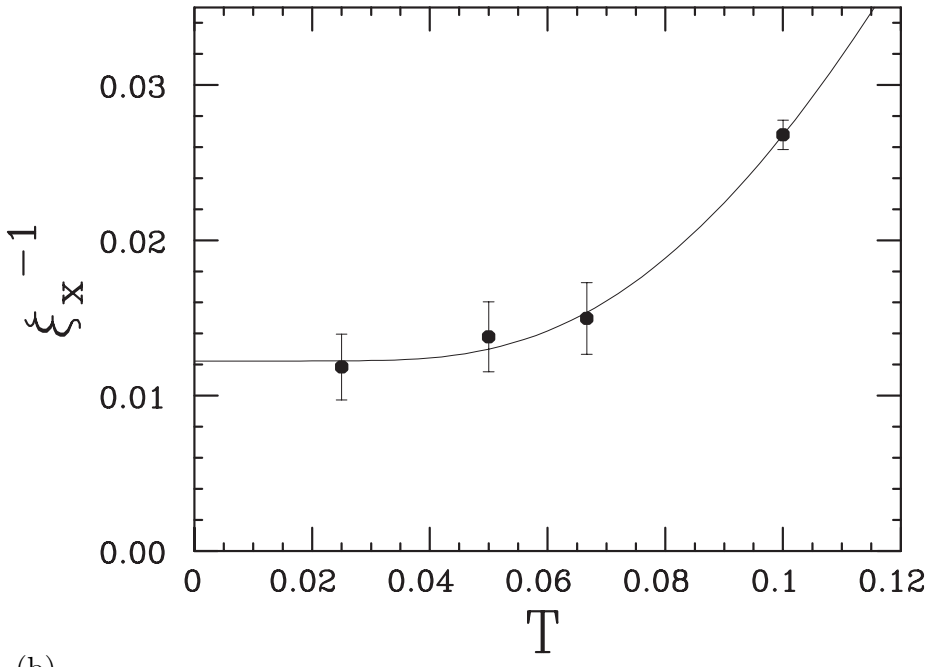

(b)

Figure 2.2 The temperature dependence of the correlation length of the $S = 2$ Heisenberg chain: (a) $0 < T \leq 1.0$ and (b) a magnified figure of (a) in the region $0 < T \leq 0.1$. The fitting line of (2.23) is also indicated.

the correlation length is nearly proportional to the temperature. As the temperature is lowered, however, the correlation length slows down its growth below the temperature around $T \sim 0.1$ and is saturated to a value.

We fitted the four data points in Fig. 2.2 (b) to the function

$$\xi_x(T)^{-1} = \xi_x(0)^{-1} + cT \exp\left(-\frac{\Delta E}{T}\right) \tag{2.23}$$

by the least-squares method, and obtained the estimate

$$\xi_x(0)^{-1} = 0.012(2). \tag{2.24}$$

Here we added the prefactor T to the exponential term of the fitting function (2.23) so that the function may become $\xi^{-1} \propto T$ at high temperatures. The result obtained by the fitting is indicated in Fig. 2.2 (b). The estimate agrees well with the value obtained with naive usage of (2.5), $\xi_x^{-1} \simeq 0.011$.

The correlation length is almost constant below the temperature $T = 1/15 \simeq 0.067$. This fact suggests that we have reached the ground state in this region. This is consistent with the value $\Delta E \simeq 0.048$ derived from (2.4) for $S = 2$. (Unfortunately, we have not obtained enough data to estimate the magnitude of the energy gap. The error of the estimate by (2.23) is large: $\Delta E = 0.2(2)$.)

In Fig. 2.3 we plotted the data for the cases $S = 1/2$, 1, $3/2$ and 2 together, scaling the temperature by a factor $1/S(S+1)$:

$$\overline{T} \equiv T/S(S+1). \tag{2.25}$$

This scaling is equivalent to re-defining the Hamiltonian in the form

$$\mathcal{H} \equiv \frac{1}{S(S+1)} \sum \boldsymbol{S}_i \cdot \boldsymbol{S}_{i+1}. \tag{2.26}$$

All the data fall on a line $\xi_x^{-1} \simeq 1.3\overline{T}$ rather well except at low temperatures, where, in the cases $S = 1$ and $S = 2$, the lines turn to finite values on the ordinate. We clearly distinguish the $S = 1$ and $S = 2$ models from the $S = 1/2$ and $S = 3/2$ models.

In the limit $S \to \infty$ the Hamiltonian (2.26) may converge to the classical Heisenberg model

$$\mathcal{H}_{\text{classical}} \equiv \sum \tilde{\boldsymbol{S}}_i \cdot \tilde{\boldsymbol{S}}_{i+1}, \tag{2.27}$$

where the length of the spins is normalized to $|\tilde{\boldsymbol{S}}| = 1$. The exact solution of the model [Fisher 64] yields

$$\left\langle \tilde{S}_i^z \tilde{S}_{i+r}^z \right\rangle = \frac{1}{3} u^r \qquad \text{with} \qquad u \equiv \coth(1/T) - T. \tag{2.28}$$

Hence we have

$$\xi^{-1} = -\log u \simeq T \qquad \text{as} \quad T \to 0, \tag{2.29}$$

which is also drawn in Fig. 2.3.

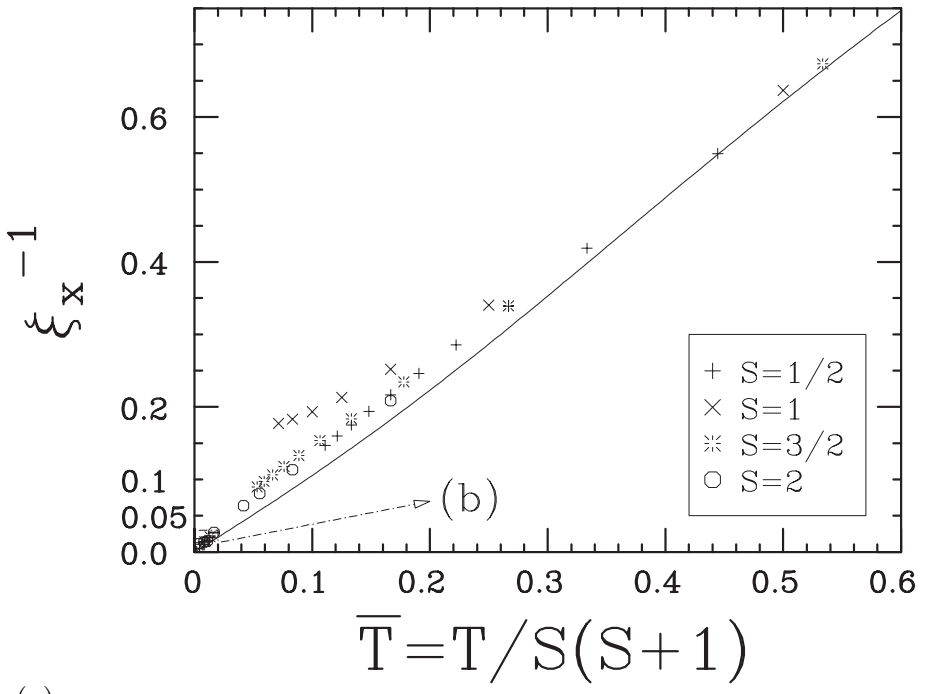

(a)

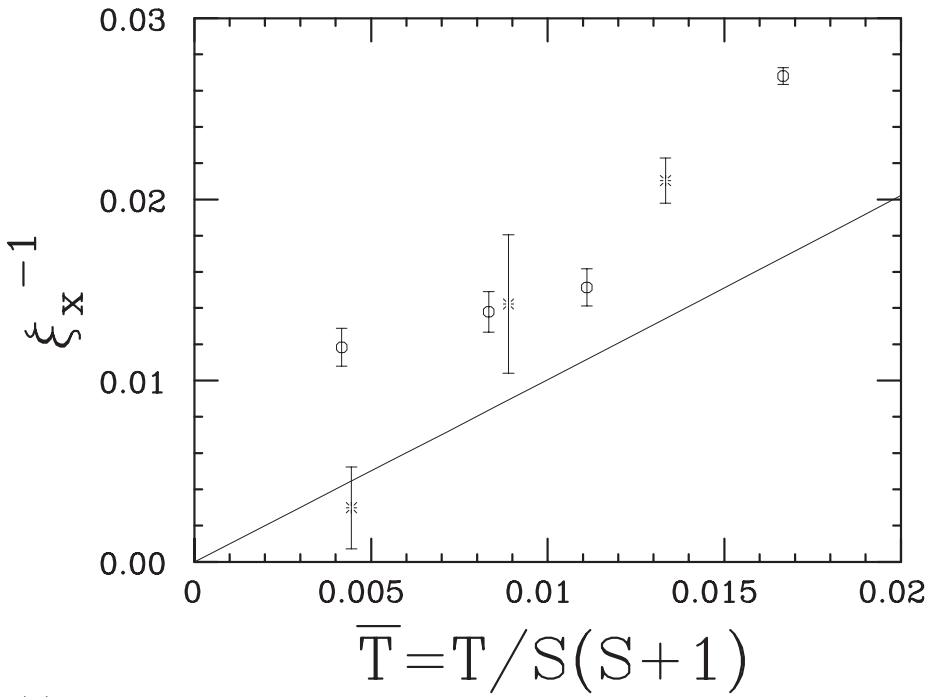

(b)

Figure 2.3 The correlation length of the $S = 1/2$ (+), 1 ($\times$), 3/2 ($*$) and 2 ($\circ$) models versus the scaled temperature $\overline{T} \equiv T/S(S+1)$: (a) $0 < \overline{T} < 0.6$ and (b) a magnified figure of (a) in the region $0 < \overline{T} < 0.02$. The exact solution of the classical model is also plotted here (the solid line).

2.4 Summary

We numerically investigated the one-dimensional Heisenberg antiferromagnet, particularly the $S = 2$ model. We concentrated on the temperature dependence of the correlation length.

We observed the behavior $\xi \propto T^{-1}$ for the $S = 1/2$, 1, 3/2, 2 models except the region $T < \Delta E$ of the integer-spin cases; the exponent $\nu = 1$ coincides with the value in the classical limit.

At the temperatures $T < 0.1$ we observed the saturation of the correlation length of the $S = 2$ model, distinguishing it from the $S = 3/2$ case. This observation confirmed the Haldane conjecture. We stress here that the usage of the Monte Carlo power method is essential to this observation; we might have found the behavior $\xi \propto T^{-1}$ if we used only the data for $T > 0.2$ obtained by the transfer-matrix method.

We conclude that the correlation length of the $S = 2$ model is saturated to the value $\xi^{-1} \simeq 0.012(2)$. The approximate formula (2.5) by Haldane explains the value well. Hence we expect that the formula gives the values for $S \geq 3$ rather precisely; namely $\xi^{-1}(S = 3) \simeq 6.3 \times 10^{-4}$, $\xi^{-1}(S = 4) \simeq 3.4 \times 10^{-5}$ and so on.

2.A Proofs of propositions

In this appendix we briefly mention proofs of the two propositions stated below (2.15).

The proof of the first proposition is given by a straightforward extension of the proof in the $S = 1/2$ case [Koma 89].

When the spin chain is under the periodic-boundary condition we have (2.10). When it is under the open-boundary condition, on the other hand, the expression should be modified to

$$Z_n(N) = \left\langle \varphi_n \left| \mathcal{T}_n^N \right| \varphi_n \right\rangle . \tag{2.30}$$

Here the vector $|\varphi_n\rangle$ is a superposition of all the bases which satisfy the condition

$$S_{2j} = S_{2j+1} \qquad \text{for} \quad j = 0, 1, \ldots, n-1. \tag{2.31}$$

The notation of the subscripts of the spin variables is indicated in Fig. 2.1 (a). Owing to the condition (2.31), the vector $|\varphi_n\rangle$ has non-vanishing elements only in the subspace $M_{\text{stag}} = 0$.

In the thermodynamic limit $N \to \infty$, the largest eigenvalue of the block $M_{\text{stag}} = 0$ gives the free-energy density of the open system. On the other hand, the largest eigenvalue of the whole matrix gives the free-energy density of the periodic system. Hence these two eigenvalues must coincide; otherwise the free-energy density in the thermodynamic limit depends on the boundary condition, which contradicts with the extensivity of the free energy.

The proof of the second proposition is also the same as in the $S = 1/2$ case [Takahashi 91a]. Since the operator S^z does not change the direction of spins, the condition

$$|\langle \phi_1 | S^z | \phi_\nu \rangle| \neq 0 \tag{2.32}$$

is satisfied only when the vector $|\phi_\nu\rangle$ belongs to the same block as the one $|\phi_1\rangle$ belongs to, namely, the $M_{\text{stag}} = 0$ block. The operator S^x, on the other hand, raises or lowers a

spin by unity; therefore the vector $|\phi_\nu\rangle$ satisfying the condition

$$|\langle\phi_1\,|S^x|\,\phi_\nu\rangle| \neq 0 \tag{2.33}$$

must belong to either of the blocks $M_{\text{stag}} = \pm 1$.

Chapter 3

Ground-State Phase Transition of $S = 1/2$ Alternating-Bond Chains[†]

A world-line Monte Carlo method of studying the ground state of a quantum system is proposed. An application of the method to the one-dimensional $S = 1/2$ alternating-bond model is reported. Anisotropy dependence of order parameters suggesting ground-state phase transitions is observed.

3.1 Introduction

The study of ground-state phase transitions driven by quantum fluctuation is now one of the most interesting problems in condensed-matter physics. Critical points are defined in a parameter space of the relevant model, at which an energy gap from the ground state vanishes in the thermodynamic limit. At these critical points, correlation functions of the system show power-law behavior instead of exponential decay, and the correlation length diverges.

In investigating ground-state phase transitions using quantum Monte Carlo methods, however, there arises a problem, namely, the difficulty of taking the zero-temperature limit. We investigate the relevant system first at finite temperatures, and take the zero-temperature limit to extract the ground-state property. This can be performed practically at temperatures low enough to satisfy the inequality $T \ll \Delta E$. Here ΔE denotes the energy gap just above the ground state. Near phase boundaries the energy gap is narrow, and hence it is difficult to satisfy the condition $T \ll \Delta E$.

Moreover, when we treat frustrated spin systems or fermion systems, the negative-sign problem becomes quite serious at low temperatures.

Some attempts to circumvent the problems have been proposed [Kalos 74, Kuti 82, Blankenbecler 83, Sugiyama 86]. They are more or less based on the following formula:

$$\mathrm{e}^{-\beta\mathcal{H}}\,|\psi\rangle \longrightarrow \mathrm{e}^{-\beta E_{\mathrm{g}}}\,|\psi_{\mathrm{g}}\rangle \qquad \text{as} \quad \beta \to \infty, \tag{3.1}$$

where $|\psi_{\mathrm{g}}\rangle$ is the ground-state vector, E_{g} is the ground-state energy, and $|\psi\rangle$ is a trial vector which is not orthogonal to $|\psi_{\mathrm{g}}\rangle$. If the trial vector is orthogonal to the first excited state, the extraction of the ground state may be performed even at rather high

[†]The content of this chapter will be published in [Hatano 93b].

temperatures (though the variable $T = 1/\beta$ loses its meaning as the temperature). A quantity in the ground state is given by

$$\langle Q \rangle_{\rm g} \equiv \langle \psi_{\rm g} | Q | \psi_{\rm g} \rangle = \lim_{\beta \to \infty} \langle\langle Q \rangle\rangle_\beta \tag{3.2}$$

with

$$\langle\langle Q \rangle\rangle_\beta \equiv \frac{\left\langle \psi \left| {\rm e}^{-\beta \mathcal{H}} Q {\rm e}^{-\beta \mathcal{H}} \right| \psi \right\rangle}{\left\langle \psi \left| {\rm e}^{-2\beta \mathcal{H}} \right| \psi \right\rangle}. \tag{3.3}$$

The limit procedure $\beta \to \infty$ itself is simulated, by interpreting multiplications of a transfer matrix as a Markov process, in several ways, for example, in the Green's-function Monte Carlo method [Kalos 74] and in the projector Monte Carlo method [Kuti 82, Blankenbecler 83], to which we refer as the diffusion Monte Carlo methods. However, Hetherington [Hetherington 84] pointed out that a systematic error appears in the diffusion Monte Carlo simulations when the number of steps is large. Repeating multiplications of a stochastic matrix M to a state vector, we obtain the stationary state of a Markov process:

$$M^N |\psi\rangle \longrightarrow |\psi_{\rm stationary}\rangle \qquad \text{as} \quad N \to \infty. \tag{3.4}$$

(Here the matrix element M_{ij} denotes the probability that a random walker hops from the j-th state to the i-th state.) The convergence to the stationary state is proved only when the stochastic matrix M satisfies the condition

$$\sum_i M_{ij} = 1 \qquad \text{for all } j \quad . \tag{3.5}$$

A transfer matrix which does not satisfy this condition is used to define the Markov process in the diffusion Monte Carlo methods.

Here we propose an application of the world-line quantum Monte Carlo algorithm [Suzuki 76b, Suzuki 77b] to the formula (3.3). We demonstrate the efficiency of the present method, studying the $S = 1/2$ alternating-bond spin chains [Hida 92a]. The improvement in the convergence for $\beta \to \infty$ is observed.

In the present method we first fix the parameter β to estimate quantities by a simulation. Analyzing the data we evaluate the quantities in the ground state. Hence the present method is free from such systematic error as that appearing in the diffusion Monte Carlo methods.

In the present world-line approach, trial functions of a wide class are available, as shown below. An approach similar to the present one has been frequently employed in studies on the Hubbard model [Sugiyama 86, Sorella 89]. In these studies the fermion degrees of freedom are traced out by the Stratonovich-Hubbard transformation [Stratonovich 57, Hubbard 59, Hirsch 83b], and auxiliary-field degrees of freedom are sampled by simulations. In these approaches the trial function $|\psi\rangle$ is necessarily a direct product of one-particle states:

$$|\psi\rangle \equiv \prod_{m=1}^{M} \left(\sum_{i=1}^{N} F_{im} c_i^\dagger \right) |0\rangle \, . \tag{3.6}$$

It is possible in the thermodynamic limit that an overlap between the ground state and the trial function becomes exponentially small compared to the full extent of the Hilbert space.

3.2 $S = 1/2$ alternating-bond chains and the Haldane problem

In this section we mention properties of the $S = 1/2$ alternating-bond spin chain and its relation with the Haldane problem.

The Hamiltonian of the $S = 1/2$ alternating-bond spin chain is described by

$$\mathcal{H} \equiv \frac{1}{2}\sum_{i=1}^{N/2}\left(\sigma_{2i-1}^{x}\sigma_{2i}^{x} + \sigma_{2i-1}^{y}\sigma_{2i}^{y} + \lambda\sigma_{2i-1}^{z}\sigma_{2i}^{z}\right) - \frac{J_{\mathrm{F}}}{2}\sum_{i=1}^{N/2}\boldsymbol{\sigma}_{2i}\cdot\boldsymbol{\sigma}_{2i+1}. \tag{3.7}$$

The antiferromagnetic coupling of the first term is defined to be one-half. The boundary is either free or periodic ($\sigma_{N+1} = \sigma_1$).

We consider the parameter region $J_{\mathrm{F}} > 0$. In the limit $J_{\mathrm{F}} \to \infty$, we expect that every pair of spins σ_{2i} and σ_{2i+1} form a triplet, and effectively becomes an $S = 1$ spin. We thereby obtain the $S = 1$ antiferromagnetic chain with the anisotropy λ:

$$\mathcal{H}_{S=1} = \sum_{i=1}^{N/2}\left(S_{i-1}^{x}S_{i}^{x} + S_{i-1}^{y}S_{i}^{y} + \lambda\sigma_{i-1}^{z}\sigma_{i}^{z}\right). \tag{3.8}$$

For this model with $S = 1$, Haldane conjectured [Haldane 83a, Haldane 83b, Affleck 89] that, in a region $\lambda_{\mathrm{c1}} < \lambda < \lambda_{\mathrm{c2}}$, (i) there is a phase in which an energy gap exists just above the unique ground state, and (ii) the spin correlation decays exponentially in the ground state.

In the limit $J_{\mathrm{F}} = 0$, on the other hand, the model (3.7) becomes a set of mutually independent dimers. We can write down the unique ground state of the model in the region $\lambda > -1$, that is, the direct product of singlets located on antiferromagnetic bonds:

$$|\psi_{\mathrm{ground}}\rangle = \bigotimes_{i=1}^{N/2}|\mathrm{singlet}\rangle_i = \bigotimes_{i=1}^{N/2}\frac{1}{\sqrt{2}}\left(|\uparrow_{2i-1}\downarrow_{2i}\rangle - |\downarrow_{2i-1}\uparrow_{2i}\rangle\right). \tag{3.9}$$

The first excited states are given by the ones in which one of the singlets is excited to a triplet:

$$|\psi_{\mathrm{excited}}\rangle = |\mathrm{triplet}\rangle_j \bigotimes_{i(\neq j)}|\mathrm{singlet}\rangle_i. \tag{3.10}$$

There exists an energy gap of the magnitude

$$\Delta E = \min\left[2, \lambda + 1\right]. \tag{3.11}$$

Recently Hida [Hida 92a, Hida 92b] observed that no clear phase boundary exists on the line $\lambda = 1$ for $J_{\mathrm{F}} \geq 0$. When one increases the parameter J_{F}, the ground state of the dimer model, (3.9), continuously becomes the ground state conjectured by Haldane. The energy gap (3.11) never closes along this line.

This observation is comparable with construction of the valence-bond-solid state, which is the exact ground state of an $S = 1$ model with an extra interaction term [Affleck 88]:

$$\mathcal{H} \equiv \sum_{i=1}^{N/2}\left[\boldsymbol{S}_i\cdot\boldsymbol{S}_{i+1} + \frac{1}{3}\left(\boldsymbol{S}_i\cdot\boldsymbol{S}_{i+1}\right)^2\right]. \tag{3.12}$$

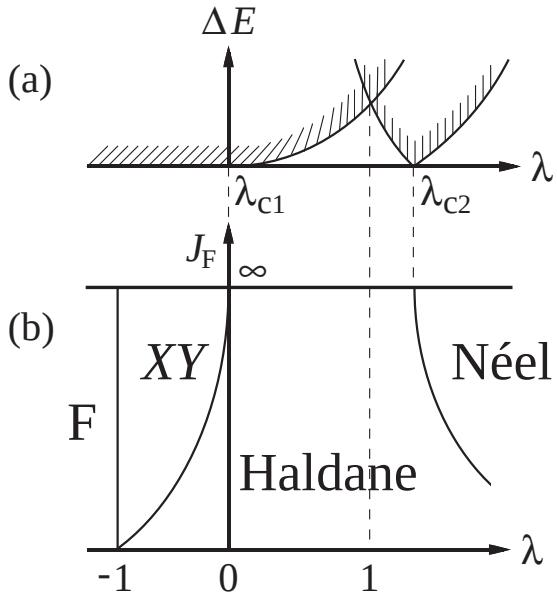

Figure 3.1 (a) Anisotropy dependence of the magnitude of the energy gap of the model with $S = 1$. (b) An expected phase diagram of the alternating-bond spin chain.

The valence-bond-solid state is defined as follows; consider a direct product of singlets, (3.9). We symmetrize the wave functions of each pair of spins σ_{2i} and σ_{2i+1}. This state is the exact ground state of (3.12). It is considered [Affleck 88] that the state satisfies the Haldane conjecture, and hence is an good approximant of the ground state of the $S = 1$ isotropic Heisenberg model (namely the model (3.8) with $\lambda = 1$). We notice that the procedure $J_{\rm F} \to \infty$ is a physical interpretation of the definition of the valence-bond-solid state.

When we change the value of the parameter λ of the $S = 1$ model, (3.8), ground-state phase transitions are expected to occur [Haldane 83a, Haldane 83b, Kolb 83, Parkinson 85b, Kubo 86, Nomura 89b, Sakai 90b, Kubo 92]; see Fig. 3.1 (a). In the region $-1 < \lambda < \lambda_{\rm c1} \simeq 0$, we have the XY phase; the energy spectrum is continuous above the ground state. In the region $\lambda_{\rm c1} < \lambda < \lambda_{\rm c2}$, we have the Haldane phase; an energy gap is open just above the unique ground state. In the region $\lambda > \lambda_{\rm c2}$, we have the Néel phase; an energy gap is open above the two degenerate ground states. At the point $\lambda = \lambda_{\rm c2}$, the energy gap is closed and the correlation length diverges.

Hereafter we investigate the model (3.7) with finite $J_{\rm F}$. When we change λ of the $S = 1/2$ model with fixed $J_{\rm F}$, we expect phase transitions of the same character as the ones in the $S = 1$ model [Kohmoto 92]; see Fig. 3.1 (b). The transitions have been studied by means of the series-expansion method [Yamanaka 92].

An order parameter characterizing the Haldane phase of the $S = 1$ model is known as the string order parameter [Den Nijs 89], which is defined by

$$O^{\alpha}_{\rm string}(k) \equiv -\exp\left(i\pi \sum_{j=1}^{k-1} S^{\alpha}_{j}\right) S^{\alpha}_{k} \qquad \text{for} \quad \alpha = x, y, z. \tag{3.13}$$

This definition yields the string correlation

$$G^{\alpha}_{\rm string}(k-l) \equiv O^{\alpha}_{\rm string}(k) O^{\alpha}_{\rm string}(l) = -S^{\alpha}_{k} \exp\left(i\pi \sum_{j=k+1}^{l-1} S^{\alpha}_{j}\right) S^{\alpha}_{l}. \tag{3.14}$$

An $S = 1/2$ version of the string order parameter can be defined by

$$O^{\alpha}_{\rm string}(k) \equiv -\frac{1}{2}\exp\left(\frac{i\pi}{2}\sum_{j=1}^{2k-2}\sigma^{\alpha}_{j}\right)\left(\sigma^{\alpha}_{2k}+\sigma^{\alpha}_{2k+1}\right) = \frac{(-1)^k}{2}\left(\prod_{j=1}^{2k-2}\sigma^{\alpha}_{j}\right)\left(\sigma^{\alpha}_{2k}+\sigma^{\alpha}_{2k+1}\right). \tag{3.15}$$

Different versions can be considered; see [Takada 92, Hida 92c]. The bulk order parameter is given by

$$O^{\alpha}_{\rm string} \equiv \frac{1}{N}\sum_{k}(-1)^k\left(\prod_{j=1}^{2k-2}\sigma^{\alpha}_{j}\right)\left(\sigma^{\alpha}_{2k}+\sigma^{\alpha}_{2k+1}\right). \tag{3.16}$$

The string correlation is now given by

$$G^{\alpha}_{\rm string}(k-l) = \frac{(-1)^{k-l}}{4}\left(\sigma^{\alpha}_{2k}+\sigma^{\alpha}_{2k+1}\right)\left(\prod_{j=2k+1}^{2l-2}\sigma^{\alpha}_{j}\right)\left(\sigma^{\alpha}_{2l}+\sigma^{\alpha}_{2l+1}\right). \tag{3.17}$$

In the Haldane phase the string order parameter does not vanish and the string correlation ranges over the system.

An order parameter characterizing the Néel phase of the $S = 1$ phase can be defined by the staggered magnetization:

$$O^{\alpha}_{\rm N\acute{e}el}(k) \equiv (-1)^k S^{\alpha}_{k}. \tag{3.18}$$

The $S = 1/2$ version of the order parameter is hence given by

$$O^{\alpha}_{\rm N\acute{e}el}(k) \equiv \frac{(-1)^k}{2}\left(\sigma^{\alpha}_{2k}+\sigma^{\alpha}_{2k+1}\right). \tag{3.19}$$

The bulk order parameter is given by

$$O^{\alpha}_{\rm N\acute{e}el} \equiv \frac{1}{N}\sum_{k}(-1)^k\left(\sigma^{\alpha}_{2k}+\sigma^{\alpha}_{2k+1}\right). \tag{3.20}$$

The staggered correlation is written in the form

$$G^{\alpha}_{\rm N\acute{e}el}(k-l) = \frac{(-1)^{k-l}}{4}\left(\sigma^{\alpha}_{2k}+\sigma^{\alpha}_{2k+1}\right)\left(\sigma^{\alpha}_{2l}+\sigma^{\alpha}_{2l+1}\right). \tag{3.21}$$

In the Néel phase the Néel order parameter does not vanish and the staggered correlation ranges over the system.

3.3 Method of numerical calculation

In the present section we describe a quantum Monte Carlo method of studying ground states and its application to the alternating-bond chain.

To evaluate the quantity (3.3), we have employed the world-line quantum Monte Carlo method based on the Suzuki-Trotter transformation [Suzuki 76b, Suzuki 77b]. Following the standard procedure [Suzuki 87b], we first decompose the density matrix as follows:

$$\mathrm{e}^{-\beta\mathcal{H}} = \left(\mathrm{e}^{-\beta A/(2n)}\mathrm{e}^{-\beta B/n}\mathrm{e}^{-\beta A/(2n)}\right)^n + O\left(\frac{\beta^3}{n^2}\right), \tag{3.22}$$

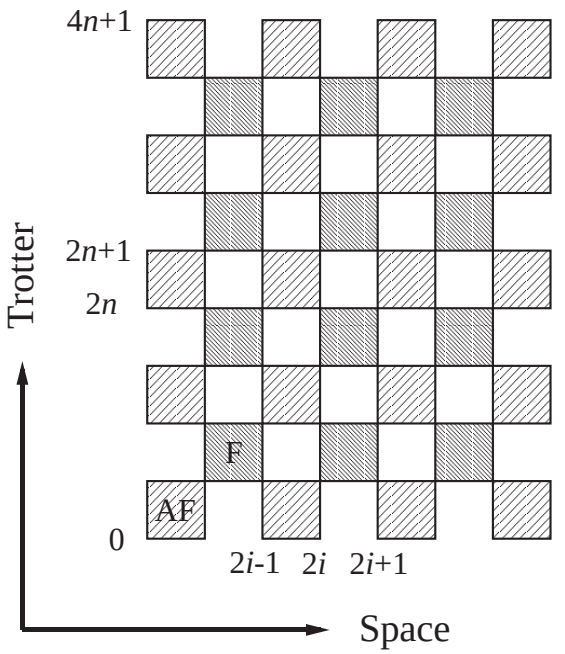

Figure 3.2 The mapped Ising-spin system of the checkerboard type. The restricted boundary conditions are required on the spins $\{\sigma\}_0$ and $\{\sigma\}_{4n+1}$.

with

$$\mathcal{H} = A + B. \tag{3.23}$$

We should keep the Trotter number n larger than β to eliminate the correction term $O(\beta^3/n^2)$. Application of the decomposition yields

$$\left\langle \psi \left| \mathrm{e}^{-2\beta\mathcal{H}} \right| \psi \right\rangle = \lim_{n\to\infty} \left\langle \psi \left| \mathrm{e}^{-\beta A/(2n)} \mathrm{e}^{-\beta B/n} \left(\mathrm{e}^{-\beta A/n} \mathrm{e}^{-\beta B/n} \right)^{2n-1} \mathrm{e}^{-\beta A/(2n)} \right| \psi \right\rangle. \tag{3.24}$$

Next we prepare an orthonormal set of bases which diagonalizes the operators $\{\sigma_i^z\}$. We insert the resolution of the unit operator $\hat{1}$ between each pair of exponential operators in (3.22). At the same time we expand the trial function with respect to the bases as

$$|\psi\rangle = \sum F(\{\sigma\}) \, |\{\sigma\}\rangle \, . \tag{3.25}$$

Thus we interpret the denominator of (3.3) as the partition function of an Ising spin system of the checkerboard type [Hirsch 81, Hirsch 82]:

$$Z_n \equiv \sum F(\{\sigma\}_0) W(\{\sigma\}_0, \{\sigma\}_1, \ldots, \{\sigma\}_{4n+1}) F(\{\sigma\}_{4n+1}), \tag{3.26}$$

where

$$\begin{aligned} & W(\{\sigma\}_0, \{\sigma\}_1, \{\sigma\}_2, \ldots, \{\sigma\}_{4n+1}) \\ & \equiv \left\langle \{\sigma\}_0 \left| \, \mathrm{e}^{-\beta A/(2n)} \, \right| \{\sigma\}_1 \right\rangle \left\langle \{\sigma\}_1 \left| \, \mathrm{e}^{-\beta B/n} \, \right| \{\sigma\}_2 \right\rangle \\ & \quad \cdots \times \left\langle \{\sigma\}_{4n-1} \left| \, \mathrm{e}^{-\beta B/n} \, \right| \{\sigma\}_{4n} \right\rangle \left\langle \{\sigma\}_{4n} \left| \, \mathrm{e}^{-\beta A/(2n)} \, \right| \{\sigma\}_{4n+1} \right\rangle. \end{aligned} \tag{3.27}$$

See Fig. 3.2.

On the other hand, in the finite-temperature algorithm based on the Suzuki-Trotter formula [Suzuki 76b, Suzuki 77b], we transform the partition function of the quantum system

$$\mathrm{Tr}\, \mathrm{e}^{-\beta\mathcal{H}} \tag{3.28}$$

into that of the corresponding Ising system. This system and the system (3.26) differ in boundary conditions. The system is given by

$$Z_n = \sum_{\{\sigma\}} W(\{\sigma\}_0, \{\sigma\}_1, \{\sigma\}_2, \ldots, \{\sigma\}_{2n-1}, \{\sigma\}_0). \tag{3.29}$$

In the finite-temperature algorithm we require the periodic-boundary conditions $\{\sigma\}_{2n} = \{\sigma\}_0$. In the formulation (3.26) we require constrained-boundary conditions on the spins $\{\sigma\}_0$ and $\{\sigma\}_{4n+1}$; a spin configuration $\{\sigma\}_0$ appears with a rate determined by the Boltzmann factor $W(\{\sigma\}_0)$ times the extra factor $F(\{\sigma\}_0)$.

When we perform the importance sampling of (3.26), we have to flip the spins $\{\sigma\}_0$ and $\{\sigma\}_{4n+1}$,

$$\{\sigma\} \longrightarrow \{\sigma\}', \tag{3.30}$$

according to the ratio $R = R_1 R_2$,

$$R_1 \equiv \frac{W(\{\sigma\}_0')}{W(\{\sigma\}_0)} \tag{3.31}$$

and

$$R_2 \equiv \frac{F(\{\sigma\}_0')}{F(\{\sigma\}_0)}. \tag{3.32}$$

Since the interactions of the Ising system are of short range, the factor R_1 can be calculated easily. The factor R_2 can also be calculated for a wide class of trial functions. The other spins are flipped only according to the factor R_1.

It is preferable to choose a trial function with $f(\{\sigma\}) \geq 0$ for all $\{\sigma\}$; otherwise the Boltzmann weight in (3.26) can be negative, and we may have the negative-sign problem even if $W \geq 0$. It is also natural to choose a function with $f \geq 0$; in models where $W \geq 0$, the Hamiltonian is a non-negative matrix at least after a unitary transformation. In this case the ground state is a non-negative vector owing to the Perron-Frobenius theorem, namely $f_{\rm g}(\{\sigma\}) \geq 0$. Hence we can increase the overlap between the trial function and the ground-state function by choosing $f \geq 0$.

The same procedure as (3.22)-(3.27) yields

$$\langle\langle Q \rangle\rangle_\beta \simeq \frac{1}{Z_n} \sum_{\{\sigma\}} \tilde{Q} f W f, \tag{3.33}$$

where

$$\tilde{Q}(\{\sigma\}_{2n}, \{\sigma\}_{2n+1}) \equiv \frac{\left\langle \{\sigma\}_{2n} \left| {\rm e}^{-\beta A/(2n)} Q {\rm e}^{-\beta A/(2n)} \right| \{\sigma\}_{2n+1} \right\rangle}{\left\langle \{\sigma\}_{2n} \left| {\rm e}^{-\beta A/n} \right| \{\sigma\}_{2n+1} \right\rangle}. \tag{3.34}$$

Measurement of $\tilde{Q}$ thereby gives a Monte Carlo estimate of $\langle\langle Q \rangle\rangle_\beta$.

Hereafter we describe application of the method to the $S = 1/2$ alternating-bond chains.

In order to ensure positivity of the Hamiltonian, we apply the following unitary transformations,

$$\left\{ \begin{array}{lcl} \sigma_i^x & \longrightarrow & -\sigma_i^x \\ \sigma_i^y & \longrightarrow & -\sigma_i^y \\ \sigma_i^z & \longrightarrow & \sigma_i^z \end{array} \right. \qquad \text{for} \quad i = 4k+2, 4k+3, \quad k = 0, 1, \ldots. \tag{3.35}$$

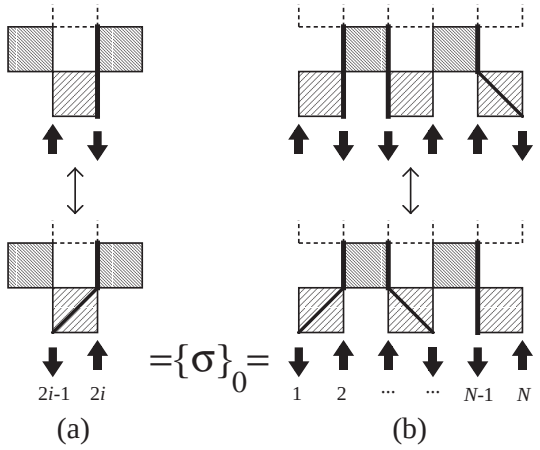

Figure 3.3 Flips of the spins $\{\sigma\}_0$ due to the use of the present trial functions. The shaded squares denote four-spin interactions of the transformed Ising system. The thick lines on the lattices denote the world lines which connect downward spins: (a) local-exchange flip for (3.9); (b) global-exchange flip for (3.40).

Now the Hamiltonian is written in the form

$$\mathcal{H}^{\mathrm{AF}} = \sum_{i=1}^{N/2} \mathcal{H}_i^{\mathrm{AF}} = \sum_i \left(-\sigma_{2i-1}^x \sigma_{2i}^x - \sigma_{2i-1}^y \sigma_{2i}^y + \lambda \sigma_{2i-1}^z \sigma_{2i}^z \right) \tag{3.36}$$

and

$$\mathcal{H}^{\mathrm{F}} = \sum_i \mathcal{H}_i^{\mathrm{F}} = -J_{\mathrm{F}} \sum_i \boldsymbol{\sigma}_{2i} \cdot \boldsymbol{\sigma}_{2i+1}. \tag{3.37}$$

We have employed the Suzuki-Trotter transformation (3.22) with

$$A = \mathcal{H}^{\mathrm{AF}} \qquad \text{and} \qquad B = \mathcal{H}^{\mathrm{F}}, \tag{3.38}$$

which leads to the checkerboard decomposition [Hirsch 81, Hirsch 82] as is depicted in Fig. 3.2. The Boltzmann factor is a product of the local factors

$$\begin{aligned} w^{\mathrm{AF}} &\equiv \left\langle \sigma_{2i-1}, \sigma_{2i} \left| \mathrm{e}^{-\beta \mathcal{H}_i^{\mathrm{AF}}} \right| \sigma'_{2i-1}, \sigma'_{2i} \right\rangle \\ \text{and} \qquad w^{\mathrm{F}} &\equiv \left\langle \sigma_{2i}, \sigma_{2i+1} \left| \mathrm{e}^{-\beta \mathcal{H}_i^{\mathrm{F}}} \right| \sigma'_{2i}, \sigma'_{2i+1} \right\rangle . \end{aligned} \tag{3.39}$$

We choose the trial function for the Haldane phase as the direct product of the singlets, (3.9), on account of Hida's observation [Hida 92a]. In this case we prepare a local-exchange flip for the spins $\{\sigma\}_0$ and $\{\sigma\}_{4n+1}$; see Fig. 3.3 (a). It is expected that the trial function is orthogonal to the first excited state, which is close to the state in which one of the singlets is excited to a triplet.

As for the Néel phase we choose the trial function as

$$|\psi_{\mathrm{N}}\rangle = \frac{1}{\sqrt{2}} \left(|\uparrow\uparrow\downarrow\downarrow\uparrow\uparrow \cdots\rangle + |\downarrow\downarrow\uparrow\uparrow\downarrow\downarrow \cdots\rangle \right). \tag{3.40}$$

In this case we prepare a global flip for the spins $\{\sigma\}_0$ and $\{\sigma\}_{4n+1}$; see Fig. 3.3 (b). In the Néel phase we expect that the first excited state is a domain-wall excitation, which is orthogonal to (3.40).

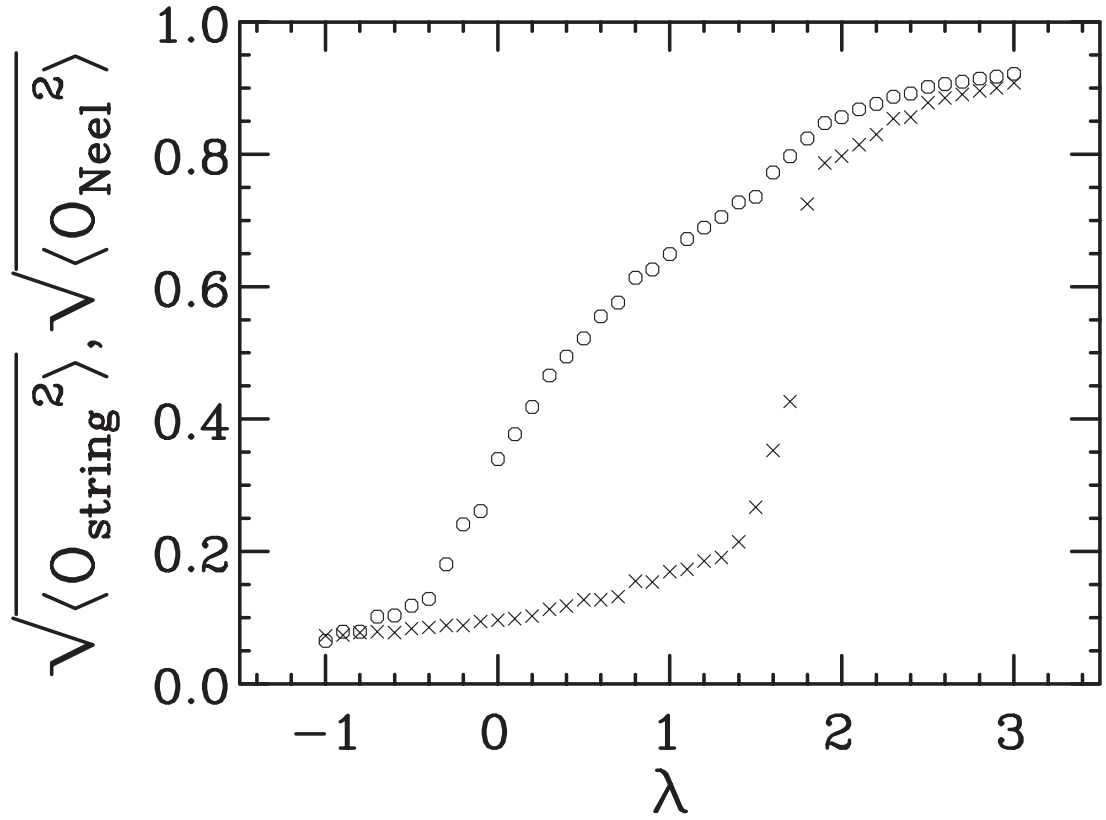

Figure 3.4 Anisotropy dependence of the string order parameter (◯) and the Néel order parameter (×). The size of the error bar of each data point is less than of nearly equal to the symbol size.

3.4 Results

We have calculated the root-mean-squares of the z-component of the order parameters, (3.16) and (3.20). We use the system of length $N = 200$ under the periodic-boundary condition.

The root-mean-squares of the order parameters converge to the order parameters themselves, respectively, in the limit $N \to \infty$. Assuming the behavior of the correlations as

$$\langle G^z(k-l)\rangle_{\rm g} \simeq \langle O^z\rangle_{\rm g}^2 + c\exp\left(\frac{|k-l|}{\xi}\right), \tag{3.41}$$

we have

$$\begin{aligned}\frac{1}{N}\sqrt{\left\langle\left(\sum O^z(k)\right)^2\right\rangle_{\rm g}} &= \frac{1}{N}\sqrt{\sum_{k,l}\langle G^z(k-l)\rangle_{\rm g}} \\ &\simeq \sqrt{\langle O^z\rangle_{\rm g}^2 + \frac{2c\xi}{N}} \longrightarrow \langle O^z\rangle_{\rm g} \qquad \text{as} \quad N\to\infty. \end{aligned}\tag{3.42}$$

The result for $J_{\rm F} = 5$ is shown in Fig. 3.4. The phase transitions may take place at $\lambda = \lambda_{\rm c1} \sim -0.3$ and at $\lambda = \lambda_{\rm c2} \sim 1.6$.

We have found the convergence

$$\sqrt{\langle O^2 \rangle} \propto \frac{1}{\sqrt{N}} \to 0 \qquad \text{as} \quad N \to \infty \tag{3.43}$$

at $\lambda = -0.5$ for the string order parameter, and at $\lambda = 1.4$ for the Néel order parameter. This asymptotic behavior means that the system is disordered there.

For a more precise determination of the location of the critical points, we have to analyze the data in terms of the finite-size scaling theory, which will be reported elsewhere.

3.5 Discussions

We compare the present method with the finite-temperature algorithm due to the Suzuki-Trotter transformation [Suzuki 76b, Suzuki 77b]. In the latter approach the convergence to the ground state in the limit $\beta \to \infty$ is achieved when $\beta \gg \Delta E$. If the trial function chosen in the present approach is orthogonal to the first excited state, we can extract the ground state using (3.1) with a smaller value of β. We can thereby attain the convergence of the limit $n \to \infty$ even for small Trotter numbers. This leads to the suppression of statistical errors. This difference of the convergence for $\beta \to \infty$ may be more effective near phase boundaries, where the energy gap tends to be closed.

In the present case we actually observed improvements in the convergence for $\beta \to \infty$ both in the Haldane phase and in the Néel phase. In Fig. 3.5 we show the β-dependence of the string order parameter for $\lambda = 0$ (a), and the Néel order parameter for $\lambda = 2.0$ (b) at $J_{\mathrm{F}} = 5$. In each case our model is located near one of the phase boundaries. Employing the trial functions (3.9) and (3.40), we achieved clear improvements in the convergence.

Moreover, the present approach combined with the finite-temperature algorithm can be used for confirmation of the convergence for $\beta \to \infty$. We note that the lower bounds of the order parameters in the ground state are given by the finite-temperature algorithm, while the upper bounds are given by the present ground-state algorithm; see Fig. 3.5. The order parameter usually grows monotonically as the temperature is lowered. On the other hand, starting from a trial vector with an artificially strong order, we approach the final estimate from above.

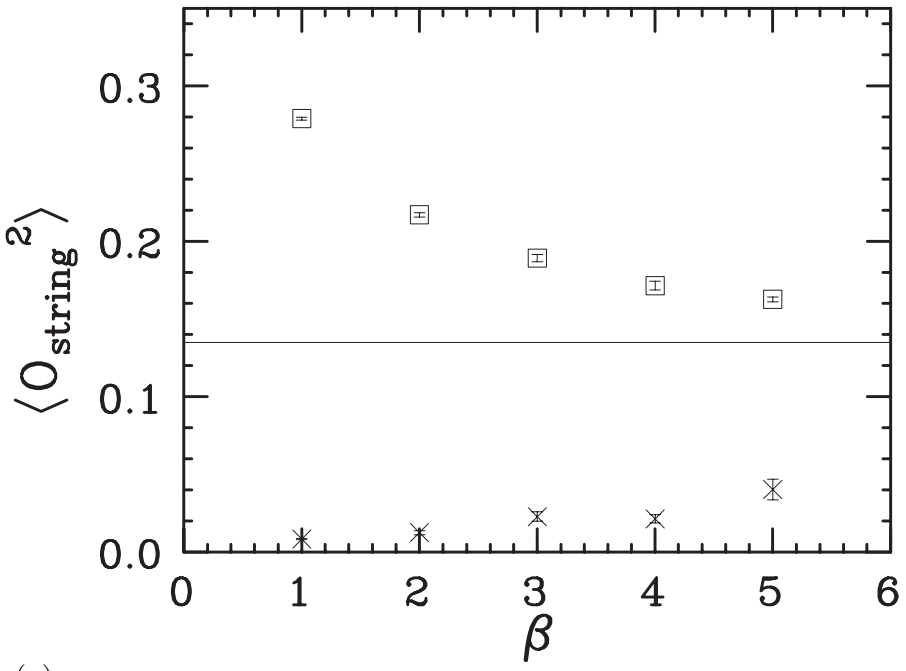

(a)

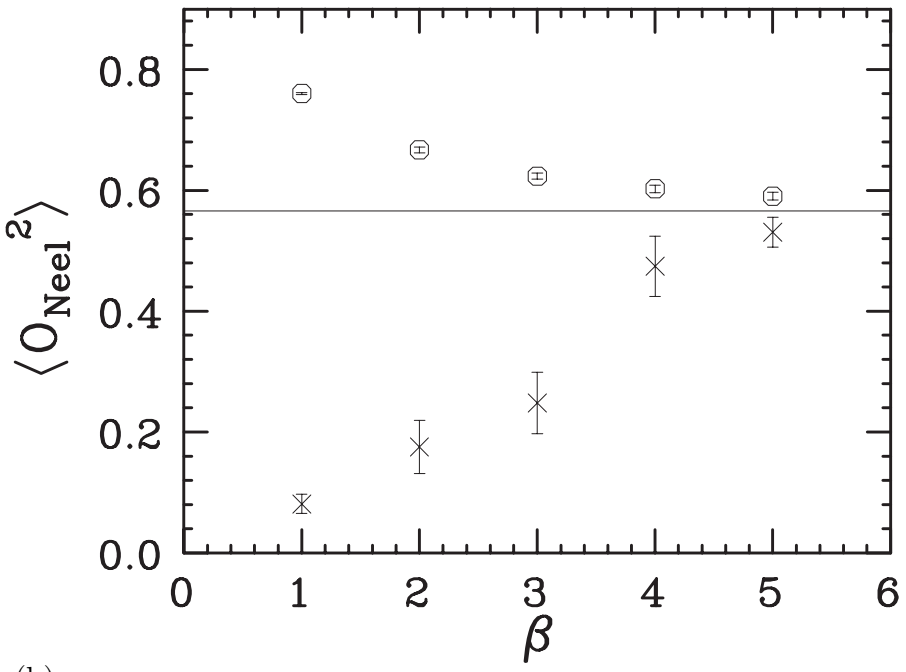

(b)

Figure 3.5 β-dependence of the order parameters at $J_{\rm F} = 5$: (a) The string order parameter at $\lambda = 0$ from the simulation using (3.9) ($\boxplus$) and from the simulation using the finite-temperature algorithm ($\times$). We fixed $\beta/n = 0.2$. (b) The Néel order parameter at $\lambda = 2.0$ by the simulation with (3.40) ($\bigcirc$) and by the simulation with the finite-temperature algorithm ($\times$). We fixed $\beta/n = 0.1$. The solid line in each figure indicates the final estimate.

Chapter 4

Negative-Sign Problem and the Reweighting Method[‡]

The deteriorated statistics, or the negative-sign problem, appearing in quantum Monte Carlo simulations is discussed. The origin of the negative-sign problem is described. It is proposed to apply the reweighting method to the quantum Monte Carlo simulations in order to circumvent the negative-sign problem. An argument on estimation of the statistical error is given.

4.1 Introduction

Since Toulouse proposed the idea of the "frustration" [Toulouse 77], many researchers have been interested in the problem to study how the frustration destroys a long-range order. The effect of the frustration may appear most prominently in quantum systems at low temperatures, where quantum fluctuation also affects physical properties of the relevant system strongly.

The J_1-J_2 model, for example, has been studied extensively in the context of investigation of the high-T_c superconductivity. The Hamiltonian of the model is given by

$$\mathcal{H} \equiv J_1 \sum_{\text{n.n.}} \boldsymbol{\sigma}_i \cdot \boldsymbol{\sigma}_j + J_2 \sum_{\text{n.n.n.}} \boldsymbol{\sigma}_i \cdot \boldsymbol{\sigma}_j, \tag{4.1}$$

where the operators $\boldsymbol{\sigma}_i$ denote the Pauli matrices. Here the first summation runs over the nearest-neighbor pairs on a square lattice, while the second summation runs over the next-nearest-neighbor pairs on the lattice; see Fig. 4.1. The coupling constants are defined to be positive; hence there is a frustration on every triangle (x, y)-$(x \pm 1, y)$-$(x, y \pm 1)$. Hereafter we use the notation

$$\alpha \equiv \frac{J_2}{J_1}. \tag{4.2}$$

The connection between the J_1-J_2 model and the high-T_c superconductors is explained as follows. Materials exhibiting the high-T_c superconductivity may be approximated by the Hubbard model on the square lattice. In the strong-coupling limit of the half-filled Hubbard model, we have the antiferromagnetic Heisenberg model on the square lattice

[‡]A part of this chapter was published in [Hatano 92].

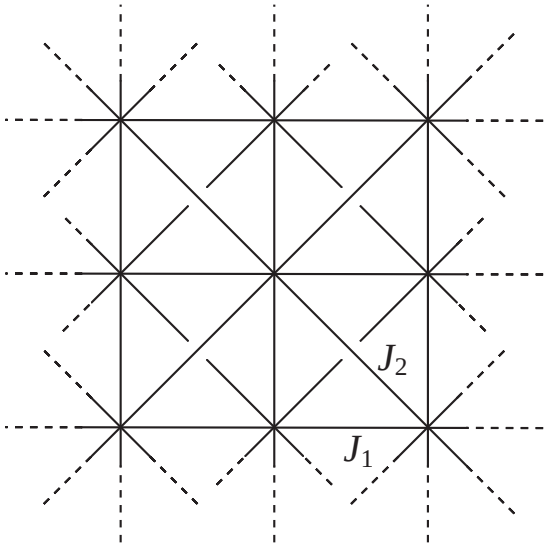

Figure 4.1 The J_1-J_2 model.

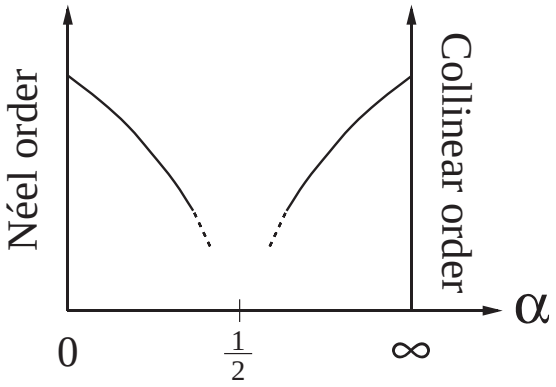

Figure 4.2 The Néel order persists when $\alpha \ll 1$, and the collinear order does when $\alpha \gg 1$. The existence of any order in the intermediate strongly-frustrated region, $\alpha \simeq 0.5$, is not known.

[Cleveland 76]: that is, the model (4.1) with $J_2 = 0$. Though the absence of the Néel order of the model at finite temperatures was proved [Mermin 66, Ruelle 69, Griffiths 72], the ground state is considered to have the Néel order, or to be an insulator; see for a review [Manousakis 91]. It may be necessary for appearance of a superconducting phase to destroy the insulating Néel order. Hence we introduce frustrations into the model, which yields the J_1-J_2 model, (4.1).

The main interest here is the question whether the Néel order persists or not in the strongly frustrated region, $\alpha \equiv J_2/J_1 \simeq 0.5$ [Chandra 88, Hirsch 89b, Wen 89, Dagotto 89a, Figueirido 89, Gelfand 89, Dagotto 89b, Sano 91, Oguchi 90, Nishimori 90, Xu 90, Mila 91]; see Fig. 4.2. When the system is weakly frustrated ($\alpha \ll 1$), many studies suggest that the Néel order is weakened and yet exists. When the next-nearest-neighbor coupling dominates the system ($\alpha \gg 1$), the system approximately breaks up into two square lattices penetrating each other. We may have the Néel order on each lattice, which is called the collinear phase. A disordered ground state may appear between the Néel phase and the collinear phase.

Another interesting example of the frustrated quantum systems is the triangular

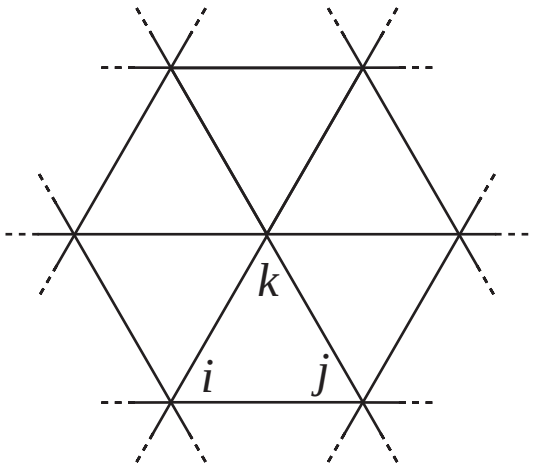

Figure 4.3 The triangular antiferromagnet. The chiral order parameter, (4.3), is defined on a triangle i-j-k.

antiferromagnet. The Hamiltonian,

$$\mathcal{H} \equiv \sum_{\langle i,j \rangle} \left[J_{xy} \left(\sigma_i^x \sigma_j^x + \sigma_i^y \sigma_j^y \right) + J_z \sigma_i^z \sigma_j^z \right], \tag{4.3}$$

is now defined on a triangular lattice; see Fig. 4.3. Providing $J_{xy}, J_z > 0$, we have frustration on every triangle.

For the classical model, there may be a phase transition with respect to the chiral order parameter [Villain 77a, Villain 77b, Villain 77c, Teitel 83, Miyashita 84, Lee 84a, Lee 86, Miyashita 86, Kawashima 89],

$$O^z_{\text{chiral}} \equiv \frac{1}{2\sqrt{3}} \sum_{\triangle} \left(\boldsymbol{\sigma}_i \times \boldsymbol{\sigma}_j + \boldsymbol{\sigma}_j \times \boldsymbol{\sigma}_k + \boldsymbol{\sigma}_k \times \boldsymbol{\sigma}_i \right)_z . \tag{4.4}$$

Here the summation runs over all the upright triangles of the lattice. The set of the subscripts i, j and k denotes three sites which surround the triangle i-j-k anticlockwise as is shown in Fig. 4.3. Below a temperature the inversion symmetry

$$O^z_{\text{chiral}} \longleftrightarrow -O^z_{\text{chiral}} \tag{4.5}$$

may break spontaneously. (In two dimensions, continuous symmetries do not break spontaneously at finite temperatures; however, a discrete symmetry can break.)

The problem here is whether the chiral order persists for the quantum system. Numerical calculations and analytic arguments suggest the existence of the transition around the XY-model region, $J_z \simeq 0$ [Fujiki 86, Fujiki 87a, Fujiki 87b, Nishimori 88, Matsubara 88, Fujiki 91, Momoi 92a, Momoi 92b, Masui 92].

As regards numerical studies on quantum systems, the approximate transformation from a d-dimensional quantum system to a $(d+1)$-dimensional classical system via the Suzuki-Trotter formula [Trotter 59, Suzuki 76a, Suzuki 77c],

$$\mathrm{e}^{-\beta\mathcal{H}} = \lim_{n\to\infty} \left(\mathrm{e}^{-\beta\mathcal{H}_1/n} \mathrm{e}^{-\beta\mathcal{H}_2/n} \right)^n \qquad \text{with} \quad \mathcal{H} = \mathcal{H}_1 + \mathcal{H}_2, \tag{4.6}$$

is now employed frequently. In the world-line approach of the method [Suzuki 76b, Suzuki 77b], the partition function of the quantum system described by the Hamiltonian

$\mathcal{H}$ is transformed into the following form:

$$\begin{aligned} Z_{\rm q} &\equiv \sum_{\{\sigma\}_1} \langle \{\sigma\}_1 | \, {\rm e}^{-\beta\mathcal{H}} \, | \{\sigma\}_1 \rangle \\ &= \lim_{n\to\infty} \sum_{\{\sigma\}} \langle \{\sigma\}_1 | \, {\rm e}^{-\beta\mathcal{H}_1/n} \, | \{\sigma\}_2 \rangle \, \langle \{\sigma\}_2 | \, {\rm e}^{-\beta\mathcal{H}_2/n} \, | \{\sigma\}_3 \rangle \times \cdots \\ &\qquad \cdots \times \langle \{\sigma\}_{2n} | \, {\rm e}^{-\beta\mathcal{H}_2/n} \, | \{\sigma\}_1 \rangle \equiv \lim_{n\to\infty} \sum_{\{\sigma\}} W\{\sigma\}. \end{aligned} \tag{4.7}$$

Here each $\{|\{\sigma\}_i\rangle\}$ denotes a complete set of representation basis states. Now the approximate Boltzmann weight W is a product of local Boltzmann factors; for example, the product of the factor

$$w(\sigma_1, \sigma_2, \sigma_3, \sigma_4) \equiv \langle \sigma_1, \sigma_2 | \, {\rm e}^{-\beta\mathcal{H}_{ij}/n} \, | \sigma_3, \sigma_4 \rangle \, , \tag{4.8}$$

where $\mathcal{H}_{ij}$ denotes a local two-site Hamiltonian. Hence a suitable stochastic process for a Monte Carlo simulation can be constructed in the extended phase space

$$\{\sigma\} \equiv \{\{\sigma\}_1, \{\sigma\}_2, \cdots, \{\sigma\}_{2n}\} \, . \tag{4.9}$$

Unfortunately, the method is not applicable to the frustrated spin systems at low temperatures because of the negative-sign problem. In the case of frustrated spin systems, the Boltzmann weight becomes negative for some states. (If there are no frustrations, though the local weights (4.8) may be negative, the whole product of them is always positive. In this case we are free from the negative-sign problem.) We cannot carry out a Monte Carlo simulation of the system as it is. The Boltzmann weight of a state is interpreted as the probability of appearance of the state in the course of the simulation, and the probability must be positive. A prescription used so far to circumvent the difficulty results in deteriorated statistics at low temperatures.

Here we propose a method of easing the negative-sign problem. First, we describe the origin of the negative-sign problem in Section 4.2. We present an argument on exact estimation of a statistical error. In Appendix 4.A and Appendix 4.B we show examples of applications of the argument of Section 4.2. In Section 4.3 we propose application of the reweighting method to the quantum Monte Carlo simulation, in order to overcome the negative-sign problem.

4.2 Negative-sign problem

In this section we describe the origin of the negative-sign problem. An argument on estimation of the statistical error is given. Examples of application of the present argument are given in Appendix 4.A and Appendix 4.B.

The estimation of the statistical error is important because of the following reason. It has been known by experience that the negative-sign problem depends on the quantization axis of spins, or the spin representation [Loh 85b]. The spin representation which eases the negative-sign problem may be related to the ground-state spin-configuration of the models. A trivial example is that, if one makes use of the eigenstates of the models, the Boltzmann weight is always positive. From both the physical and practical point

of view, optimization of the spin representation is an interesting subject. Studies on the optimization, however, has not been done extensively. One of the reasons of this reservation may be lack of methods by which one can discuss exactly the dependence of the negative-sign problem on the spin representation. The growth rate of the statistical error for a specific spin representation has been obtained only after massive Monte Carlo calculations, which may result in waste of CPU time! We want to estimate the statistical error before massive simulations; this is our motivation here. By the argument described below, one can estimate it performing exact diagonalization of small systems. The argument can be used for preliminary trial of a quantum Monte Carlo algorithm.

As is shown in the previous section, when we apply the Suzuki-Trotter transformation to the frustrated spin systems, we have a classical system whose Boltzmann weight may be negative:

$$Z_n \equiv \sum_{\{\sigma\}} W\{\sigma\} \tag{4.10}$$

where $W\{\sigma\} < 0$ for some configurations $\{\sigma\}$.

The naive solution of the negative-sign problem is to use the following identity [Hirsch 82, Takasu 86] for measurement of a quantity Q:

$$\langle Q \rangle_n = \frac{\sum QW}{\sum W} = \frac{\sum QRW'}{\sum RW'} = \frac{\sum QRW'}{\sum W'} \Big/ \frac{\sum RW'}{\sum W'}. \tag{4.11}$$

Here we have prepared another classical system whose Boltzmann weight is the absolute value of the classical system (4.10):

$$Z'_n \equiv \sum_{\{\sigma\}} W'\{\sigma\} \tag{4.12}$$

with

$$W'\{\sigma\} \equiv |W\{\sigma\}|\,. \tag{4.13}$$

The symbol R in (4.11) stands for the sign of W, namely

$$R\{\sigma\} \equiv \mathrm{sign}(W\{\sigma\}). \tag{4.14}$$

Hereafter we refer to the system (4.12) as the "positive-weight" system.

The quantity Q, (4.11), is thereby measured in simulations of the system defined by the new Boltzmann weight W':

$$\langle Q \rangle_n = \frac{\langle QR \rangle'_{\mathrm{MCS}}}{\langle R \rangle'_{\mathrm{MCS}}}. \tag{4.15}$$

where $\langle \cdots \rangle'_{\mathrm{MCS}}$ stands for Monte Carlo average in simulations of the system W'. The denominator of (4.15),

$$\langle R \rangle'_{\mathrm{MCS}} = \frac{\sum RW'}{\sum W'} = \frac{\sum W}{\sum W'} = \frac{Z_n}{Z'_n}. \tag{4.16}$$

is often called the negative-sign ratio.

The first part of the negative-sign problem is thereby solved. Nevertheless this solution is exactly the point from which the second part of the problem comes; a statistical error of the negative-sign ratio grows rapidly at low temperatures or for large systems.

The fact is understood as follows. The numerator of (4.16) is, in the limit $n \to \infty$, the partition function of the quantum system, $Z_{\rm q}$. For the time being, we assume that the denominator of (4.16), Z'_n, converges to the partition function of another quantum system, $Z'_{\rm q}$. This assumption is confirmed later. We have

$$Z_{\rm q} = {\rm e}^{-\beta F} \qquad \text{and} \qquad Z'_{\rm q} = {\rm e}^{-\beta F'}, \tag{4.17}$$

where F (F') stands for the free energy of the system $Z_{\rm q}$ ($Z'_{\rm q}$). The negative-sign ratio is given by

$$\langle R \rangle'_{\rm MCS} = {\rm e}^{-\beta(F-F')} \qquad \text{as} \quad n \to \infty. \tag{4.18}$$

The value $\langle R \rangle'_{\rm MCS}$ is bounded to the above by unity, and therefore

$$F > F'. \tag{4.19}$$

First, at low temperatures we can replace F and F' by the ground-state energies $E_{\rm g}$ and $E'_{\rm g}$ of the systems $Z_{\rm q}$ and $Z'_{\rm q}$ respectively, and hence [Morgenstern 89, Loh 90, Hamann 90, Hatano 91b]

$$\langle R \rangle'_{\rm MCS} \simeq {\rm e}^{-\beta(E_{\rm g}-E'_{\rm g})} \qquad \text{as} \quad \beta \to \infty. \tag{4.20}$$

Second, assuming the extensivity of the free energy, we have [Hirsch 82]

$$\langle R \rangle'_{\rm MCS} \simeq {\rm e}^{-\beta(f-f')N} \qquad \text{as} \quad N \to \infty, \tag{4.21}$$

where N is the system size, and f (f') is the free-energy density of the system $Z_{\rm q}$ ($Z'_{\rm q}$).

The statistical error of the negative-sign ratio is given by [Muller-Krumbhaar 73]

$$\Delta \langle R \rangle'_{\rm MCS} = \sqrt{\frac{2\tau+1}{M}} \sqrt{\langle R^2 \rangle'_{\rm MCS} - \langle R \rangle'^{\,2}_{\rm MCS}} = \sqrt{\frac{2\tau+1}{M}} \sqrt{1 - \langle R \rangle'^{\,2}_{\rm MCS}}, \tag{4.22}$$

where τ denotes auto-correlation time of the simulation dynamics, and M denotes the number of Monte Carlo steps. The relative error of the negative-sign ratio behaves as

$$\frac{\Delta \langle R \rangle'_{\rm MCS}}{\langle R \rangle'_{\rm MCS}} = \sqrt{\frac{2\tau+1}{M}} \sqrt{\frac{1}{\langle R \rangle'^{\,2}_{\rm MCS}} - 1} = \sqrt{\frac{2\tau+1}{M}} \sqrt{\left(\frac{Z'_{\rm q}}{Z_{\rm q}}\right)^2 - 1} \tag{4.23}$$

$$\simeq \sqrt{\frac{2\tau+1}{M}} \times \begin{cases} {\rm e}^{\beta(E_{\rm g}-E'_{\rm g})} \gg 1 & \text{as} \quad \beta \to \infty, \\ {\rm e}^{\beta(f-f')N} \gg 1 & \text{as} \quad N \to \infty. \end{cases} \tag{4.24}$$

At low temperatures or for large systems, the statistical error grows rapidly, and hence we cannot precisely estimate the negative-sign ratio and physical quantities (4.15) by Monte Carlo simulations.

The deteriorated statistics (4.24) can be roughly interpreted as follows [Morgenstern 89]; see Fig. 4.4. At low temperatures the canonical distribution of the quantum system in the Hilbert space has a sharp peak in the vicinity of the true ground state $\psi_{\rm g}$ (see Fig. 4.4). On the other hand, the importance sampling in actual simulations

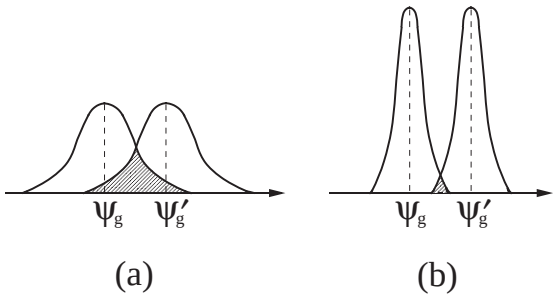

Figure 4.4 The distribution functions of states for $Z_{\rm q}$ and $Z'_{\rm q}$. The overlap between them (the shaded part) decreases rapidly, when the peaks of the distributions become sharp; compare (a) and (b).

is based on the positive-weight system $Z'_{\rm q}$. Configurations generated in the simulations follow the distribution which has a peak in the vicinity of the ground state $\psi'_{\rm g}$ of the positive-weight system. If the ground states $\psi_{\rm g}$ and $\psi'_{\rm g}$ are appreciably different from each other, the two canonical distributions scarcely overlap. Thus we count many configurations in vain. (The excess configurations are cancelled with each other in (4.16), owing to the sign R.) Effective number of configurations sampled in simulations may decreases exponentially, hence the deteriorated statistics.

The same argument can be made in the case of simulating a large system. As the system size increases, the peak width of the canonical distribution of the system decreases as $1/\sqrt{N}$ according to the central-limit theorem. The overlap between the canonical distributions of the original quantum system and the positive-weight system thereby decreases.

This interpretation of the origin of the negative-sign problem motivates us to find out the explicit form of the Hamiltonian $\mathcal{H}'$ of the positive-weight system $Z'_{\rm q}$. Making use of it, we can exactly estimate the growth rate of the statistical error of the negative-sign ratio in (4.23).

The form $\mathcal{H}'$ can be obtained as follows.

By definition, the positive-weight partition function is

$$Z'_{\rm q} = \lim_{n\to\infty} {\rm Tr} \left[T' \left(-\frac{\beta}{n} \right) \right]^n , \tag{4.25}$$

where T' is the transfer matrix defined by

$$\langle \{\sigma\}_1 | \, T' \, | \{\sigma\}_3 \rangle = \sum_{\{\sigma\}_2} \left| \langle \{\sigma\}_1 | \, {\rm e}^{-\beta \mathcal{H}_1/n} \, | \{\sigma\}_2 \rangle \right| \cdot \left| \langle \{\sigma\}_2 | \, {\rm e}^{-\beta \mathcal{H}_2/n} \, | \{\sigma\}_3 \rangle \right| . \tag{4.26}$$

Let us define the Hamiltonian $\mathcal{H}'$ as an expansion coefficient of the transfer matrix, i.e.,

$$T' \left(-\frac{\beta}{n} \right) = I - \frac{\beta}{n} \mathcal{H}' + O\left(\frac{\beta^2}{n^2} \right) , \tag{4.27}$$

where I denotes the identity matrix. Indeed, the definition of the exponential function

$${\rm e}^x \equiv \lim_{n\to\infty} \left(1 + \frac{x}{n} \right)^n \tag{4.28}$$

yields

$$Z'_{\rm q} = {\rm Tr} \, {\rm e}^{-\beta \mathcal{H}'} . \tag{4.29}$$

The expansion of the original transfer matrices gives

$$\langle \{\sigma\}_1 | \, \mathrm{e}^{-\beta \mathcal{H}_i/n} \, | \{\sigma\}_2 \rangle = I - \frac{\beta}{n} \langle \{\sigma\}_1 | \, \mathcal{H}_i \, | \{\sigma\}_2 \rangle + O\left(\frac{\beta^2}{n^2}\right), \tag{4.30}$$

for $i = 1, 2$. On the other hand, we define partial Hamiltonians of the positive-weight system by the expansion of the matrices in the right-hand side of (4.26):

$$\left| \langle \{\sigma\}_1 | \, \mathrm{e}^{-\beta \mathcal{H}_i/n} \, | \{\sigma\}_2 \rangle \right| = I - \frac{\beta}{n} \langle \{\sigma\}_1 | \, \mathcal{H}'_i \, | \{\sigma\}_2 \rangle + O\left(\frac{\beta^2}{n^2}\right). \tag{4.31}$$

We compare (4.31) with (4.30) element by element. For a sufficiently large n, all the diagonal elements of (4.30) are positive owing to the leading unity. Therefore each diagonal element of (4.31) equals to that of (4.30). This yields, in the first order of β/n

$$\langle \{\sigma\}_1 | \, \mathcal{H}'_i \, | \{\sigma\}_1 \rangle \equiv \langle \{\sigma\}_1 | \, \mathcal{H}_i \, | \{\sigma\}_1 \rangle \, . \tag{4.32}$$

On the other hand, some of the off-diagonal elements may be negative, because of the leading term $\langle \{\sigma\}_1 | \, \mathcal{H}'_i \, | \{\sigma\}_2 \rangle$. In the first order of β/n, taking the absolute value of the off-diagonal elements leads to

$$\langle \{\sigma\}_1 | \, \mathcal{H}'_i \, | \{\sigma\}_2 \rangle \equiv \left| \langle \{\sigma\}_1 | \, \mathcal{H}_i \, | \{\sigma\}_2 \rangle \right| \qquad \text{for} \quad \{\sigma\}_1 \neq \{\sigma\}_2. \tag{4.33}$$

Finally, we obtain the positive-weight Hamiltonian $\mathcal{H}'$ with

$$\langle \{\sigma\}_1 | \, \mathcal{H}' \, | \{\sigma\}_2 \rangle \equiv \langle \{\sigma\}_1 | \, \mathcal{H}'_1 \, | \{\sigma\}_2 \rangle + \langle \{\sigma\}_1 | \, \mathcal{H}'_2 \, | \{\sigma\}_2 \rangle \, . \tag{4.34}$$

Now that we know the explicit expressions of $\mathcal{H}$ and $\mathcal{H}'$, we can calculate the partition functions Z_{q} and Z'_{q} at least for small systems, and estimate the statistical (4.23) *before* we perform Monte Carlo simulations.

We give, in Appendices 4.A and 4.B, examples of the application of the present argument. In Appendix 4.A we discuss the negative-sign problem of the fractal decomposition. In Appendix 4.B we discuss the dependence of the negative-sign problem on the spin representation.

Incidentally, we point out that, as for usual cell-decompositions [Suzuki 87b, Takasu 86 Nakamura 92a, Nakamura 92b], the above discussion does not depend even quantitatively on ways of setting up unit cells. If we enlarge the unit cell, the behavior in the limit $n \to \infty$,(4.24), does not change.

Finally, the discussion here cannot be applied directly to the negative-sign problem in the auxiliary-field algorithm [Hirsch 83c, Hirsch 85a]. It may be a challenging problem to find out a method of estimating dependence of the negative-sign problem on the way of the Stratonovich-Hubbard decoupling [Batrouni 90].

4.3 Reweighting method

In this section we propose an application of the reweighting method to the quantum Monte Carlo simulations in order to circumvent the negative-sign problem.

In the previous section we have observed that the negative-sign problem comes from the difference between the original Hamiltonian $\mathcal{H}$ and the positive-weight Hamiltonian $\mathcal{H}'$. This situation is against the spirit of the importance sampling. In the importance-sampling method we efficiently sample configurations whose Boltzmann weights are large. In the method (4.12)-(4.16), however, we sample many configurations in vain.

We notice that the choice of the positive-weight system, (4.13), is not necessary for the formulae (4.11)-(4.16) to hold. The formulae hold for any set of Boltzmann weight $\{W'\}$ if we change the definition of the negative-sign ratio from (4.14) to the form

$$R\{\sigma\} \equiv \frac{W\{\sigma\}}{W'\{\sigma\}}. \tag{4.35}$$

Hence we can define another positive-weight Hamiltonian $\mathcal{H}'$. The Boltzmann weight W' is obtained through the Suzuki-Trotter transformation, (4.6)-(4.8):

$$Z'_{\rm q} = \mathrm{Tr}\, \mathrm{e}^{-\beta'\mathcal{H}'} = \lim_{n\to\infty} \sum_{\{\sigma\}} W'. \tag{4.36}$$

(It is possible to choose β' different from β.) We may ease the negative-sign problem by preparing a positive-weight system more similar to the original system [Nakamura 92a, Nakamura 92b].

The formulae (4.11)-(4.16) have been used in Monte Carlo simulations of classical systems as the "reweighting method". The method was proposed at first for evaluation of the free energy [Salsburg 59, Valleau 72, Torrie 74]. Recently the method is re-proposed for studies on phase transitions, under the name of the "histogram method" [Ferrenberg 88, Ferrenberg 89, Hu 92]. The histogram method has been successfully applied to the Ising model [Ferrenberg 91] and to the random Potts model [Chen 92]. The validity of the method is examined in [Munger 91].

The conditions which the positive-weight system $\mathcal{H}'$ should satisfy are given as follows: (i) The Boltzmann weight W' resulting from $\mathcal{H}'$ is always positive. (ii) The ground state of the positive-weight Hamiltonian is similar to the expected ground state of the original Hamiltonian; for example, the positive-weight system has the same order as the one the original system has. (iii) To put the condition (ii) more practically, the statistical error of the negative-sign ratio is small.

Let us describe an example. We consider the J_1-J_2 model, (4.1). In the region $J_2 \ll J_1$, we expect that the Néel order insists. When we apply the prescription (4.10)-(4.14), the positive-weight system $\mathcal{H}'$ turns out to be described by

$$\mathcal{H}'_{\rm abs} = J_1 \sum_{\langle i,j\rangle} \boldsymbol{\sigma}_i \cdot \boldsymbol{\sigma}_j + J_2 \sum\nolimits'_{\langle i,j\rangle} \left(-\sigma_i^x\sigma_j^x - \sigma_i^y\sigma_j^y + \sigma_i^z\sigma_j^z\right), \tag{4.37}$$

according to the argument (4.25)-(4.34). The ferromagnetic off-diagonal interaction of the second term of (4.37) may destroy the expected Néel order too strongly. Then the ground state of the positive-weight Hamiltonian (4.37) may differ from the true ground state so much that we have the deteriorated statistics.

We can define a positive-weight Hamiltonian for the reweighting method which satisfies the conditions (i) and (ii) above, in the form [Nakamura 92a, Nakamura 92b],

$$\mathcal{H}'_{\rm rwt} \equiv J_1 \sum_{\langle i,j\rangle} \boldsymbol{\sigma}_i \cdot \boldsymbol{\sigma}_j + J_2 \sum\nolimits'_{\langle i,j\rangle} \sigma_i^z\sigma_j^z. \tag{4.38}$$

Because of the absence of the antiferromagnetic off-diagonal interaction of the second term, the Boltzmann weight W' resulting from (4.38) is always positive; hence the condition (i) is satisfied.

Concerning the condition (ii), we can expect that the Néel order insists for the Hamiltonian $\mathcal{H}'_{\rm rwt}$ more strongly than for $\mathcal{H}'_{\rm abs}$. Though we cannot solve the negative-sign problem completely by employing $\mathcal{H}'_{\rm rwt}$, we may reach a lower temperature using $\mathcal{H}'_{\rm rwt}$ than using $\mathcal{H}'_{\rm abs}$. When the collinear order is expected to exist (for $\alpha \gg 1$), we should define another positive-weight Hamiltonian which induces the collinear order.

In order to confirm that the Hamiltonian (4.38) satisfies the condition (iii), we need to estimate the statistical error of the negative-sign ratio which appears in the reweighting method. The estimation can be made in a way similar to (4.22)-(4.23), which we describe in the following.

The formula (4.23) should be modified to

$$\frac{\Delta \langle R \rangle'_{\rm MCS}}{\langle R \rangle'_{\rm MCS}} = \sqrt{\frac{2\tau+1}{M}} \sqrt{\frac{\left\langle R^2 \right\rangle'_{\rm MCS}}{\langle R \rangle'^{\,2}_{\rm MCS}} - 1}. \tag{4.39}$$

Using the definition (4.35), we have

$$\frac{\left\langle R^2 \right\rangle'_{\rm MCS}}{\langle R \rangle'^{\,2}_{\rm MCS}} = \frac{\sum \left(\frac{W}{W'}\right)^2 W' \Big/ \sum W'}{\left(\sum \frac{W}{W'} W' \Big/ \sum W'\right)^2} = \frac{\sum W' \times \sum \frac{W^2}{W'}}{\left(\sum W\right)^2}. \tag{4.40}$$

The factors $\sum W$ and $\sum W'$ in the right-hand side of (4.40) are the partition functions Z_n and Z'_n respectively, which turn out to be $Z_{\rm q}$ and $Z'_{\rm q}$ in the limit $n \to \infty$.

Concerning the factor $\sum W^2/W'$, we can develop an argument similar to (4.25)-(4.34). Thus we have

$$\lim_{n\to\infty} \sum \frac{W^2}{W'} = Z''_{\rm q} = {\rm Tr}\, {\rm e}^{-\beta'' \mathcal{H}''}. \tag{4.41}$$

Here the new Hamiltonian $\mathcal{H}''$ is defined as follows. The diagonal elements of $\mathcal{H}''$ is given by

$$\langle \{\sigma\}_1 | \left(-\beta'' \mathcal{H}''\right) | \{\sigma\}_1 \rangle = \langle \{\sigma\}_1 | \left(-2\beta \mathcal{H} + \beta' \mathcal{H}'\right) | \{\sigma\}_1 \rangle , \tag{4.42}$$

while the off-diagonal elements is defined by

$$\langle \{\sigma\}_1 | \left(-\beta'' \mathcal{H}''\right) | \{\sigma\}_2 \rangle = \frac{\left[\langle \{\sigma\}_1 | \left(-\beta \mathcal{H}\right) | \{\sigma\}_2 \rangle\right]^2}{\langle \{\sigma\}_1 | \left(-\beta' \mathcal{H}'\right) | \{\sigma\}_2 \rangle} \qquad \text{for} \quad \{\sigma\}_1 \neq \{\sigma\}_2, \tag{4.43}$$

provided $\langle \{\sigma\}_1 | \left(-\beta' \mathcal{H}'\right) | \{\sigma\}_2 \rangle \neq 0$.

Finally we obtain

$$\frac{\left\langle R^2 \right\rangle'_{\rm MCS}}{\langle R \rangle'^{\,2}_{\rm MCS}} \simeq \frac{Z'_{\rm q} Z''_{\rm q}}{Z_{\rm q}^2} \qquad \text{as} \quad n \to \infty, \tag{4.44}$$

and hence

$$\frac{\Delta \langle R \rangle'_{\rm MCS}}{\langle R \rangle'_{\rm MCS}} \simeq \sqrt{\frac{2\tau+1}{M}} \sqrt{\frac{Z'_{\rm q} Z''_{\rm q}}{Z_{\rm q}^2} - 1}. \tag{4.45}$$

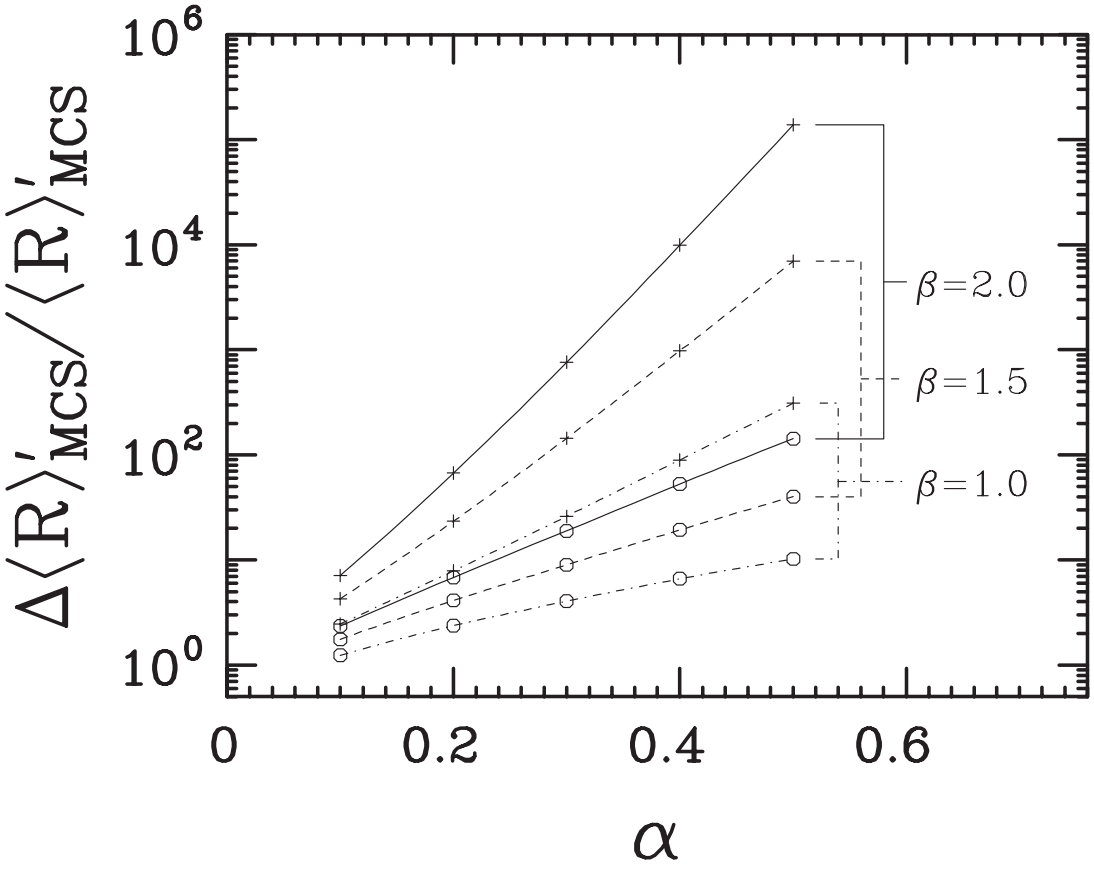

Figure 4.5 The error estimate (4.45) except the prefactor $\sqrt{(2\tau+1)/M}$ in the case of the usage of $\mathcal{H}'_{\rm rwt}$ (◯). We compare it with (4.23) for $\mathcal{H}'_{\rm abs}$ (+). The temperature is defined as $\beta = 1.0$ (– · –), $\beta = 1.5$ (– – –) and $\beta = 2.0$ (——).

We applied the formula (4.45) to the J_1-J_2 model, (4.1), coupled with the positive-weight Hamiltonian (4.38). We diagonalized the Hamiltonians $\mathcal{H}$, $\mathcal{H}'_{\rm rwt}$ and $\mathcal{H}''$ of size 3×3, and obtained the error estimate (4.45) except the prefactor $\sqrt{(2\tau+1)/M}$. The result is shown in Fig. 4.5. (For simplicity we confine ourselves to the case $\beta = \beta'$, that is, the temperature of the positive-weight system equals to that of the original system.) We also calculate the error estimate (4.23) using the Hamiltonian $\mathcal{H}'_{\rm abs}$, (4.37), and compared it with the error estimate (4.45).

Near $\alpha \sim 0.5$ we observe a great improvement of the error. The error estimate of (4.45) for $\mathcal{H}'_{\rm rwt}$ is about 10^3 times smaller than that of (4.23) for $\mathcal{H}'_{\rm abs}$ at the temperature $T = 1/\beta = 0.5$.

Note that we did not estimate the auto-correlation time τ in the prefactors of (4.23) and (4.45). The correlation time for $\mathcal{H}'_{\rm rwt}$ is indeed greater than that for $\mathcal{H}'_{\rm abs}$. This is caused by the absence of the off-diagonal interaction in (4.14); appearance of some of the world-line configurations is suppressed. This slow dynamics is a problem accompanying the present reweighting method. We might solve the problem by employing some cluster spin-flip dynamics.

The present method has been successfully applied to the J_1-J_2 model [Nakamura 92a, Nakamura 92b, Nakamura 92c]; see Fig. 4.6.

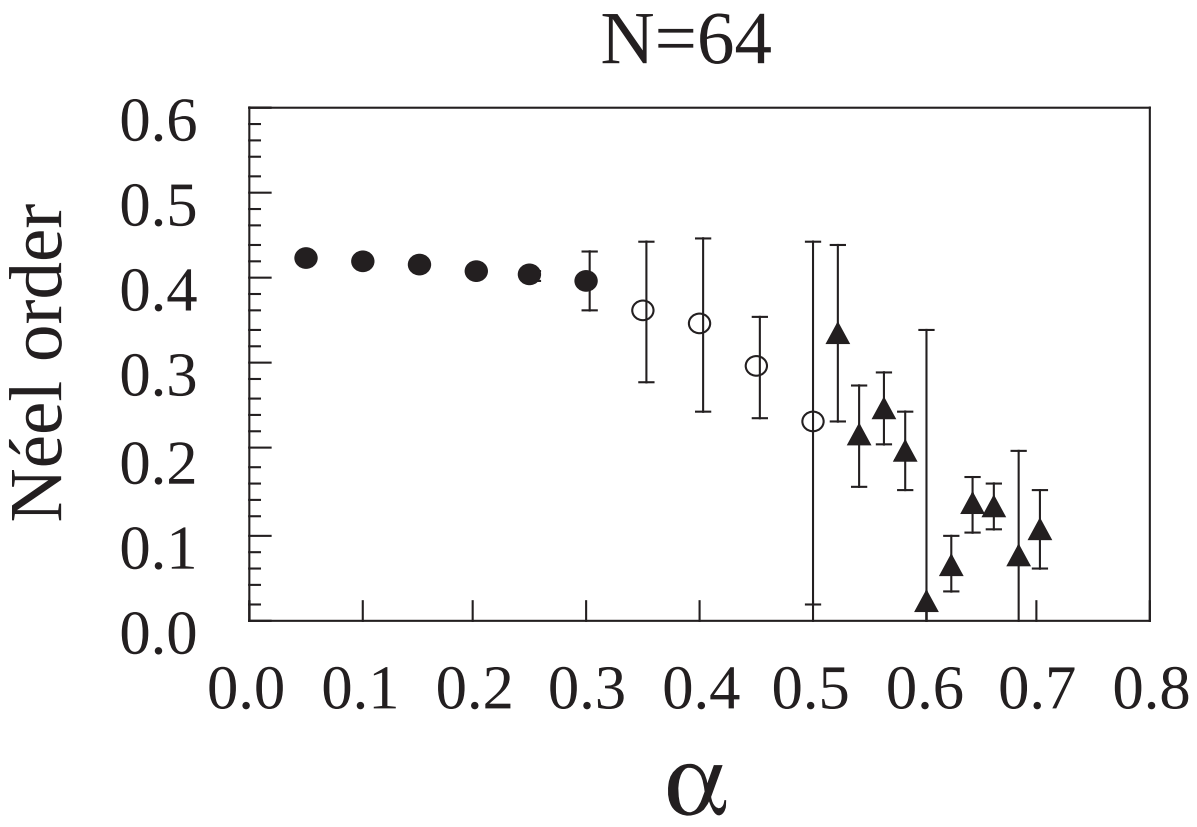

Figure 4.6 The Néel order parameter estimated for the 8×8 system by the reweighting quantum Monte Carlo simulation. (From [Nakamura 92c].)

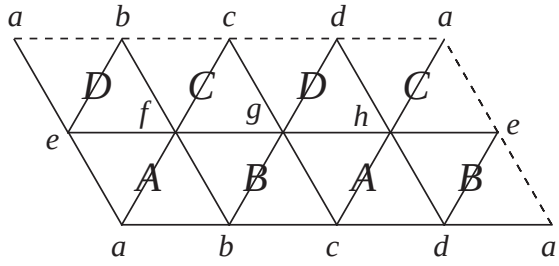

Figure 4.7 We treat the XXZ model on a triangular lattice of size 4×2. We decompose the system into four parts, as is described in (4.46).

4.4 Summary

In this chapter we have discussed on the negative-sign problem. We have presented the argument on the exact estimation of the statistical error of the negative-sign ratio. Based on the discussion, we have proposed the application of the reweighting method to the quantum Monte Carlo simulations to circumvent the negative-sign problem. We would like to stress that we have pointed out the possibility of choosing the positive-weight system different from (4.13). Indeed the method may not necessarily always work; however, the optimization of the positive-weight system becomes possible.

4.A Fractal decompositions and the negative-sign problem§

In the present appendix we describe an example of the application of the argument given in Section 4.2. We conclude that Monte Carlo simulations by the fractal decomposition are critical at low temperatures because of the negative-sign problem.

The calculations in the present appendix were performed for the spin 1/2 antiferromagnetic XXZ model on the triangular lattice, (4.3), of size 4×2 with periodic boundary conditions, as illustrated in Fig. 4.7. Hereafter the following three cases of the parameters J_{xy} and J_z are examined; namely the Ising-like case ($J_{xy} = 1/4$, $J_z = 1$), the isotropic Heisenberg case ($J_{xy} = J_z = 1$), and the XY-like case ($J_{xy} = 1$, $J_z = 1/4$).

To apply the Suzuki-Trotter decomposition to the density matrix $\exp(-\beta\mathcal{H})$, the total Hamiltonian is decomposed into the following four parts [Takasu 86]:

$$\mathcal{H} = \mathcal{H}_A + \mathcal{H}_B + \mathcal{H}_C + \mathcal{H}_D, \tag{4.46}$$

as illustrated in Fig. 4.7.

We compare the following two kinds of the Suzuki-Trotter decomposition with each other. (a) the second-order decomposition [Suzuki 85d, Fye 86],

$$\mathrm{e}^{-\beta\mathcal{H}} = \left[S_2\left(-\frac{\beta}{n}\right)\right]^n + O\left(\frac{\beta^3}{n^2}\right), \tag{4.47}$$

where

$$S_2(x) \equiv \mathrm{e}^{x\mathcal{H}_A/2}\mathrm{e}^{x\mathcal{H}_B/2}\mathrm{e}^{x\mathcal{H}_C/2}\mathrm{e}^{x\mathcal{H}_D}\mathrm{e}^{x\mathcal{H}_C/2}\mathrm{e}^{x\mathcal{H}_B/2}\mathrm{e}^{x\mathcal{H}_A/2} = \mathrm{e}^{x\mathcal{H}} + O(x^3), \tag{4.48}$$

§The content of this section was published in [Hatano 91b].

and (b) the fourth-order decomposition [Suzuki 90, Suzuki 91]

$$\mathrm{e}^{-\beta\mathcal{H}} = \left[S_4\left(-\frac{\beta}{n}\right)\right]^n + O\left(\frac{\beta^5}{n^4}\right), \tag{4.49}$$

where

$$S_4(x) \equiv S_2(p_2 x)S_2(p_2 x)S_2((1-4p_2)x)S_2(p_2 x)S_2(p_2 x) = \mathrm{e}^{x\mathcal{H}} + O(x^5), \tag{4.50}$$

with

$$4p_2^3 + (1-4p_2)^3 = 0, \quad \text{or} \quad p_2 = (4-\sqrt[3]{4})^{-1} \simeq 0.41449\cdots. \tag{4.51}$$

The parameter p_2 is chosen to cancel out the third-order corrections of the product of the five operators S_2 in (4.50). The fourth-order correction proves to vanish automatically [Suzuki 90, Suzuki 91]. Note that the propagator $S_4(-\beta)$ yield a *to-and-fro* path in the direction of the imaginary time $\tau = 0 \to \beta$, owing to the part $(1-4p_2) < 0$ in (4.50).

Following the procedure (4.7), we have

$$Z_{\mathrm{q}} \simeq Z_2(\beta) = \mathrm{Tr}\,\left[S_2\left(-\frac{\beta}{n_2}\right)\right]^{n_2} = \sum_{\{\sigma\}} W_2(\{\sigma\}) \tag{4.52}$$

and

$$Z_{\mathrm{q}} \simeq Z_4(\beta) = \mathrm{Tr}\,\left[S_4\left(-\frac{\beta}{n_4}\right)\right]^{n_4} = \sum_{\{\sigma\}} W_4(\{\sigma\}). \tag{4.53}$$

For the present case, there do exist [Takasu 87] some configurations $\{\sigma\}$ whose weights $W(\{\sigma\})$ are negative. Furthermore for the fractal decomposition, it is essential [Suzuki 91] that negative temperatures appear at some interactions, e.g., we have the negative coefficient $(1-4p_4)\beta \simeq -0.658\beta < 0$ in the decomposition (4.50). Then negative Boltzmann weights appear even in non-frustrated systems, as well as in frustrated ones.

The positive-weight system is given by the transfer matrix

$$\begin{aligned}&\langle\{\sigma\}_1|S_2'(-\beta)|\{\sigma\}_7\rangle \\ &\quad\equiv \left|\left\langle\{\sigma\}_1|\mathrm{e}^{-\beta\mathcal{H}_A}|\{\sigma\}_2\right\rangle\right|\left|\left\langle\{\sigma\}_2|\mathrm{e}^{-\beta\mathcal{H}_B/2}|\{\sigma\}_3\right\rangle\right|\cdots\left|\left\langle\{\sigma\}_6|\mathrm{e}^{-\beta\mathcal{H}_B/2}|\{\sigma\}_7\right\rangle\right|.\end{aligned} \tag{4.54}$$

instead of (4.26). The operator (4.54) gives the partition function of the new system to be simulated in the following form:

$$Z_2'(\beta) \equiv \mathrm{Tr}\,\left[S_2'\left(-\frac{\beta}{n_2}\right)\right]^{n_2} = \sum_{\{\sigma\}} |W_2(\{\sigma\})|\,. \tag{4.55}$$

As for the fractal decomposition (4.50), the following operator should be used instead of (4.54):

$$S_4'(-\beta) \equiv S_2'(-p_2\beta)S_2'(-p_2\beta)S_2(-(1-4p_2)\beta)S_2'(-p_2\beta)S_2'(-p_2\beta). \tag{4.56}$$

Note that the part $S_2(-(1-4p_2)\beta)$ must be a non-prime-operator, because the coupling $(1-4p_2)J_{xy}$ turns ferromagnetic here owing to the inequality $(1-4p_2) < 0$. The partition function to be simulated is given by

$$Z_4'(\beta) \equiv \mathrm{Tr}\,\left[S_4'\left(-\frac{\beta}{n_4}\right)\right]^{n_4} = \sum_{\{\sigma\}} |W_4(\{\sigma\})|\,. \tag{4.57}$$

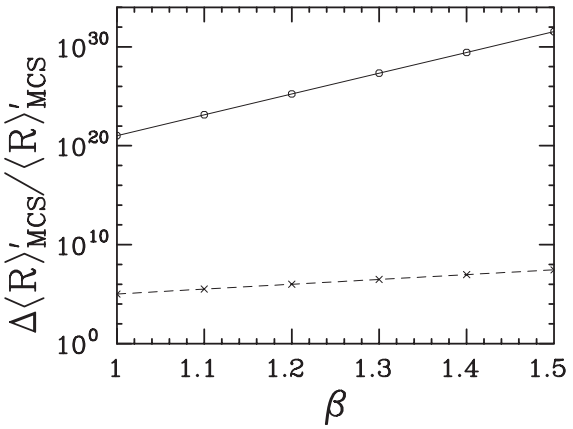

Figure 4.8 We calculated the error estimate (4.23) in the XY-like case, using the second-order decomposition, S_2, (– – –), and using the fourth-order decomposition, S_4, (——).

The systems $Z'_2(\beta)$ and $Z'_4(\beta)$ defined by (4.55) and (4.57) converge in the limit of $n \to \infty$ as follows:

$$Z_{\rm q2} = \lim_{n\to\infty} Z'_2(\beta) = {\rm Tr}\ {\rm e}^{-\beta\mathcal{H}'_2}, \quad \text{and} \quad Z_{\rm q4} = \lim_{n\to\infty} Z'_4(\beta) = {\rm Tr}\ {\rm e}^{-\beta\mathcal{H}'_4}. \tag{4.58}$$

The Hamiltonian $\mathcal{H}'_2$ is defined by the operator expansion of (4.27) of S'_2 in the following form:

$$S'_2\left(-\frac{\beta}{n}\right) = I - \frac{\beta}{n}\mathcal{H}'_2 + O\left(\frac{\beta^2}{n^2}\right), \tag{4.59}$$

with

$$\mathcal{H}'_2 \equiv \sum_{\langle i,j\rangle}\left[-J_{xy}(\sigma_i^x\sigma_j^x + \sigma_i^y\sigma_j^y) + J_z\sigma_i^z\sigma_j^z\right]. \tag{4.60}$$

The expansion of the operator $S'_4(-\frac{\beta}{n})$ defined by (4.56) gives the definition of $\mathcal{H}'_4$ as follows:

$$\begin{aligned} S'_4(-\frac{\beta}{n}) &= \left(I - p_2\frac{\beta}{n}\mathcal{H}'_2\right)^2\left(I - (1-4p_2)\frac{\beta}{n}\mathcal{H}\right)\left(I - p_2\frac{\beta}{n}\mathcal{H}'_2\right)^2 + O\left(\frac{\beta^2}{n^2}\right) \\ &= I - \frac{\beta}{n}\mathcal{H}'_4 + O\left(\frac{\beta^2}{n^2}\right), \end{aligned} \tag{4.61}$$

with

$$\begin{aligned} \mathcal{H}'_4 &= 4p_2\mathcal{H}'_2 + (1-4p_2)\mathcal{H} \\ &= \sum_{\langle i,j\rangle}\left[-(8p_2-1)J_{xy}(\sigma_i^x\sigma_j^x + \sigma_i^y\sigma_j^y) + J_z\sigma_i^z\sigma_j^z\right]. \end{aligned} \tag{4.62}$$

The coefficient $(8p_2 - 1)$ originates from the total length $4|p_2| + |1 - 4p_2|(> 1)$ of the to-and-fro path mentioned below (4.51).

We have calculated the error estimates using Z'_2 and Z'_4 for a sufficiently large Trotter number n ($\gg \beta$); see Fig. 4.8. We observe the deteriorated statistics, particularly in the case of the fractal decomposition S_4.

We calculated the ground-state energy, $E_{\rm g}$, $E'_{\rm g2}$ and $E'_{\rm g4}$, of $\mathcal{H}$, $\mathcal{H}'_2$, and $\mathcal{H}'_4$, respectively, by exact diagonalization; see Table 4.1. The energy of the system $Z'_4(\beta)$ becomes far lower than those of the other two systems. The ferromagnetic interaction of $\mathcal{H}'_2$, $-J_{xy}$,

	Ising-like		Heisenberg		XY-like	
	$E_{\rm g}$ or $E'_{\rm g}$	$E_{\rm g} - E'_{\rm g}$	$E_{\rm g}$ or $E'_{\rm g}$	$E_{\rm g} - E'_{\rm g}$	$E_{\rm g}$ or $E'_{\rm g}$	$E_{\rm g} - E'_{\rm g}$
$Z_{\rm exact}$	-12.0	—	-24.0	—	-18.0	—
Z'_2	$-13.3\cdots$	$1.3\cdots$	$-33.6\cdots$	$9.6\cdots$	$-29.4\cdots$	$11.4\cdots$
Z'_4	$-22.0\cdots$	$10.0\cdots$	$-70.4\cdots$	$46.4\cdots$	$-66.5\cdots$	$48.5\cdots$

Table 4.1 The ground-state energies of the systems $Z_{\rm exact}$, Z'_2, and Z'_4 in the limit of $n \to \infty$.

results in the inequality $E'_{\rm g2} < E_{\rm g}$. Moreover the enhanced ferromagnetic interaction of $\mathcal{H}'_4$, $-(8p_2 - 1)J_{xy} \simeq -2.3J_{xy}$, results in the inequality $E'_{\rm g4} < E'_{\rm g2}$.

The argument shown in Fig. 4.4 can be explained by an illustrative example, that is the XXZ model on a triangular. The energy eigenvalues of the system are $3J_z$, $-J_z - 2J_{xy}$, and $-J_z + 4J_{xy}$. The ground-state energy in the case of $J_z, J_{xy} > 0$ is $E_{\rm g} = -J_z - 2J_{xy}$. When the coupling J_{xy} is switched to ferromagnetic, $-J_{xy}$, as in (4.60), the ground-state energy becomes $E'_{\rm g2} = -J_z - 4J_{xy} (< E_{\rm g})$. The eigenvector of this eigenvalue is different from the one of the eigenvalue $E_{\rm g} = -J_z - 2J_{xy}$. Thereby we have the situation shown in Fig. 4.4. For the Hamiltonian, (4.62), the ground-state energy becomes $E'_{\rm g4} = -J_z - 4(8p_2 - 1)J_{xy}$, which is even lower than $E'_{\rm g2}$. The distribution peak around the eigenvector of $E'_{\rm g4}$ becomes narrower, and hence the statistics is further deteriorated.

To summarize the present appendix, though the fractal decomposition is useful in transfer-matrix calculations, Monte Carlo simulations by the fractal decomposition are critical at low temperatures.

4.B Representation basis and the negative-sign problem¶

We describe another example of the application of the argument in Section 4.2. We show the dependence of the negative-sign problem on the choice of the representation bases $|\{\sigma\}\rangle$.

We treat the antiferromagnetic XXZ model (with exchange interactions J_z and J_{xy}) on a triangular lattice, (4.3), or

$$\begin{aligned} -\beta\mathcal{H} &\equiv \sum_{\langle i,j\rangle} \left[K_{xy}\sigma_i^x\sigma_j^x + K_{xy}\sigma_i^y\sigma_j^y + K_z\sigma_i^z\sigma_j^z \right] \\ &= \sum_{\langle i,j\rangle} \left[2K_{xy}\left(\sigma_i^+\sigma_j^- + \sigma_i^-\sigma_j^+\right) + K_z\sigma_i^z\sigma_j^z \right], \end{aligned} \tag{4.63}$$

where

$$K_z \equiv \beta J_z \qquad \text{and} \qquad K_{xy} \equiv \beta J_{xy}. \tag{4.64}$$

In (4.63) we assume implicitly that the representation basis is the direct product of the eigenstates of z-components of spins. Hereafter (4.63) will be referred to as the "S_z representation".

¶The content of this section was published in [Hatano 92].

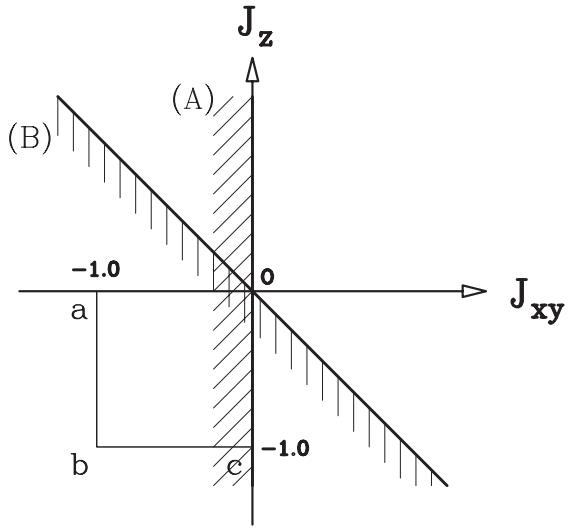

Figure 4.9 The region of appearance of the negative-sign problem; (A) the S_z representation and (B) the S_x representation.

We also test, as the representation basis, the direct product of the eigenstates of x-component of spins. This is equivalent to the rotation of the quantization axis. We rewrite (4.63) in the form

$$\begin{aligned} -\beta\mathcal{H} &\equiv \sum_{\langle i,j\rangle}\left[K_{xy}\sigma_i^z\sigma_j^z + K_{xy}\sigma_i^y\sigma_j^y + K_z\sigma_i^x\sigma_j^x\right] \\ &= \sum_{\langle i,j\rangle}\Big[K_{xy}\sigma_i^z\sigma_j^z + (K_z+K_{xy})\left(\sigma_i^+\sigma_j^- + \sigma_i^-\sigma_j^+\right) \\ &\qquad + (K_z-K_{xy})\left(\sigma_i^+\sigma_j^+ + \sigma_i^-\sigma_j^-\right)\Big]. \end{aligned} \tag{4.65}$$

Hereafter (4.65) will be referred to as the "S_x representation".

As is shown below, we observe the following results: First, we can avoid the negative-sign problem in the region $-K_z < K_{xy} < 0$ by using the S_x representation; see Fig. 4.9. Next, the energy difference

$$\Delta \equiv E_{\rm g} - E'_{\rm g} \tag{4.66}$$

in (4.24) is smaller for the S_x representation than for the S_z representation in the antiferromagnetic XY-like region ($|K_{xy}| > |K_z|$), though the difference is not so big unfortunately; see Fig. 4.10.

Provided that $K_{xy} < 0$, the positive-weight Hamiltonian through the S_z representation is obtained by

$$-\beta\mathcal{H}'_{S_z} = \sum_{\langle i,j\rangle}\left[2\,|K_{xy}|\left(\sigma_i^+\sigma_j^- + \sigma_i^-\sigma_j^+\right) + K_z\sigma_i^z\sigma_j^z\right]. \tag{4.67}$$

The term

$$K_{xy}\left(\sigma_i^+\sigma_j^- + \sigma_i^-\sigma_j^+\right) \tag{4.68}$$

of (4.63) results in negative matrix elements. In most quantum Monte Carlo calculations, the Hamiltonian (4.63) is decomposed into several partial Hamiltonians of cells on the lattice [Suzuki 87b, Takasu 86, Nakamura 92a, Nakamura 92b]. For such cell-decompositions, each K_{xy} term in the summand of (4.63) corresponds to one off-diagonal element of (4.30). Hence the definition (4.33) yields (4.67).

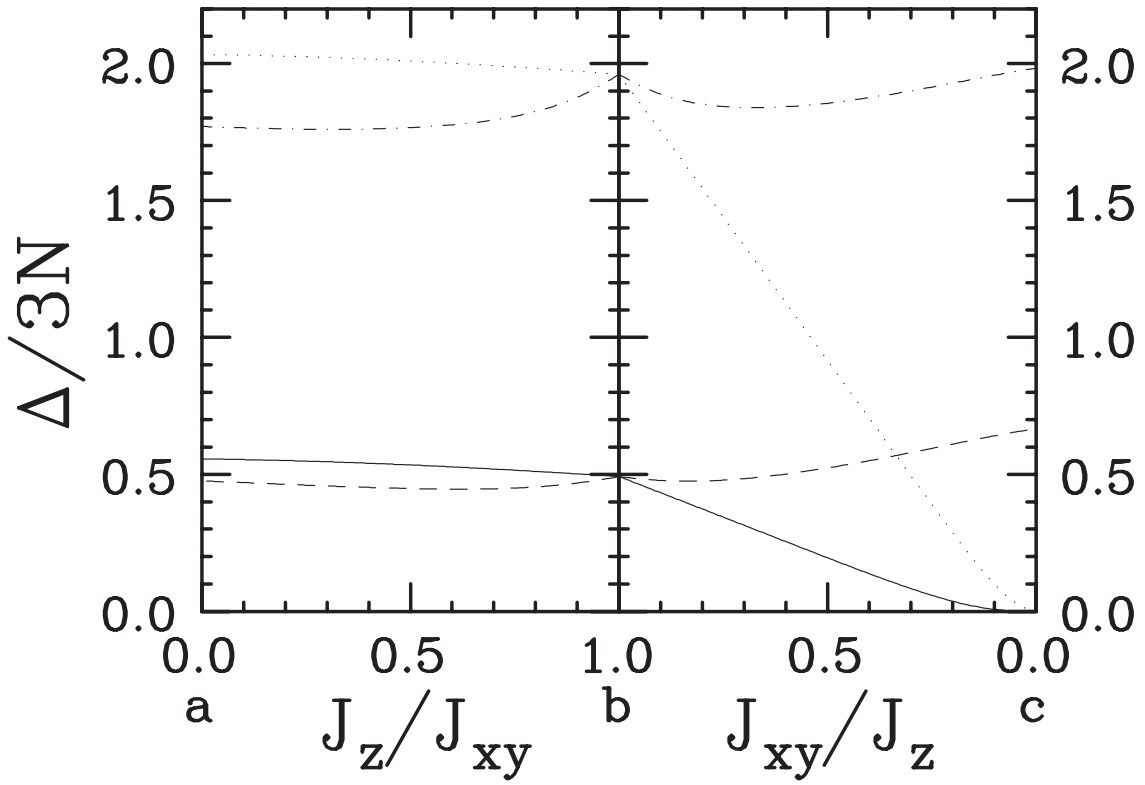

Figure 4.10 The energy difference Δ per bond evaluated for the 3×3 system in the antiferromagnetic region ($J_{xy}, J_z < 0$): the S_z representation (——) and the S_x representation (– – –). The symbols a, b and c on the abscissa correspond to the parameter points indicated in Fig. 4.9. The results calculated with the fractal decomposition are also plotted; the S_z representation ($\cdots$) and the S_x representation (– · –).

As for the model on bipartite lattices, the Hamiltonian (4.67) is connected with the Hamiltonian (4.63) through a unitary transformation [Makivic 91], which does not change the energy spectrum of the model. This fact justifies the neglect of the sign of the Boltzmann weights in simulations of the model on bipartite lattice.

As for the XY model ($J_z = 0$) on frustrated lattices, it turns out that, in the S_z representation, we simulate a ferromagnetic model to understand the fully frustrated model, which inevitably results in the deteriorated statistics.

Meanwhile, the off-diagonal elements of the S_x representation come from the second and third terms of the right-hand side of (4.65). We can select the sign of the third term arbitrarily by further rotations of the axis, and consequently only the second term may cause the negative-sign problem. Hence the problem appears in the region $K_z + K_{xy} < 0$, which is different from that of the case of the S_z representation (Fig. 4.9).

In the region $K_z, K_{xy} < 0$, the positive-weight Hamiltonian through the S_x representation is now

$$\begin{aligned} -\beta\mathcal{H}'_{S_x} &= \sum_{\langle i,j\rangle} \Big[K_{xy}\sigma_i^z\sigma_j^z + |K_z + K_{xy}| \left(\sigma_i^+\sigma_j^- + \sigma_i^-\sigma_j^+\right) \\ &\qquad + |K_z - K_{xy}| \left(\sigma_i^+\sigma_j^+ + \sigma_i^-\sigma_j^-\right)\Big]. \end{aligned} \tag{4.69}$$

We evaluated the energy difference Δ in the cases of (4.67) and (4.69) for the 3×3 system with periodic boundary conditions, and we obtained the results shown in Fig. 4.10.

Incidentally, in Appendix 4.A we reported on the negative-sign problem in the fractal decomposition [Suzuki 90, Suzuki 91]

$$S_4(x) \equiv S_2(px)^2 S_2((1-4p)x) S_2(px)^2 = \mathrm{e}^{x\mathcal{H}} + O(x^5), \tag{4.70}$$

with

$$p \equiv (4 - \sqrt[3]{4})^{-1} \tag{4.71}$$

and

$$S_2(x) \equiv \mathrm{e}^{x\mathcal{H}_1/2}\mathrm{e}^{x\mathcal{H}_2}\mathrm{e}^{x\mathcal{H}_1/2} = \mathrm{e}^{x\mathcal{H}} + O(x^3). \tag{4.72}$$

The positive-weight Hamiltonian corresponding to the decomposition (4.70) was found to be different from (4.67). Our conclusion was that [Hatano 91b] the convergence of the fractal decomposition,

$$\lim_{n\to\infty} \mathrm{Tr} \left[S_4\left(-\frac{\beta}{n}\right)\right]^n, \tag{4.73}$$

is rather rapid, but the negative-sign problem is more serious for the fractal decomposition than for the usual one.

Here we also evaluated Δ through the decomposition (4.70) and compared the cases of the S_z and S_x representations. The results plotted in Fig. 4.10 show that, for the fractal decomposition, the energy difference Δ is also suppressed in the XY-like region.

Chapter 5

Quantum Monte Carlo and Related Methods[‖]

Quantum Monte Carlo methods are reviewed with emphasis on their methodological aspects. Methods based on the Suzuki-Trotter approximation are mainly described.

5.1 Introduction

In this chapter we review quantum Monte Carlo methods, emphasizing its methodological aspects. In this section, before reviewing quantum Monte Carlo methods, we briefly describe the Monte Carlo method for the classical statistical mechanics. (For more detailed reviews on the classical Monte Carlo methods, see [Binder 79, Binder 84, Binder 92].) In addition, we introduce some quantum models.

In the classical statistical mechanics we obtain an expectation value of a quantity Q in the following form:

$$\langle Q \rangle \equiv \frac{\sum Q \mathrm{e}^{-\beta E}}{\sum \mathrm{e}^{-\beta E}}, \tag{5.1.1}$$

where the summation runs over all the possible configurations of the system. The number of the summands is huge for many-body systems, and we could not calculate the whole summation in many cases. We sample some of the summands by Monte Carlo methods.

A straightforward application of the simple sampling results in deteriorated statistics at low temperatures. At low temperatures only a small part of all the configurations contributes to the summation in (5.1.1) because of the factor $\mathrm{e}^{-\beta E}$. If we sample configurations uniformly, most of the sampled configurations have little contribution to (5.1.1).

It is preferable that we sample configurations at a rate proportional to the factor $\mathrm{e}^{-\beta E}$. Then the expectation value is given by

$$\langle Q \rangle = \frac{1}{M} \sum_{t=1}^{M} Q(t), \tag{5.1.2}$$

where the summation runs over the sampled configurations. The larger the weight $\mathrm{e}^{-\beta E}$

[‖]A part of this chapter will be published in [Hatano 93c].

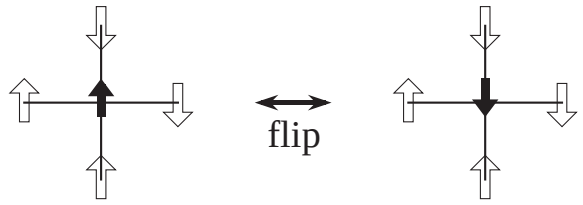

Figure 5.1 A flip trial of an Ising spin.

of a configuration is, the more frequently the configuration is sampled. Thus we can recover from the deteriorated statistics. This is the essence of the importance sampling.

The Monte Carlo dynamics for the importance sampling is proposed first by Metropolis [Metropolis 53]. We use a Markov process to define the dynamics. Consider the Ising model. We define a flip trial of an Ising spin; see Fig. 5.1. By flipping the spin, we change the energy of the system from E to E'. We calculate the following ratio:

$$R \equiv \frac{\mathrm{e}^{-\beta E'}}{\mathrm{e}^{-\beta E}}. \tag{5.1.3}$$

Because of locality of the interaction, we can calculate the ratio easily by knowing the configuration of only the neighboring spins. The probability of flipping the spin is given by

$$P_{\text{flip}} = \min\left[1, R\right] \qquad \text{or} \qquad P_{\text{flip}} \equiv \frac{R}{1+R}, \tag{5.1.4}$$

according to the Metropolis algorithm or the heat-bath algorithm respectively. We compare the probability with a random number P_{rnd}; when $P_{\text{rnd}} < P_{\text{flip}}$, we actually flip the spin and proceed to another flip trial.

Let us introduce two quantum mechanical models, namely the Heisenberg model and the Hubbard model.

The quantum Heisenberg model is described by the Hamiltonian

$$\mathcal{H} = -J \sum_{\langle i,j \rangle} \boldsymbol{\sigma}_i \cdot \boldsymbol{\sigma}_j, \tag{5.1.5}$$

where $\boldsymbol{\sigma}$ denotes the Pauli operators σ^x, σ^y and σ^z. The noncommutability,

$$[\sigma^\mu, \sigma^\nu] \neq 0 \qquad \text{for} \quad \mu \neq \nu, \tag{5.1.6}$$

results in quantum fluctuations.

Another interesting model is the Hubbard Hamiltonian [Hubbard 63], which is a model to describe strongly correlated electrons on a lattice:

$$\mathcal{H} \equiv K + V. \tag{5.1.7}$$

Here K denotes the kinetic energy of tight-binding electrons,

$$K \equiv -t \sum_{\langle i,j \rangle} \sum_{\sigma=\uparrow,\downarrow} \left(c^\dagger_{i\sigma} c_{j\sigma} + c^\dagger_{j\sigma} c_{i\sigma} \right), \tag{5.1.8}$$

and V is the on-site Coulomb energy plus the chemical potential,

$$V \equiv U \sum_i \left(n_{i\uparrow} - \frac{1}{2} \right) \left(n_{i\downarrow} - \frac{1}{2} \right) - \mu \sum_i \sum_{\sigma=\uparrow,\downarrow} n_{i\sigma}. \tag{5.1.9}$$

The noncommutability

$$[K, V] \neq 0 \tag{5.1.10}$$

results in quantum fluctuations.

Naive extension of the procedure (5.1.3)-(5.1.4) to quantum systems results in a difficulty. In the quantum statistical mechanics we calculate the expectation value of a quantity in the form

$$\langle Q \rangle \equiv \frac{\mathrm{Tr}\, Q\mathrm{e}^{-\beta\mathcal{H}}}{\mathrm{Tr}\, \mathrm{e}^{-\beta\mathcal{H}}} = \frac{\sum_{\psi} \left\langle \psi \left| Q\mathrm{e}^{-\beta\mathcal{H}} \right| \psi \right\rangle}{\sum_{\psi} \left\langle \psi \left| \mathrm{e}^{-\beta\mathcal{H}} \right| \psi \right\rangle}, \tag{5.1.11}$$

instead of (5.1.1). In order to simulate the system as it is, we have to calculate the ratio

$$R \equiv \frac{\left\langle \psi' \left| \mathrm{e}^{-\beta\mathcal{H}} \right| \psi' \right\rangle}{\left\langle \psi \left| \mathrm{e}^{-\beta\mathcal{H}} \right| \psi \right\rangle} \tag{5.1.12}$$

for a flip trial $\psi \longrightarrow \psi'$. Hence we have to diagonalize the matrix $\mathcal{H}$, which is practically impossible for large systems.

This difficulty is essential in the quantum statistical mechanics. In the classical Monte Carlo dynamics it is because of the locality of the interaction that the calculation of the ratio (5.1.3) is easy. In the quantum mechanical system, however, the quantum coherence ranges over the whole system. Even if the interaction term in the Hamiltonian is local, the effect of the term is not local.

We review several methods of studying quantum systems in the following sections. The main subject there is how to calculate the density matrix $\mathrm{e}^{-\beta\mathcal{H}}$ in order to simulate the system.

The Suzuki-Trotter decomposition, which is adopted in most methods introduced here, is described in Section 5.2. A numerical calculation and an analytic argument are given in Appendix 5.A and in Appendix 5.B, respectively, in connection with the fractal decomposition.

The decomposition has been applied to the world-line approach (Section 5.3), the transfer-matrix method (Section 5.5), the Monte Carlo power method (Section 5.6) and the auxiliary-field approach (Section 5.7). Appendix 5.C is a supplement to Section 5.3. Appendices 5.D and 5.E are supplements to Section 5.7.

The negative-sign problem, which appears in some cases, is explained in Section 5.4. This section is also an introduction of Chapter 4, where a new proposal for relief of this difficulty is presented.

Modifications of some approaches for the purpose of studying ground-state properties is described in Section 5.8. The diffusion Monte Carlo methods, which is also devised for studies on the ground state, are mentioned in (5.9).

The decoupled-cell method (Section 5.9) and Handscomb's method (Section 5.10), in which the Suzuki-Trotter approximation is not utilized, are also mentioned.

5.2 Suzuki-Trotter decomposition

Here we describe the method of calculating the density matrix $\mathrm{e}^{-\beta\mathcal{H}}$ approximately. The method is utilized in many methods mentioned later. We also describe the construction

of higher-order approximants.

Generally speaking, when we find an m-th order approximant $f_m(x)$ of the exponential operator $\mathrm{e}^{-x\mathcal{H}}$,

$$f_m(x) = \mathrm{e}^{-x\mathcal{H}} + O(x^{m+1}), \tag{5.2.1}$$

the density matrix is approximated by

$$\mathrm{e}^{-\beta\mathcal{H}} = \left(\mathrm{e}^{-\beta\mathcal{H}/n}\right)^n = \left(f_m\left(\frac{\beta}{n}\right)\right)^n + O\left(\frac{\beta^{m+1}}{n^m}\right). \tag{5.2.2}$$

The extrapolation $n \to \infty$ reproduces the original density matrix. The problem is how to find the approximant f_m. It is preferable that the approximant retains some symmetry properties of the original exponential operator.

In the Feynman path-integral approach [Feynman 65] the perturbational approximant

$$\mathrm{e}^{-\beta\mathcal{H}/n} = 1 - \frac{\beta}{n}\mathcal{H} + O\left(\frac{\beta^2}{n^2}\right) \tag{5.2.3}$$

has been usually used. The Suzuki-Trotter decomposition [Suzuki 76a, Suzuki 77c, Suzuki 85b], on the other hand, takes the form

$$\mathrm{e}^{-\beta\mathcal{H}/n} \simeq \mathrm{e}^{-\beta p_1 A_1/n}\mathrm{e}^{-\beta p_2 A_2/n}\cdots, \tag{5.2.4}$$

where we decompose the total Hamiltonian into partial Hamiltonians A_l so that it may be easy to diagonalize each partial Hamiltonians. Approximants of this type, when imitating time-evolution operators, retain the unitarity. Moreover it is easy to obtain higher-order approximants as is shown below. In the present section we concentrate on approximants of this type.

When we extrapolate an approximant $[f_m(\beta/n)]^n$ to the limit $n \to \infty$, the correction vanishes as n^{-m}. On the other hand, the time necessary to calculate the approximant $[f_m(\beta/n)]^n$, in general, increases proportionally to the Trotter number n. Thus approximants with m large can improve the procedure of the extrapolation $n \to \infty$.

The simplest example of the decomposition is [Trotter 59, Suzuki 76a]

$$Q_1(x) \equiv \prod_{i=1}^{q} \mathrm{e}^{-x\mathcal{H}_i} = \mathrm{e}^{-x\mathcal{H}} + O\left(x^2\right) \tag{5.2.5}$$

with

$$\mathcal{H} = \sum_{i=1}^{q} \mathcal{H}_i \tag{5.2.6}$$

and

$$[\mathcal{H}_i, \mathcal{H}_j] \neq 0 \qquad \text{for} \quad i \neq j. \tag{5.2.7}$$

Here the symbol $\prod_{i=1}^{q}$ indicates that operators are multiplied in the ascending order $i = 1, 2, \ldots, q$.

Suzuki showed the following fact [Suzuki 85d, Suzuki 90]: when an approximant S_{2m-1}, correct up to the power of x^{2m-1}, satisfies the relation

$$S_{2m-1}(x)S_{2m-1}(-x) = 1, \tag{5.2.8}$$

then the approximant is actually correct up to the power of x^{2m}. An approximant Q_{2m-1}, if it does not satisfy (5.2.8), thus produces the approximant S_{2m} as follows (the symmetrization) [Suzuki 90]:

$$S_m(x) = Q_{m-1}\left(\frac{x}{2}\right) Q_{m-1}^{-1}\left(-\frac{x}{2}\right). \tag{5.2.9}$$

Application of this fact to (5.2.5) yields

$$S_2(x) \equiv \left(\prod_{i=1}^{q-1} \mathrm{e}^{-x\mathcal{H}_i/2}\right) \mathrm{e}^{-x\mathcal{H}_q} \left(\prod_{i=q-1}^{1} \mathrm{e}^{-x\mathcal{H}_i/2}\right) = \mathrm{e}^{-x\mathcal{H}} + O\left(x^3\right), \tag{5.2.10}$$

where the symbol $\prod_{i=q-1}^{1}$ indicates that operators are multiplied in the descending order $i = q, q-1, \ldots, 1$.

Moreover, Suzuki [Suzuki 90, Suzuki 91, Yoshida 90] discovered a new way to construct approximants correct up to arbitrarily higher orders, namely the fractal decomposition. The main idea of the fractal decomposition is its recursive way of construction; an appropriate combination of lower-order approximants yields a higher-order approximant in such a way that the lowest-order corrections of the former cancel out with each other.

Let us concentrate only on symmetrized approximants, that is, approximants which satisfy (5.2.8). An approximant S_{2m} is constructed of S_{2m-2} in the form:

$$S_{2m}(x) \equiv \prod_{j=1}^{2r-1} S_{2m-2}(p_{2m,j}x) \tag{5.2.11}$$

with the coefficients $\{p_{2m,j}\}$ satisfying the normalization condition

$$\sum_{j=1}^{2r-1} p_{2m,j} = 1, \tag{5.2.12}$$

the cancellation condition

$$\sum_{j=1}^{2r-1} p_{2m,j}^{2m-1} = 0 \tag{5.2.13}$$

and the symmetrization condition

$$p_{2m,j} = p_{2m,2r-j} \qquad \text{for} \quad j = 1, 2, \ldots, r-1. \tag{5.2.14}$$

The cancellation condition (5.2.13) ensures that the approximant is correct up to the power of x^{2m-1}, and the symmetrization condition (5.2.13) ensures that up to the power of x^{2m}.

The number of product $2r-1$ is arbitrary as long as the set of the conditions has a solution; in the case $r = 3$, for example, we have [Suzuki 90, Suzuki 91]

$$\begin{aligned} & p_{2m,1} = p_{2m,2} = p_{2m,4} = p_{2m,5} = \left(4 - 4^{1/(2m-1)}\right)^{-1} (> 0) \\ \text{and} \qquad & p_{2m,3} = 1 - 4p_{2m,1} (< 0). \end{aligned} \tag{5.2.15}$$

In Appendix 5.A we show an example of the application of the fractal decomposition [Hatano 91b]. The rapid convergence for $n \to \infty$ of a fractal decomposition is confirmed there.

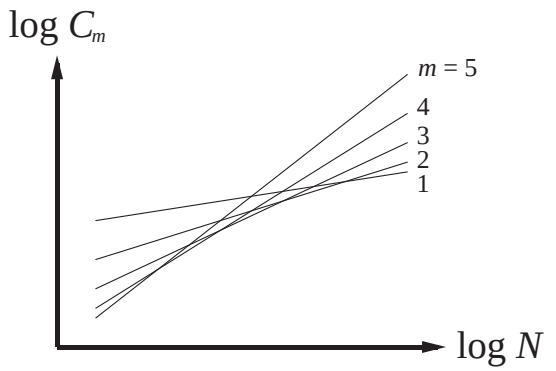

Figure 5.2 The magnitude of the correction as a function of the number of multiplications.

An interesting feature of the fractal decomposition is the structure of time evolution. Suzuki [Suzuki 91] proved generally that some of coefficients of an approximant of the form (5.2.4) is necessarily negative except in the case of first- and second-order approximants. Thereby the path along which a wave function is developed with exponential operators runs back and forth on the time axis. The dimensionality of the path, or the coefficients of the decomposition $\beta\mathcal{H} \to \{\beta A_1, \beta A_2, \ldots, \beta A_q\}$ is fractal in the limit $m \to \infty$ [Suzuki 90,Suzuki 91]; this is the reason why the decomposition is called the "fractal decomposition". It seems that the fractal path is necessary for the recovery of quantum effects.

Incidentally, which decomposition is the most advantageous of all the $\{S_{2m}\}$? Let us leave out the application to Monte Carlo simulations for a while, and discuss the direct calculation of the products of the exponential operators. In the comparison between the fractal decompositions $\{S_{2m}\}$, we have to consider the following two factors. When we use a higher-order decomposition, (i) the magnitude of the correction decreases as β^{2m+1}/n^{2m}, while (ii) the computational time increases as $n(2r)^m$. (Here we assume that the coefficient of the correction term β^{2m+1}/n^{2m} does not grow rapidly as m increases.)

The dependence $n(2r)^m$ is given as follows. The number of the multiplications necessary to construct a decomposition S_{2m} in (5.2.11) is of the order of $(2r)^m$. When we use the decomposition to construct the approximant (5.2.2) with a Trotter number n, the total number of multiplications is of the order of $n(2r)^m$.

Consider that we can afford the computational time to execute the multiplications N times. We can attain the Trotter number n given by

$$n \simeq \frac{N}{(2r)^m}. \tag{5.2.16}$$

The magnitude of the correction term of (5.2.2) is then of the order of

$$\frac{\beta^{2m+1}}{n^{2m}} \simeq \frac{\beta^{2m+1}(2r)^{2m^2}}{N^{2m}} \equiv C_m(N). \tag{5.2.17}$$

We schematically show the function $C_m(N)$ in Fig. 5.2. An actual example is given in Fig. 5.13 of Appendix 5.A.

When we fix the number of the multiplications, N, the most precise is the m_1-th order decomposition, where m_1 is defined by

$$\frac{\partial}{\partial m} \log C_m(N)\bigg|_{m=m_1} = 0, \qquad \text{or} \qquad m_1 = \frac{\log(N/\beta)}{2\log(2r)}. \tag{5.2.18}$$

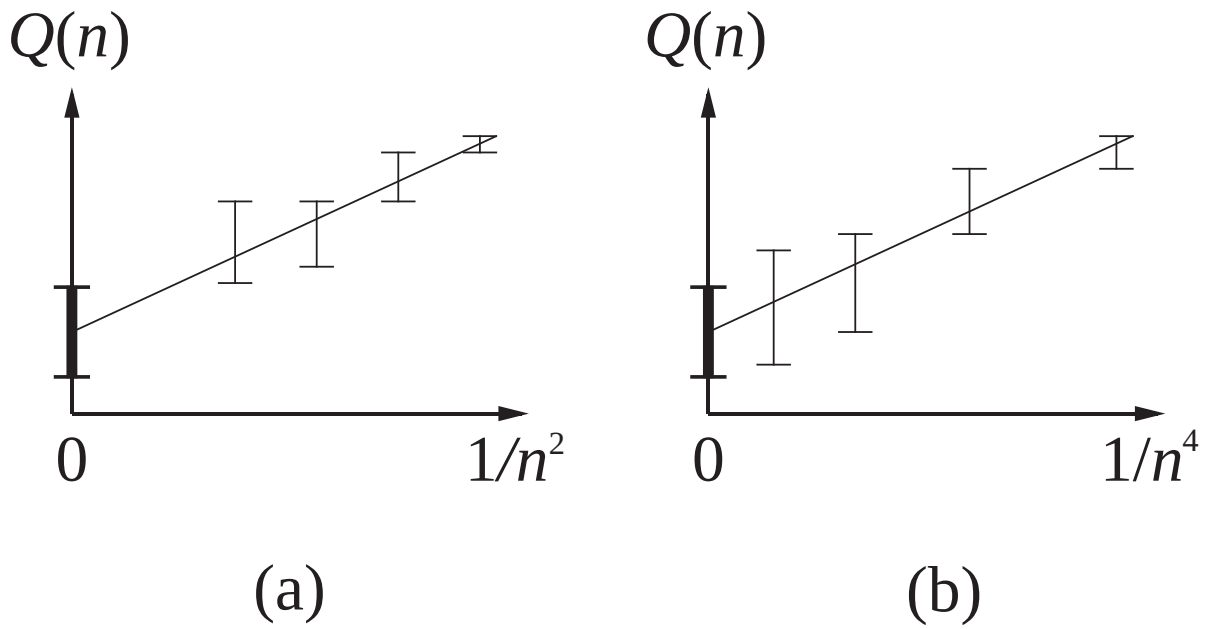

Figure 5.3 The schematic situations of the extrapolation $n \to \infty$ for a relevant quantity $Q(n)$ measured in quantum Monte Carlo simulations with (a) the decomposition S_2 and (b) the fractal decomposition S_4.

Conversely, when we fix, to a value C, the magnitude of the correction we can allow, the most time-saving is the m_2-th decomposition, where m_2 is given by

$$\frac{\partial}{\partial m} \log N_m(C)\Big|_{m=m_2} = 0, \qquad \text{or} \qquad m_2 = \sqrt{\frac{\log(\beta/C)}{\log(2r)}}. \tag{5.2.19}$$

Here $N_m(C)$ is the inverse function of $C_m(N)$.

Thus we can optimize the choice of a fractal decomposition. When we optimize most, the correction decreases rapidly as

$$C_{m_1}(N) = \frac{\beta^{m_1+1}}{N^{m_1}} \sim N^{-\alpha \log N}, \tag{5.2.20}$$

where α is an appropriate constant.

As for the application of the fractal decomposition to Monte Carlo calculations, we have to take into account another factor, namely the negative-sign problem. (The negative-sign problem is mentioned in Section 5.4 and in Chapter 4. The problem in the case of the fractal decomposition is described particularly in Appendix 4.A.) The negative-sign problem appears more severely in the fractal decomposition than in the second-order decomposition, because some of the coefficients $\{p_{2m,j}\}$ are negative for the fractal decompositions. Since the statistics deteriorates owing to the negative-sign problem, Monte Carlo simulations with the use of the fractal decomposition are critical at low temperatures.

The schematic situations of the extrapolation $n \to \infty$ are shown in Fig. 5.3. The error bar for the finally estimated value $Q(n = \infty)$ results both from the finiteness of

the Trotter number n and from statistical errors appearing in Monte Carlo simulations. It can be stated that the fractal decomposition has a merit with respect to the former, a demerit with respect to the latter.

Recently Suzuki has developed a general scheme for higher-order approximants [Suzuki 92a, Suzuki 92b]. Using these approximants, we can reduce the number of the multiplications of the exponential operators. As far as we calculate the approximants directly, this general scheme is quite useful.

Unfortunately, the negative coefficients of $\{p_{2m,j}\}$ cannot be excluded, and hence the application of the decompositions to Monte Carlo simulations is still critical at low temperatures.

In Appendix 5.B we show a theorem concerning the correction term of the Trotter-like decomposition.

5.3 World-line approach

In this section we review one of the quantum Monte Carlo methods which utilize the Suzuki-Trotter decomposition reviewed above. Some formulae for measurement of physical quantities with Monte Carlo simulations are given in Appendix 5.C.

In the following we consider, as an example, the one-dimensional $S = 1/2$ Heisenberg ferromagnet:

$$\mathcal{H} = -\sum_{i=0}^{N} \boldsymbol{\sigma}_i \cdot \boldsymbol{\sigma}_{i+1}. \tag{5.3.1}$$

Not all the thermodynamic properties of the model are known [Schlottmann 85, Takahashi 85, Takada 86], because we have not found all the eigenvalues and eigenvectors of the Hamiltonian so far. In order to obtain the average of a quantity Q, namely,

$$\langle Q \rangle_{\mathrm{q}} \equiv \frac{1}{Z_{\mathrm{q}}} \mathrm{Tr}\, Q \mathrm{e}^{-\beta\mathcal{H}} \tag{5.3.2}$$

$$\text{with} \qquad Z_{\mathrm{q}} \equiv \mathrm{Tr}\, \mathrm{e}^{-\beta\mathcal{H}}, \tag{5.3.3}$$

it is necessary to use the Suzuki-Trotter decomposition.

Here we use the simplest approximant

$$\mathrm{e}^{-\beta\mathcal{H}} \simeq \left(\mathrm{e}^{-\beta A/n} \mathrm{e}^{-\beta B/n}\right)^n, \tag{5.3.4}$$

dividing the Hamiltonian (5.3.1) into two parts:

$$\mathcal{H} = A + B \tag{5.3.5}$$

with

$$A \equiv -\sum_{i=0}^{N/2-1} \boldsymbol{\sigma}_{2i} \cdot \boldsymbol{\sigma}_{2i+1} \qquad \text{and} \qquad B \equiv -\sum_{i=0}^{N/2-1} \boldsymbol{\sigma}_{2i+1} \cdot \boldsymbol{\sigma}_{2i+2}. \tag{5.3.6}$$

Though there are many alternatives to the approximant as was mentioned in the previous section, we concentrate on the one (5.3.4)-(5.3.6) here for simplicity; it is straightforward to generalize the following argument to the alternatives.

We thereby approximately describe the partition function (5.3.3) of the quantum system $\mathcal{H}$ as follows [Suzuki 76b, Suzuki 77a, Suzuki 86b, Suzuki 87b]:

$$\begin{aligned} Z_{\mathrm{q}} &= \sum_{\{\sigma\}_0} \left\langle \{\sigma\}_0 \left| \mathrm{e}^{-\beta\mathcal{H}} \right| \{\sigma\}_0 \right\rangle && (5.3.7) \\ &\overset{(5.3.4)}{\simeq} \sum_{\{\sigma\}_0} \left\langle \{\sigma\}_0 \left| \left(\mathrm{e}^{-\beta A/n}\mathrm{e}^{-\beta B/n}\right)^n \right| \{\sigma\}_0 \right\rangle \\ &= \sum_{\{\sigma\}} \left\langle \{\sigma\}_0 \left| \mathrm{e}^{-\beta A/n} \right| \{\sigma\}_1 \right\rangle \left\langle \{\sigma\}_1 \left| \mathrm{e}^{-\beta B/n} \right| \{\sigma\}_2 \right\rangle \\ &\qquad \cdots \left\langle \{\sigma\}_{2n-1} \left| \mathrm{e}^{-\beta B/n} \right| \{\sigma\}_0 \right\rangle . && (5.3.8) \end{aligned}$$

Here every state vector $|\{\sigma\}_l\rangle$ is a direct product of eigenstates of σ_i^z:

$$|\{\sigma\}_l\rangle \equiv |\sigma_{0,l}\rangle\, |\sigma_{1,l}\rangle \cdots |\sigma_{N,l}\rangle\,, \tag{5.3.9}$$

where $\sigma_i^z\, |\sigma_{i,l}\rangle = \sigma_{i,l}\, |\sigma_{i,l}\rangle$ with $\sigma_{i,l} = \pm 1$. A set of vectors $\{|\{\sigma\}_l\rangle\}$ for each l is hence complete and orthogonal in the Hilbert space. We have inserted resolution of the unit operator

$$\hat{1} \equiv \sum_{\{\sigma\}_l} |\{\sigma\}_l\rangle\, \langle\{\sigma\}_l| \tag{5.3.10}$$

into each pair of exponential operators of (5.3.8). Consequently, the summation in the last line of (5.3.8) runs over all the configuration of the $2n(N+1)$ variables $\sigma_{i,l}$:

$$\begin{aligned} \{\sigma\} \equiv \{ \quad & \sigma_{0,0}, && \sigma_{1,0}, && \sigma_{2,0}, && \ldots, && \sigma_{N,0}, \\ & \sigma_{0,1}, && \sigma_{1,1}, && \sigma_{2,1}, && \ldots, && \sigma_{N,1}, \\ & \cdots, && \cdots, && \cdots, && \cdots, && \cdots, \\ & \sigma_{0,2n-1}, && \sigma_{1,2n-1}, && \sigma_{2,2n-1}, && \ldots, && \sigma_{N,2n-1} \}. \end{aligned} \tag{5.3.11}$$

We identify each summand of (5.3.8) with one of the Boltzmann factors of a classical system:

$$W\{\sigma\} \equiv \prod_{l=0}^{n-1} \left\langle \{\sigma\}_{2l} \left| \mathrm{e}^{-\beta A/n} \right| \{\sigma\}_{2l+1} \right\rangle \left\langle \{\sigma\}_{2l+1} \left| \mathrm{e}^{-\beta B/n} \right| \{\sigma\}_{2l+2} \right\rangle \tag{5.3.12}$$

with the periodic boundary condition $\{\sigma\}_{2n} \equiv \{\sigma\}_0$. The partition function of the quantum system Z_{q} is approximated by the partition function of the classical system,

$$Z_n \equiv \sum_{\{\sigma\}} W\{\sigma\}. \tag{5.3.13}$$

Suzuki [Suzuki 76b] pointed out the following fact: when a d-dimensional quantum Hamiltonian comprises only short-range interactions, it is possible in general to arrange the Suzuki-Trotter decomposition so that the resulting classical system may be a $(d+1)$-dimensional system with *short-range* interactions. We call the additional dimensional axis the Trotter direction.

The above general statement actually holds in the case (5.3.13). Since each summand of A (or B) in (5.3.6) is commutable with others, we can express the exponential operators in (5.3.12) as

$$\begin{aligned} \mathrm{e}^{-\beta A/n} &= \prod_{i=0}^{N/2-1} \exp\left(\frac{\beta}{n}\boldsymbol{\sigma}_{2i}\cdot\boldsymbol{\sigma}_{2i+1}\right) \\ \text{and}\quad \mathrm{e}^{-\beta B/n} &= \prod_{i=0}^{N/2-1} \exp\left(\frac{\beta}{n}\boldsymbol{\sigma}_{2i+1}\cdot\boldsymbol{\sigma}_{2i+2}\right). \end{aligned} \tag{5.3.14}$$

We easily obtain matrix elements of them in the following forms:

$$\begin{aligned} \left\langle \{\sigma\}_{2l} \left| \mathrm{e}^{-\beta A/n} \right| \{\sigma\}_{2l+1} \right\rangle &= \prod_{i=0}^{N/2-1} w(2i, 2l) \\ \left\langle \{\sigma\}_{2l+1} \left| \mathrm{e}^{-\beta B/n} \right| \{\sigma\}_{2l+2} \right\rangle &= \prod_{i=0}^{N/2-1} w(2i+1, 2l+1) \end{aligned} \tag{5.3.15}$$

with

$$\begin{aligned} w(i,l) &\equiv \left\langle \sigma_{i,l}, \sigma_{i+1,l} \left| \exp\left(\frac{\beta}{n}\boldsymbol{\sigma}_i\cdot\boldsymbol{\sigma}_{i+1}\right) \right| \sigma_{i,l+1}, \sigma_{i+1,l+1} \right\rangle \\ &\qquad\qquad |\uparrow\uparrow\rangle \quad |\uparrow\downarrow\rangle \quad |\downarrow\uparrow\rangle \quad |\downarrow\downarrow\rangle \\ &= \begin{array}{c} \langle\uparrow\uparrow| \\ \langle\uparrow\downarrow| \\ \langle\downarrow\uparrow| \\ \langle\downarrow\downarrow| \end{array} \begin{pmatrix} a & & & \\ & b & c & \\ & c & b & \\ & & & a \end{pmatrix}. \end{aligned} \tag{5.3.16}$$

Here the symbol $\uparrow$ stands for $\sigma_{i,l} = 1$, the symbol $\downarrow$ stands for $\sigma_{i,l} = -1$, and

$$\begin{aligned} a &\equiv \mathrm{e}^{\beta/n} \\ b &\equiv \mathrm{e}^{-\beta/n}\cosh(2\beta/n) \\ c &\equiv \mathrm{e}^{-\beta/n}\sinh(2\beta/n). \end{aligned} \tag{5.3.17}$$

Finally we obtain the Boltzmann factors (5.3.12) as

$$W\{\sigma\} = \prod_{\substack{i=0 \\ i+l=\text{even}}}^{N} \prod_{l=0}^{2n-1} w(i,l). \tag{5.3.18}$$

We can interpret [Suzuki 76b] this as the Boltzmann factor of a two-dimensional spin systems with four-spin interactions w; the system is depicted in Fig. 5.4. (The decomposition (5.3.6) is called the checkerboard decomposition [Hirsch 81, Hirsch 82].) Monte Carlo calculation with the importance-sampling method [Metropolis 53] is applicable to the system if $W\{\sigma\} \geq 0$ for all $\{\sigma\}$.

The following fact should be noted when one performs a Monte Carlo simulation of the system: some spin configurations $\{\sigma\}$ have vanishing Boltzmann factors, and should be omitted from configurations sampled in the simulation. The four-spin interaction (5.3.16) follows a conservation law similar to the one in the six-vertex model [Barma 78], namely,

$$\sigma_{i,l} + \sigma_{i+1,l} = \sigma_{i,l+1} + \sigma_{i+1,l+1}. \tag{5.3.19}$$

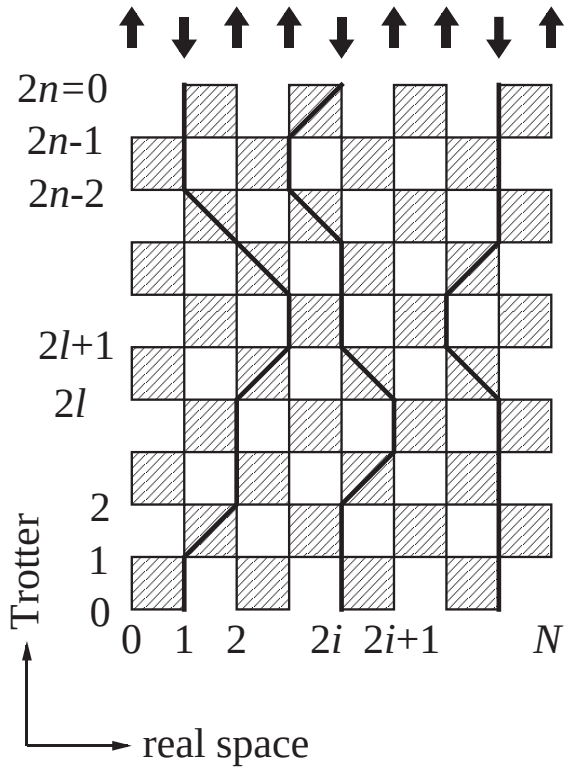

Figure 5.4 The classical Ising-spin system mapped with the Suzuki-Trotter decomposition. The thick line on the lattice denotes the world line which connects downward spins. Because of a conservation rule, the world lines never terminate.

Hence the number of downward spins on the row $l = 0$ is conserved throughout all the rows l. A spin configuration $\{\sigma\}$ which breaks this conservation law does not contribute to the partition function (5.3.13). For a configuration which follows the rule, we can draw lines which run through the corresponding down spins in the Trotter direction [Hirsch 81] as is shown in Fig. 5.4. The lines are called *world lines*. There is one-to-one correspondence between an allowed spin configuration and a world-line configuration, provided that we require the world lines not to intersect. Thus the summation in (5.3.13) runs only over possible world-line configurations after all.

We sample some of them in Monte Carlo simulations, creating, annihilating and moving world lines according to the Boltzmann weights (5.3.18). The process of creating and annihilating world lines is called a global flip, while the process of moving them is called a local flip.

Once we obtain a set of data of the classical systems with a fixed temperature and various Trotter numbers, the Trotter extrapolation to the limit $n \to \infty$ yields data of the quantum system. Behavior of the correction to the quantum limit is well-known as was described in the preceding section. We have to note that Trotter numbers must be large enough to ensure sufficient convergence. A practical condition of the convergence might be given by $n > \beta$.

In order to improve the convergence for $n \to \infty$, the following method has been employed. The correction depends on the way of the decomposition of the Hamiltonian. We expect that the coefficient of the correction term $1/n^2$ of the approximant (5.3.4) is

smaller in the case of the decomposition

$$\begin{aligned} A &\equiv -\sum_{i=0}^{N/2m-1}\sum_{j=0}^{m-1}\boldsymbol{\sigma}_{mi+j}\cdot\boldsymbol{\sigma}_{mi+j+1} \\ \text{and}\quad B &\equiv -\sum_{i=0}^{N/2m-1}\sum_{j=m}^{2m-1}\boldsymbol{\sigma}_{mi+j}\cdot\boldsymbol{\sigma}_{mi+j+1} \end{aligned} \tag{5.3.20}$$

than in the case (5.3.6). We thereby exactly treat quantum fluctuations inside the cluster of size m. This approach is first introduced to the quantum transfer-matrix method [Tsuzuki 85, Tsuzuki 86, Betsuyaku 86a], which will be described in Section 5.5. We refer to this approach as the cluster-transfer-matrix method. Okabe and Kikuchi [Okabe 87] first applied a decomposition of this type to a Monte Carlo study on the one-dimensional Heisenberg model. Nomura [Nomura 89a, Nomura 89b] studied $S = 1$ models by simulations based on this approach.

Computational time necessary in the world-line Monte Carlo simulation is proportional to the number of spins of the classical system (5.3.13), namely, to Nn. This is shorter than in the Monte Carlo simulation with the auxiliary-field approach described in Section 5.7. This merit comes from the fact that the classical system consists of short-range interactions.

Thus the method has been successfully applied to quantum ferromagnets [Suzuki 77b, Cullen 83, De Raedt 84a, De Raedt 84b, Loh 85a, Loh 85b, Ding 90b, Ding 92, Makivic 92b], to quantum antiferromagnets on bipartite lattices [Miyashita 88, Reger 88, Ding 90a, Makivic 91, Ding 91], and to one-dimensional fermion systems [De Raedt 81, Hirsch 81, Hirsch 82, Hirsch 83a, Hirsch 84a, Hirsch 84b]. On the other hand for frustrated antiferromagnets and higher-dimensional fermion systems, a problem arises, namely, the negative-sign problem, which is mentioned in the next section.

Some measurement formulae for physical quantities are given in Appendix 5.C.

5.4 Negative-sign problem

In this section we review the negative-sign problem, which is one of the most serious problems in the quantum Monte Carlo method.

There are two parts of the negative-sign problem. The first part comes of the fact that the Boltzmann weight (5.3.18) becomes negative for some configurations $\{\sigma\}$, when we treat frustrated antiferromagnets or fermion systems. We can solve this part using the reweighting method as is shown below. If the first part is solved, the statistics of Monte Carlo data obtained deteriorates at low temperatures; this is the second part.

The problem appears when the spin system is frustrated, that is, when the number of antiferromagnetic bonds around a plaquette of the lattice is odd.

Consider, as an example, the Heisenberg antiferromagnet on a triangle:

$$\mathcal{H} = \boldsymbol{\sigma}_1\cdot\boldsymbol{\sigma}_2 + \boldsymbol{\sigma}_2\cdot\boldsymbol{\sigma}_3 + \boldsymbol{\sigma}_3\cdot\boldsymbol{\sigma}_1. \tag{5.4.1}$$

We use the approximant

$$\mathrm{e}^{-\beta\mathcal{H}} \simeq \left(\mathrm{e}^{-\beta\boldsymbol{\sigma}_1\cdot\boldsymbol{\sigma}_2/n}\mathrm{e}^{-\beta\boldsymbol{\sigma}_2\cdot\boldsymbol{\sigma}_3/n}\mathrm{e}^{-\beta\boldsymbol{\sigma}_3\cdot\boldsymbol{\sigma}_1/n}\right)^n. \tag{5.4.2}$$

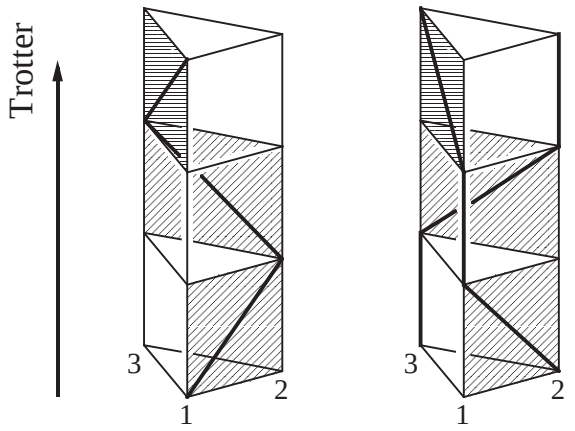

Figure 5.5 World-line configurations of the triangular antiferromagnet. These configurations have negative Boltzmann weights.

The procedure explained in the previous section gives

$$Z_n = \sum_{\{\sigma\}} W\{\sigma\} \tag{5.4.3}$$

with

$$W\{\sigma\} \equiv \prod_{l=0}^{n} w(1,3l)w(2,3l+1)w(3,3l+2). \tag{5.4.4}$$

The local Boltzmann weight w is now given by (5.3.16) with

$$\begin{aligned} a &\equiv \mathrm{e}^{-\beta/n}, \\ b &\equiv \mathrm{e}^{\beta/n}\cosh(2\beta/n) \\ \text{and} \quad c &\equiv \mathrm{e}^{\beta/n}\sinh(2\beta/n), \end{aligned} \tag{5.4.5}$$

instead of (5.3.17). Note that, in the present antiferromagnetic case, some local weights become negative: $w(i,l) = -c$. These weights correspond to the configurations where a world line goes across a square of the four-body interaction. The total Boltzmann weight W can be negative; when $n = 1$, two configurations depicted in Fig. 5.5 have the negative weights $-c^3$.

Nevertheless, the importance sampling method is not applicable to a system if the total Boltzmann weight of the system can be negative. The Boltzmann weight of each configuration is proportional to the number of times when the configuration is generated in simulations, and needs to be positive. This is the first part of the negative-sign problem.

The problem does not appear when the lattice of the spin system is bipartite: square lattices, honeycomb lattices and cubic lattices, for example. Local configurations which give negative Boltzmann weights always appear an even number of times, and the total weight is thus positive. This fact is confirmed as follows [Makivic 91]. Consider the antiferromagnetic Hamiltonian on a bipartite lattice,

$$\mathcal{H} = \sum_{\langle i,j \rangle} \boldsymbol{\sigma}_i \cdot \boldsymbol{\sigma}_j, \tag{5.4.6}$$

and consider a decomposition similar to (5.2.2)-(5.2.4). We define the following unitary transformation U: for spins on a sublattice A, we rotate the spin space around the z axis,

$$\sigma_i^x \longrightarrow -\sigma_i^x \quad \text{and} \quad \sigma_i^y \longrightarrow -\sigma_i^y \qquad \text{for} \quad i \in A, \tag{5.4.7}$$

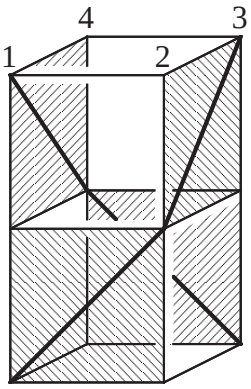

Figure 5.6 World-line configurations of the Hubbard model on a square lattice. These configurations have negative Boltzmann weights.

while we leave spins on the other sublattice B as they are. After we apply this unitary transformation, the local Boltzmann factor is always positive, and hence the total Boltzmann weight is also positive. It is impossible to define such a unitary transformation on frustrated lattices.

The negative-sign problem also appears, when we apply the world-line approach to the two- and higher-dimensional Hubbard models. The configuration depicted in Fig. 5.6, for example, gives a negative Boltzmann factor owing to the anti-commutation relation of fermions:

$$\begin{aligned}
&\left\langle \uparrow,0,\uparrow,0 \left| \mathrm{e}^{\beta t(c_{1\uparrow}^\dagger c_{2\uparrow}+c_{2\uparrow}^\dagger c_{1\uparrow})/n} \mathrm{e}^{\beta t(c_{3\uparrow}^\dagger c_{4\uparrow}+c_{4\uparrow}^\dagger c_{3\uparrow})/n} \right| 0,\uparrow,0,\uparrow \right\rangle \\
&\times \left\langle 0,\uparrow,0,\uparrow \left| \mathrm{e}^{\beta t(c_{2\uparrow}^\dagger c_{3\uparrow}+c_{3\uparrow}^\dagger c_{2\uparrow})/n} \mathrm{e}^{\beta t(c_{4\uparrow}^\dagger c_{1\uparrow}+c_{1\uparrow}^\dagger c_{4\uparrow})/n} \right| \uparrow,0,\uparrow,0 \right\rangle \\
&= \sinh^4\left(\frac{\beta t}{n}\right) \left\langle 0 \left| c_{3\uparrow} c_{1\uparrow} c_{1\uparrow}^\dagger c_{3\uparrow}^\dagger \right| 0 \right\rangle \left\langle 0 \left| c_{4\uparrow} c_{2\uparrow} c_{4\uparrow}^\dagger c_{2\uparrow}^\dagger \right| 0 \right\rangle \\
&= -\sinh^4\left(\frac{\beta t}{n}\right) < 0, \qquad (5.4.8)
\end{aligned}$$

where the base kets are defined by

$$|\uparrow,0,\uparrow,0\rangle \equiv c_{1\uparrow}^\dagger c_{3\uparrow}^\dagger |0\rangle \qquad \text{and} \qquad |0,\uparrow,0,\uparrow\rangle \equiv c_{2\uparrow}^\dagger c_{4\uparrow}^\dagger |0\rangle \qquad (5.4.9)$$

with the vacuum state $|0\rangle$. The negative sign of the weights, in this case, results from the anti-commutation relation of fermion operators.

The naive solution of the negative-sign problem is to use the following identity [Hirsch 82, Takasu 86]:

$$\frac{\sum_{\{\sigma\}} Q\{\sigma\} W\{\sigma\}}{\sum_{\{\sigma\}} W\{\sigma\}} = \frac{\sum_{\{\sigma\}} Q\{\sigma\} R\{\sigma\} W'}{\sum_{\{\sigma\}} W'} \Bigg/ \frac{\sum_{\{\sigma\}} R\{\sigma\} W'}{\sum_{\{\sigma\}} W'}. \qquad (5.4.10)$$

Here each $W'\{\sigma\}$ is the absolute value of Boltzmann weight $W\{\sigma\}$,

$$W'\{\sigma\} \equiv |W\{\sigma\}|\,, \qquad (5.4.11)$$

and $R\{\sigma\}$ is the sign of it, namely

$$R\{\sigma\} \equiv \mathrm{sign}(W\{\sigma\}). \qquad (5.4.12)$$

Hence we have $W = RW'$, which yields (5.4.10).

A quantity Q is thereby measured in simulations of the system defined by the new Boltzmann weight W':

$$\langle Q \rangle = \frac{\langle QR \rangle'_{\rm MCS}}{\langle R \rangle'_{\rm MCS}}, \tag{5.4.13}$$

where $\langle \cdots \rangle'_{\rm MCS}$ stands for Monte Carlo average in simulations of the system W'. The denominator of (5.4.13),

$$\langle R \rangle'_{\rm MCS} = \frac{\sum_{\{\sigma\}} W}{\sum_{\{\sigma\}} |W|}, \tag{5.4.14}$$

is often called the negative-sign ratio.

The first part of the negative-sign problem is thereby solved. Nevertheless this solution is exactly the point from which the second part of the problem comes; a statistical error of the negative-sign ratio grows rapidly at low temperatures or for large systems.

The fact is understood as follows. The numerator of (5.4.14) is, in the limit $n \to \infty$, the partition function of the quantum system, $Z_{\rm q}$, while the denominator of (5.4.14) converges to the partition function of another quantum system, $Z'_{\rm q}$, as is shown in Section 4.2. Thus we have

$$Z_{\rm q} = {\rm e}^{-\beta F} \qquad \text{and} \qquad Z'_{\rm q} = {\rm e}^{-\beta F'}, \tag{5.4.15}$$

where F (F') stands for the free energy of the system $Z_{\rm q}$ ($Z'_{\rm q}$). The negative-sign ratio is given by

$$\langle R \rangle'_{\rm MCS} = {\rm e}^{-\beta(F-F')} \qquad \text{as} \quad n \to \infty. \tag{5.4.16}$$

The value $\langle R \rangle'_{\rm MCS}$ is bounded from above by unity, and therefore we have

$$F > F'. \tag{5.4.17}$$

First, at low temperatures we can replace F and F' by the ground-state energies $E_{\rm g}$ and $E'_{\rm g}$ of the systems $Z_{\rm q}$ and $Z'_{\rm q}$, respectively, and hence [Morgenstern 89, Loh 90, Hatano 91b, Hatano 92]

$$\langle R \rangle'_{\rm MCS} \simeq {\rm e}^{-\beta(E_{\rm g}-E'_{\rm g})} \qquad \text{as} \quad \beta \to \infty. \tag{5.4.18}$$

Second, assuming the extensivity of the free energy, we have [Hirsch 82]

$$\langle R \rangle'_{\rm MCS} \simeq {\rm e}^{-\beta(f-f')N} \qquad \text{as} \quad N \to \infty, \tag{5.4.19}$$

where N is the system size and f (f') is the free-energy density of the system $Z_{\rm q}$ ($Z'_{\rm q}$).

The statistical error of the negative-sign ratio is given by [Muller-Krumbhaar 73]

$$\Delta \langle R \rangle'_{\rm MCS} = \sqrt{\frac{2\tau+1}{M}} \sqrt{\langle R^2 \rangle'_{\rm MCS} - \langle R \rangle'^{\,2}_{\rm MCS}} = \sqrt{\frac{2\tau+1}{M}} \sqrt{1 - \langle R \rangle'^{\,2}_{\rm MCS}}, \tag{5.4.20}$$

where τ denotes auto-correlation time of simulation dynamics, and M denotes the number of Monte Carlo steps. The relative error of the negative-sign ratio behaves as

$$\begin{aligned} \frac{\Delta \langle R \rangle'_{\rm MCS}}{\langle R \rangle'_{\rm MCS}} &= \sqrt{\frac{2\tau+1}{M}} \sqrt{\langle R \rangle'^{\,-2}_{\rm MCS} - 1} \\ &\simeq \sqrt{\frac{2\tau+1}{M}} \times \begin{cases} {\rm e}^{\beta(E_{\rm g}-E'_{\rm g})} \gg 1 & \text{as} \quad \beta \to \infty, \\ {\rm e}^{\beta(f-f')N} \gg 1 & \text{as} \quad N \to \infty. \end{cases} \end{aligned} \tag{5.4.21}$$

At low temperatures or for large systems, the statistical error grows rapidly, and hence we cannot precisely estimate the negative-sign ratio and physical quantities (5.4.13) by Monte Carlo simulations.

The negative-sign problem has been the main obstacle to Monte Carlo studies of frustrated quantum spin systems, e.g., antiferromagnets on triangular lattices and on square lattices with next-nearest-neighbor interactions (J_1-J_2 model).

Though the problem has not been completely solved, a method of relieving the difficulty has been proposed [Nakamura 92a, Nakamura 92b, Nakamura 92c] with the use of the so-called reweighting method, which has been used in simulations of classical systems. The formula (5.4.10) holds for any set of W', when we change the definition of R from (5.4.12) to

$$R\{\sigma\} \equiv \frac{W\{\sigma\}}{W'\{\sigma\}}. \tag{5.4.22}$$

We thus can take arbitrary W' instead of the specific choice $W' = |W|$ as long as the phase space of W' is equal to or larger than that of W.

From the viewpoint of the reweighting method, the negative-sign problem is explained as follows. Although the formula is correct in the limit of an infinite number of Monte Carlo steps, it is known in simulations of classical systems that the formula may yield systematic and statistical errors in the actual use of it. The errors may appear when the distribution of W in the phase space is rather different from that of W'. This is actually the case in the present problem. Configurations sampled in the simulations of $W' = \mathrm{sign}(W)$ are counted almost in vain.

We anticipate that the growth rate of the error, (5.4.21), is reduced when we take W' whose structure is more similar to that of W than to that of $|W|$. We describe the subject in detail in Chapter 4.

In another approach to the negative-sign problem, the nodal surface of the Boltzmann weight $W\{\sigma\}$ in the phase space $\{\sigma\}$ is assumed to exist [Fahy 90, Fahy 91]. This approach may be related to the fixed-node approximation in the diffusion Monte Carlo methods [Ceperley 80, Moskowitz 82].

Recently, the measurement of quantities in the ground state using the behavior (5.4.18) has been proposed.

The ground-state energy of the positive-weight system, E'_{g}, can be measured without any significant statistical errors. On the other hand, owing to the behavior $\langle R\rangle'_{\mathrm{MCS}} \propto \exp[-\beta(E_{\mathrm{g}} - E'_{\mathrm{g}})]$, we may know the energy difference $(E_{\mathrm{g}} - E'_{\mathrm{g}})$ analyzing the temperature dependence of the negative-sign ratio; see Fig. 5.7. Though the statistical error of each data points may be large, the combination of them may yield an accurate estimate of $E_{\mathrm{g}} - E'_{\mathrm{g}}$. Thus we can obtain the estimate of E_{g} [Hamann 90].

To measure other quantities, the correction-ratio method may be applicable [Furukawa 91a]. We can estimate rather precisely the quantity $\langle Q\rangle'_{\mathrm{MCS}}$ which is measured with the factor R neglected. We can correct the estimate to obtain $\langle Q\rangle_{\mathrm{MCS}}$ by the correction-ratio method.

The "ratio correction" is defined by

$$Q_{\mathrm{RC}} \equiv \frac{\sum QW}{\sum QW'} = \frac{\sum QRW'}{\sum W'} \Big/ \frac{\sum QW'}{\sum W'} = \frac{\langle QR\rangle'_{\mathrm{MCS}}}{\langle Q\rangle'_{\mathrm{MCS}}}. \tag{5.4.23}$$

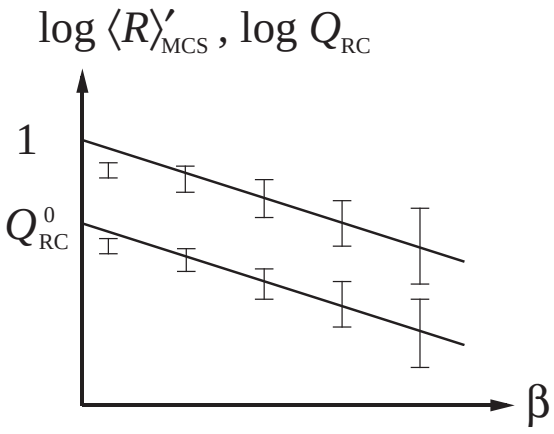

Figure 5.7 The temperature dependence of the negative-sign ratio, (5.4.18), and the ratio correction, (5.4.25).

Comparing (5.4.23) with (5.4.10), we have

$$\langle Q\rangle_{\rm MCS} = \langle Q\rangle'_{\rm MCS}\,\frac{Q_{\rm RC}}{\langle R\rangle'_{\rm MCS}}. \tag{5.4.24}$$

If both the quantities $\langle Q\rangle_{\rm MCS}$ and $\langle Q\rangle'_{\rm MCS}$ are finite at the zero temperature, that the ratio correction must behave as

$$Q_{\rm RC} \simeq Q^0_{\rm RC}{\rm e}^{-\beta(E_{\rm g}-E'_{\rm g})} \qquad \text{as} \quad \beta\to\infty \tag{5.4.25}$$

to cancel the behavior of $\langle R\rangle'_{\rm MCS}$; see Fig. 5.7. Hence we have

$$\langle Q\rangle_{\rm MCS} \simeq \langle Q\rangle'_{\rm MCS}\,Q^0_{\rm RC} \qquad \text{as} \quad \beta\to\infty. \tag{5.4.26}$$

If the asymptotic behavior (5.4.25) can be observed even at high temperatures, (which is actually the case in [Furukawa 91a]), we can avoid simulations at low temperatures, and hence suppress the statistical error.

The combination of the reweighting method and the correction-ratio method may be quite useful [Nakamura 92c].

5.5 Quantum transfer-matrix method

In this section we describe a quantum transfer-matrix method which is based on the Suzuki-Trotter decomposition.

In (5.3.7) we rewrote the density matrix of a quantum system ${\rm e}^{-\beta\mathcal{H}}$ as a product of matrices, using the Suzuki-Trotter decomposition. In Section 5.3 we described a method of performing the multiplications of the matrices by a Monte Carlo simulation. If the linear dimension of the matrices is small enough for computer memory, the multiplication of the matrices can be performed as it is [Betsuyaku 84, Suzuki 85a].

In other words we express the partition function of the classical system in Fig. 5.4 in terms of a transfer matrix as

$$Z_n = {\rm Tr}\,(T_1T_2)^n, \tag{5.5.1}$$

where T_1 and T_2 denote the matrices

$$T_1 = \left\langle \{\sigma\} \left| {\rm e}^{-\beta A/n} \right| \{\sigma\}' \right\rangle \qquad \text{and} \qquad T_2 = \left\langle \{\sigma\} \left| {\rm e}^{-\beta B/n} \right| \{\sigma\}' \right\rangle. \tag{5.5.2}$$

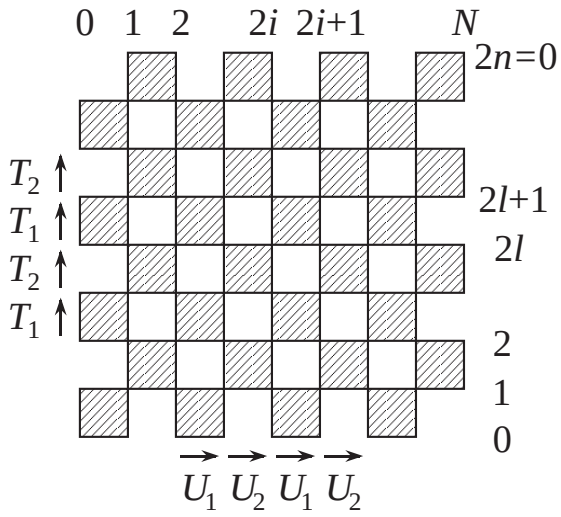

Figure 5.8 The real-space transfer matrices T_1 and T_2, and the virtual-space transfer matrices U_1 and U_2.

The matrices transfer a configuration on a row to the next row in the Trotter direction. The linear dimension of the matrices is equal to the dimension of the Hilbert space; 2^{N+1} in the case of (5.3.1).

An important feature is the locality of the interaction again as was mentioned below (5.3.13). Because of the locality, the transfer matrices are expressed as direct products of small matrices as in (5.3.14). We apply the matrices (5.3.16) to a vector successively; hence we do not have to store the whole matrix elements of T_1 and T_2. The size of the vector, when we treat an $S = 1/2$ system with 25 spins, is about 32×10^6. If we prepare an 8-byte real number for each component of the vector, the size of the memory storage is 256 megabytes, which is actually manageable on recent large-scale computers.

Note that the transfer matrix is explicitly block-diagonalized owing to the conservation law (5.3.19). Each sector is labeled with the total magnetization of spins on a row; in other words with a number of world lines. A state in a sector does not mix with states in the other sectors. Therefore the application of the transfer matrix to a state vector can be carried out in each sector separately. This aspect of the matrix is useful in reducing the size of the memory storage and computational time.

The maximum size manageable by the method above, (which is called the real-space transfer-matrix method by contrast with the method described below,) is less than 30 spins so far. An interesting reformulation of the transfer-matrix method was proposed [Suzuki 85a, Betsuyaku 85, Yokota 86] in order to treat much larger systems. The method is called the virtual-space transfer-matrix method. We describe the system in Fig. 5.4 in terms of matrices which transfer a configuration on a column to the next column in the space direction:

$$Z_n(N) = \mathrm{Tr}\,(U_1 U_2)^N. \tag{5.5.3}$$

Here we have assumed the periodic boundary condition $\sigma_N = \sigma_0$. We call U_1 and U_2 virtual-space transfer matrices; see Fig. 5.8.

Each transfer matrix is again expressed as a direct product of small matrices:

$$U_1 = \prod_{l=0}^{n-1} u(2i, 2l) \qquad \text{and} \qquad U_2 = \prod_{l=0}^{n-1} u(2i+1, 2l+1). \tag{5.5.4}$$

We derive the matrix u from the matrix (5.3.16) changing the ordering of the matrix elements as follows:

$$u(i,l) = \begin{array}{c} \\ \langle\uparrow\downarrow| \\ \langle\uparrow\uparrow| \\ \langle\downarrow\downarrow| \\ \langle\downarrow\uparrow| \end{array} \begin{array}{c} \begin{array}{cccc} |\downarrow\uparrow\rangle & |\downarrow\downarrow\rangle & |\uparrow\uparrow\rangle & |\uparrow\downarrow\rangle \end{array} \\ \begin{pmatrix} c & & & \\ & b & a & \\ & a & b & \\ & & & c \end{pmatrix} \end{array}. \tag{5.5.5}$$

Here the definition of the bra and ket vectors are changed as

$$\left.\begin{array}{l} \langle\sigma_{i,l}, \sigma_{i+1,l}| \\ |\sigma_{i,l+1}, \sigma_{i+1,l+1}\rangle \end{array}\right\} \longrightarrow \left\{\begin{array}{l} \langle\sigma_{i,l}, \sigma_{i,l+1}| \\ |\sigma_{i+1,l}, \sigma_{i+1,l+1}\rangle \end{array}\right. . \tag{5.5.6}$$

The transfer matrices U_1 and U_2 are explicitly block-diagonalized into sectors. This fact can be understood as follows. If we redefine the signs of the spins on the $(l+1)$-th column [Koma 87, Koma 89], that is,

$$\sigma_{i,l+1} \longrightarrow \sigma'_{i,l+1} \equiv -\sigma_{i,l+1} \qquad \text{for all} \quad i, \tag{5.5.7}$$

then the matrix (5.5.5) conserves the staggered magnetization. This conservation rule is derived from the original conservation law (5.3.19) as follows:

$$\sigma_{i,l} - \sigma_{i,l+1} = -\sigma_{i+1,l} + \sigma_{i+1,l+1} = \sigma'_{i+1,l} - \sigma'_{i+1,l+1}. \tag{5.5.8}$$

Hence each sector of transfer matrices is labeled with the total staggered magnetization of spins on a column:

$$M_{\text{stag}} \equiv \sum_{l=0}^{2n-1} (-1)^l \sigma_{i,l}. \tag{5.5.9}$$

The virtual-space transfer-matrix method is convenient especially in studying thermodynamic properties of long chains. Computational time grows only proportionally to the system size, and the size of necessary memory storage does not depend on the system size. (The size of the storage, on the other hand, depends on the Trotter number. We have to store a configuration of spins on a column.) Many one-dimensional systems have been thus studied. Takada and Kubo extensively studied critical properties of $S = 1/2$ XXZ chains [Takada 86] and $S = 1$ XXZ chains [Kubo 86]. Many other studies on the latter model have been reported [Betsuyaku 86b, Delica 91, Kubo 92] in connection with the Haldane problem [Haldane 83a, Haldane 83b, Affleck 89].

A remarkable feature of the virtual-space transfer-matrix method emerges when we study the thermodynamic limit of the quantum system. Several eigenvalues of the virtual-space transfer matrix describe the thermodynamic behavior of the system.

The feature comes from the following interchangeability theorem [Suzuki 85a, Suzuki 87c]. The free-energy density of the quantum N-spin system in the thermodynamic limit is written in the form

$$f_{\text{q}} = -\lim_{N\to\infty}\lim_{n\to\infty} \frac{1}{N\beta} \log Z_n(N) = -\lim_{N\to\infty}\lim_{n\to\infty} \frac{1}{N\beta} \log \text{Tr}\, (U_1 U_2)^{N/2}. \tag{5.5.10}$$

The statement of the interchangeability theorem is that we can exchange the order of the two limit operations $N \to \infty$ and $n \to \infty$: that is,

$$f_{\rm q} = -\lim_{n\to\infty}\lim_{N\to\infty}\frac{1}{N\beta}\log {\rm Tr}\,(U_1U_2)^{N/2}. \tag{5.5.11}$$

In the limit of $N \to \infty$ the partition function converges to

$$\lim_{N\to\infty} {\rm Tr}\,(U_1U_2)^{N/2} = \Lambda_1^N, \tag{5.5.12}$$

where the maximum eigenvalue of the matrix U_1U_2 is defined as Λ_1^2. The free-energy density (5.5.12) is thereby written as

$$f_{\rm q} = -\frac{1}{\beta}\lim_{n\to\infty}\log\Lambda_1. \tag{5.5.13}$$

It is remarkable that only one eigenvalue gives a thermodynamic quantity.

The virtual-space transfer-matrix method yields another useful formula for the correlation length. A spin-spin correlation function $\langle\sigma_i^\alpha\sigma_{i+L}^\alpha\rangle$ in the thermodynamic limit is written in terms of the virtual-space transfer matrix as follows:

$$\left\langle\sigma_i^\alpha\sigma_{i+L}^\alpha\right\rangle = \lim_{N\to\infty}\lim_{n\to\infty}\frac{1}{Z_n(N)}{\rm Tr}\,\sigma^\alpha(U_1U_2)^{L/2}\sigma^\alpha(U_1U_2)^{(N-L)/2}. \tag{5.5.14}$$

The correlation length is defined by

$$\xi^{-1} \equiv -\lim_{L\to\infty}\frac{1}{L}\log\left\langle\sigma_i^\alpha\sigma_{i+L}^\alpha\right\rangle. \tag{5.5.15}$$

The exchange of the limit operations is followed by

$$\lim_{L\to\infty}\lim_{N\to\infty}\frac{1}{Z_n(N)}{\rm Tr}\,\sigma^\alpha(U_1U_2)^{L}\sigma^\alpha(U_1U_2)^{(N-L)/2} = |\langle\psi_1\,|\sigma^\alpha|\,\psi_2\rangle|^2\left(\frac{\Lambda_2}{\Lambda_1}\right)^L \tag{5.5.16}$$

where the second-largest eigenvalue of the matrix U_1U_2 is defined as Λ_2^2. Thus the correlation length (5.5.15) is given by

$$\xi^{-1} = \lim_{n\to\infty}\log\left(\frac{\Lambda_1}{\Lambda_2}\right). \tag{5.5.17}$$

Suzuki and Inoue [Suzuki 87c, Inoue 88] first pointed out that it is possible to treat quantum systems analytically on the basis of these formulae (5.5.13) and (5.5.17). This approach has been further developed as the thermal Bethe-ansatz method by several researchers [Koma 87, Koma 89, Koma 90, Yamada 90, Tsunetsugu 91]. They obtained thermal Bethe-ansatz equations analytically for one-dimensional spin-1/2 models and one-dimensional Hubbard models with a finite Trotter number, and solved them numerically. As for the XYZ model without a magnetic field and the XXZ model with a magnetic field, Takahashi [Takahashi 91a, Takahashi 91b] obtained the equations in the infinite-Trotter-number limit, and thereby calculated the temperature dependence of the free energy and the correlation length numerically rigorously.

5.6 Monte Carlo power method

In this section we describe a Monte Carlo power method, by which we can numerically obtain the maximum eigenvalue of a transfer matrix.

Analytic solutions of the virtual-space transfer matrix, which are mentioned in the preceeding section, are not available for higher-spin chains. Hence we have to calculate the eigenvalues of the matrix numerically.

The most straightforward method of obtaining the maximum eigenvalue of a asymmetric matrix T is the power method; we calculate the Rayleigh quotient,

$$\lambda(N) \equiv \frac{\left\langle \phi \left| T^{N+1} \right| \phi \right\rangle}{\left\langle \phi \left| T^{N} \right| \phi \right\rangle}, \tag{5.6.1}$$

and then take the limit $N \to \infty$. If the test vector $|\phi\rangle$ and the eigenvector belonging to the maximum eigenvalue Λ_1 have an overlap, the eigenvalue emerges in the form

$$\lambda(N) = \Lambda_1 + O(\mathrm{e}^{-N/\xi}). \tag{5.6.2}$$

The correction term disappears rapidly. Thus the free-energy density (5.5.13) is given by

$$f_{\mathrm{q}} = -\frac{1}{\beta} \lim_{n\to\infty} \lim_{N\to\infty} \log \frac{\left\langle \phi \left| (U_1 U_2)^{N/2+1} \right| \phi \right\rangle}{\left\langle \phi \left| (U_1 U_2)^{N/2} \right| \phi \right\rangle}. \tag{5.6.3}$$

The problem here is the following: when we increase the Trotter number, the size of necessary memory storage grows rapidly especially in higher-spin cases. Hence the Trotter number attainable so far is less than 10 even for $S = 1$. At temperatures below $T \leq 0.1$, the convergence of the numerical data to the infinite-Trotter-number limit may not be satisfactory.

A partial solution is to use the cluster-transfer-matrix method [Tsuzuki 85, Tsuzuki 86, Betsuyaku 86a] mentioned below (5.3.20) in Section 5.3. We can reduce the magnitude of correction-term coefficients of the Suzuki-Trotter approximants, and thereby we may recover satisfactory convergence even at low temperatures. By this method, however, we have to diagonalize the matrices A and B in order to obtain $\mathrm{e}^{-\beta A/n}$ and $\mathrm{e}^{-\beta B/n}$. The diagonalization needs great memory storage, and hence the size m of manageable clusters is limited particularly in higher-spin systems.

Another solution is to use the Monte Carlo power method described below [Koma 93], by which we can estimate the Rayleigh quotient. The essential idea is a special choice of the test vector $|\phi\rangle$:

$$|\phi\rangle = \sum_{\{\sigma\}_0} |\{\sigma\}_0\rangle \,, \tag{5.6.4}$$

where $\{\sigma\}$ denotes a configuration of $2n$ spins on a column, that is,

$$\{\sigma\}_0 \equiv \{\sigma_{0,0}, \sigma_{0,1}, \ldots, \sigma_{0,2n-1}\}. \tag{5.6.5}$$

In other words we define the test vector as a superposition of all the members of the orthonormal set.

If all the elements of the transfer matrix is non-negative, the test vector (5.6.4) and the eigenvector belonging to the maximum eigenvalue necessarily has an overlap; according to the Perron-Frobenius theorem, all the components of the eigenvector is non-negative.

Employing the choice (5.6.4), we interpret the denominator of the Rayleigh quotient as

$$\begin{aligned}
&\left\langle \phi \left| (U_1 U_2)^{N/2} \right| \phi \right\rangle \\
&= \sum_{\{\sigma\}} \left\langle \{\sigma\}_0 \left| U_1 \right| \{\sigma\}_1 \right\rangle \left\langle \{\sigma\}_1 \left| U_2 \right| \{\sigma\}_2 \right\rangle \cdots \left\langle \{\sigma\}_{N-1} \left| U_2 \right| \{\sigma\}_N \right\rangle \\
&\equiv \sum_{\{\sigma\}} W\{\sigma\}, \qquad (5.6.6)
\end{aligned}$$

where each vector denotes a configuration of spins on a column. The total configuration $\{\sigma\}$ is defined by (5.3.11). We thus identify (5.6.6) with the partition function of the classical system in Fig. 5.8. On the boundaries of the system, any configurations $\{\sigma\}_0$ and $\{\sigma\}_N$ can appear, because of the choice (5.6.4). The *free boundary conditions* are required on $i = 0$ and $i = N$.

The numerator of the Rayleigh quotient is interpreted as follows:

$$\begin{aligned}
&\left\langle \phi \left| (U_1 U_2)^{N/2+1} \right| \phi \right\rangle \\
&= \sum_{\{\sigma\}} \left\langle \{\sigma\}_0 \left| U_1 \right| \{\sigma\}_1 \right\rangle \left\langle \{\sigma\}_1 \left| U_2 \right| \{\sigma\}_2 \right\rangle \cdots \left\langle \{\sigma\}_{N-1} \left| U_2 \right| \{\sigma\}_N \right\rangle \\
&\qquad \times \left\langle \{\sigma\}_N \left| U_1 \right| \{\sigma\}_{N+1} \right\rangle \left\langle \{\sigma\}_{N+1} \left| U_2 \right| \{\sigma\}_{N+2} \right\rangle \\
&= \sum_{\{\sigma\}} W\{\sigma\} Q_{\mathrm{eig}}\{\sigma\}, \qquad (5.6.7)
\end{aligned}$$

where

$$Q_{\mathrm{eig}}\{\sigma\} \equiv \sum_{\substack{\{\sigma\}_{N+1} \\ \{\sigma\}_{N+2}}} \left\langle \{\sigma\}_N \left| U_1 \right| \{\sigma\}_{N+1} \right\rangle \left\langle \{\sigma\}_{N+1} \left| U_2 \right| \{\sigma\}_{N+2} \right\rangle . \qquad (5.6.8)$$

The Rayleigh quotient hence reads

$$\lambda(N) = \frac{\sum_{\{\sigma\}} Q_{\mathrm{eig}} W}{\sum_{\{\sigma\}} W} = \langle Q_{\mathrm{eig}} \rangle_{\mathrm{MCS}} . \qquad (5.6.9)$$

In a Monte Carlo simulation of the system $W\{\sigma\}$, direct measurement of the quantity Q_{eig} on the end $i = N$ yields an estimate of the Rayleigh quotient. We can improve statistics, measuring a similar quantity on the other end $i = 0$.

It is notable that we can calculate the free energy of the system; usual Monte Carlo methods with importance sampling do not yield the free energy.

When the second-largest eigenvalue of a transfer matrix is the largest eigenvalue of a sector, the restriction of the summation enables us to obtain the eigenvalue. This feature will be actually utilized in Chapter 2 [Hatano 93a].

5.7 Auxiliary-field approach

In this section we review the auxiliary-field approach, which has been developed particularly to lattice fermion problems; for example the Hubbard model (5.1.9).

The auxiliary-field approach has been devised in order to circumvent the difficulty of the negative-sign problem of the Hubbard model, which we mention in Section 5.4. Particularly in the half-filled-band case on a bipartite lattice, we are free from the difficulty by employing the auxiliary-field approach.

The auxiliary-field approach, especially the grand-canonical Monte Carlo method, consists of the following four steps [Hirsch 83c, Hirsch 85a]. (i) We approximate the density matrix with the Suzuki-Trotter approximation, decomposing the Hamiltonian into K and V. (ii) We introduce an auxiliary Bose field to break up the Coulomb interaction between fermions (the Stratonovich-Hubbard transformation). (iii) We traces out the fermion degrees of freedom. The partition function becomes a sum with respect to the Bose-field degrees of freedom. (iv) We replace the summation by Monte Carlo summation using the importance sampling.

Because of the noncommutability (5.1.10), we cannot easily diagonalize the Hamiltonian in the 4^N-dimensional Hilbert space, when the size of the system N is large. We approximate the density matrix with the Suzuki-Trotter approximant, decomposing the Hamiltonian into two parts, K and V:

$$\mathrm{e}^{-\beta\mathcal{H}} \simeq \left(\mathrm{e}^{-\beta K/n}\mathrm{e}^{-\beta V/n}\right)^n. \tag{5.7.1}$$

Note that the kinetic-energy term breaks up in the form

$$\mathrm{e}^{-\beta K/n} = \prod_{\sigma=\uparrow,\downarrow} \mathrm{e}^{-\beta K_\sigma/n} \tag{5.7.2}$$

with

$$K_\sigma \equiv -t \sum_{\langle i,j\rangle} \left(c_{i\sigma}^\dagger c_{j\sigma} + c_{j\sigma}^\dagger c_{i\sigma}\right), \tag{5.7.3}$$

while the potential-energy term breaks up in the form

$$\mathrm{e}^{-\beta V/n} = \prod_i \mathrm{e}^{-\beta V_i/n} \tag{5.7.4}$$

with

$$V_i \equiv U\left(n_{i\uparrow} - \frac{1}{2}\right)\left(n_{i\downarrow} - \frac{1}{2}\right) - \mu \sum_{\sigma=\uparrow,\downarrow} n_{i\sigma}. \tag{5.7.5}$$

The second step is the Stratonovich-Hubbard transformation. The transformation, in the original form, is nothing but the inverse of the Gaussian integral [Stratonovich 57, Hubbard 59]. Hirsch devised another version of the transformation using a discrete Bose field, or an Ising variable [Hirsch 83b]:

$$\begin{aligned} \exp\left[-xU\left(n_\uparrow - \frac{1}{2}\right)\left(n_\downarrow - \frac{1}{2}\right) + \frac{xU}{4}\right] &= \frac{1}{2}\sum_{s=\pm1} \mathrm{e}^{xJs(n_\uparrow - n_\downarrow)} \\ &= \frac{1}{2}\sum_{s=\pm1}\prod_{\sigma=\uparrow,\downarrow} \mathrm{e}^{xJ\sigma s n_\sigma}, \end{aligned} \tag{5.7.6}$$

where the coefficient a is defined by

$$\cosh xJ = \mathrm{e}^{xU/2}. \tag{5.7.7}$$

The readers can confirm the identity (5.7.6) easily by checking it in the four cases $(n_\uparrow, n_\downarrow) = (0,0), (0,1), (1,0), (1,1)$. The coupling constant J behaves as $xJ \simeq \sqrt{xU}$ for $x \simeq 0$.

The auxiliary Ising field s plays a role of a mean field. Consider the case that an upward-spin electron occupies a site, $n_\uparrow = 1$. Then the system favors the state $s = 1$ because of the coupling $sn_\uparrow$, and hence tends to refuse occupation of the site by a downward-spin electron because of the coupling $-sn_\downarrow$. The field s is likely to point the same direction as the spin of an electron on the site. We can thus regard the field as a mean field. In fact the Hartree-Fock mean-field approximation to the Hubbard model and the saddle-point approximation of an effective action derived from (5.7.1) are equivalent to each other [Fradkin 91].

Applying the transformation (5.7.6) to each operator in the right-hand side of (5.7.4), we express the partition function of the system in the form:

$$Z_{\mathrm{q}} \simeq Z_n = A^{-1} \sum_{\{s\}} W_\uparrow\{s\} W_\downarrow\{s\}, \tag{5.7.8}$$

where

$$W_\sigma\{s\} \equiv \mathrm{Tr} \prod_{l=1}^{n} \left(\mathrm{e}^{-\beta K_\sigma/n} \mathrm{e}^{-\beta \tilde{V}_\sigma\{s\}_l/n} \right) \tag{5.7.9}$$

with a new potential energy

$$\tilde{V}_\sigma\{s\}_l \equiv -\sum_i \left(J\sigma s_{il} + \mu \right) n_{i\sigma}, \tag{5.7.10}$$

and a coefficient

$$A \equiv 2^{Nn} \mathrm{e}^{\beta UN/4}. \tag{5.7.11}$$

Note that $\{s\}$ consists of Nn pieces of Ising variables, that is, $\{s_{il}\}$ for $i = 1, 2, \ldots, N$ and $l = 1, 2, \ldots, n$.

We have described the system as the one where boson fields and fermions are interacting. The Monte Carlo method of studying such a system was given [Scalapino 81a, Blankenbecler 81, Scalapino 81b]. We only have to apply the formalism to the present problem. We can carry out the trace operation Tr in (5.7.9), which is the third step of the formulation described later. After the third step we regard (5.7.8) as the partition function of a classical system with Nn Ising spins interacting through a certain long-range interaction.

Before that we briefly mention the reason why, using this approach, we can expect the reduction of the difficulty of the negative-sign problem. Consider an auxiliary-field configuration shown in Fig. 5.9. As was discussed above, an Ising field on a site and the spin of an electron on the site tends to point the same direction. When two upward-spin electrons exist, the most favored world-line configuration is the one shown in Fig. 5.9 (a) [Hirsch 86]. This configuration gives a negative weight as was described in (5.4.8). In the auxiliary-field approach, however, the fermion degrees of freedom are traced out in (5.7.9); in other words many other world-line configurations are summed up. For example, the world-line configuration in Fig. 5.9 (b), with the auxiliary-fields fixed, gives a positive weight. We can expect that cancellation among all the configurations results in reduction of the negative weight.

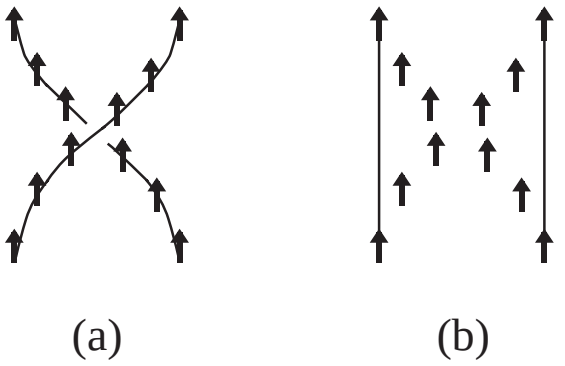

Figure 5.9 The auxiliary-field configurations (arrows) and the fermion world-line configurations (thick lines). (a) This configuration has a negative Boltzmann weight. (b) This configuration has a positive Boltzmann weight. The contributions of both the configurations are summed up, when we trace out the fermion degrees of freedom.

In the half-filled case in particular, the negative-sign problem disappears. Signs of the weight factors $W_\uparrow$ and $W_\downarrow$ are the same, and hence the product of them is always non-negative [Hirsch 83c, Hirsch 85a]. The proof is given in Appendix 5.D.

The third step is to carry out the trace operation in (5.7.9). This is possible because the operators K_σ and $\tilde{V}_\sigma$ are written in quadratic forms with respect to fermion operators:

$$-\beta K/n = c_i^\dagger \overline{K}_{ij} c_j \qquad \text{and} \qquad -\beta \tilde{V}/n = c_i^\dagger \overline{V}_{ij} c_j, \tag{5.7.12}$$

where $\overline{K}$ and $\overline{V}$ are $N \times N$ matrices defined so as to reproduce (5.7.3) and (5.7.10). Summation over repeated indices is assumed in (5.7.12). (For the time being we leave out the subscript σ.) Note that the potential energy $\tilde{V}$ depends on the auxiliary fields $\{s\}_l$, hence $\overline{V}$ does. (Hereafter the bar over a symbol indicates that the symbol denotes an $N \times N$ matrix.)

According to the equality (5.E.1) proved in Appendix 5.E, we have [Blankenbecler 81, Hirsch 85a, De Raedt 92]

$$\prod_{l=1}^{n} \left(\mathrm{e}^{c_i^\dagger \overline{K}_{ij} c_j} \mathrm{e}^{c_i^\dagger \overline{V}_{ij} c_j} \right) = \mathrm{e}^{c_i^\dagger \overline{H}_{ij} c_j}, \tag{5.7.13}$$

where the $N \times N$ matrix $\overline{H}$ is defined by

$$\prod_{l=1}^{n} \left(\mathrm{e}^{\overline{K}} \mathrm{e}^{\overline{V}} \right) = \mathrm{e}^{\overline{H}}. \tag{5.7.14}$$

The trace operation yields [Blankenbecler 81, Hirsch 85a, De Raedt 92]

$$W = \mathrm{Tr}\, \mathrm{e}^{c_i^\dagger \overline{H}_{ij} c_j} = \det \left[\overline{I} + \mathrm{e}^{\overline{H}} \right], \tag{5.7.15}$$

where $\overline{I}$ denotes the $N \times N$ identity matrix. Here we have used the equality (5.E.18) in Appendix 5.E.

Before proceeding to the fourth step we prepare a formula for measuring a physical quantity Q. Repeating the same procedure as in (5.7.1)-(5.7.14), we have

$$\langle Q \rangle_{\mathrm{q}} \simeq \frac{1}{Z_n} \sum_{\{s\}} \mathrm{Tr}\, Q \prod_{\sigma=\uparrow,\downarrow} \mathrm{e}^{c_i^\dagger \overline{H}_{ij} c_j}, = \frac{\sum_{\{s\}} \tilde{Q}\{s\} W_\uparrow\{s\} W_\downarrow\{s\}}{\sum_{\{s\}} W_\uparrow\{s\} W_\downarrow\{s\}} = \left\langle \tilde{Q} \right\rangle_{\mathrm{MCS}}, \tag{5.7.16}$$

where

$$\tilde{Q}\{s\} \equiv \frac{1}{W_\uparrow W_\downarrow} \mathrm{Tr}\, Q \prod_{\sigma=\uparrow,\downarrow} \mathrm{e}^{c_i^\dagger \overline{H}_{ij} c_j}. \tag{5.7.17}$$

Thus the average of $\tilde{Q}$ measured in a Monte Carlo simulation approximate the quantum-statistical average $\langle Q \rangle_{\rm q}$ as is mentioned in (5.C.1).

The most important quantity is the Green's functions $Q = c_{k\sigma} c_{l\sigma}^{\dagger}$. We can write other physical quantities in terms of the Green's functions in principle, using Wick's theorem. In order to obtain the equal-time Green's function we measure

$$\tilde{Q} = \overline{G}_{kl} \equiv \frac{1}{W} \mathrm{Tr}\, c_k c_l^{\dagger} \mathrm{e}^{c_i^{\dagger} \overline{H}_{ij} c_j}. \tag{5.7.18}$$

Here we have left out the spin index σ. Using a similar procedure to the one which gives (5.7.15), we have the following simple formula [Blankenbecler 81, Hirsch 85a]:

$$\overline{G} = \left(\overline{I} + \mathrm{e}^{\overline{H}} \right)^{-1}. \tag{5.7.19}$$

See the derivation of (5.E.20) in Appendix 5.E for the details. This matrix $\overline{G}$ plays an important role below. A measurement formula for the Matsubara Green's function is also given in Appendix 5.E.

The fourth step is to evaluate (5.7.16) using the importance-sampling method. In order to perform a simulation we have to calculate the ratio

$$R = R_{\uparrow} R_{\downarrow} \equiv \frac{W'_{\uparrow}}{W_{\uparrow}} \cdot \frac{W'_{\downarrow}}{W_{\downarrow}}, \tag{5.7.20}$$

as was explained in Section 5.1. Here W'_{σ} denotes the weight calculated under a new spin configuration. the new configuration differs from the old configuration by the direction of a spin. First consider a flip of a spin on the n-th layer $l = n$:

$$s_{jn} \longrightarrow s'_{jn} = -s_{jn}. \tag{5.7.21}$$

The difference between $W\{s\}$ and $W\{s\}'$ comes from the difference between $\exp(\overline{V})$ and $\exp(\overline{V}')$: see (5.7.14)-(5.7.15). Since the matrix $\overline{V}$ is diagonal, we can write down the following expression:

$$\mathrm{e}^{\overline{V}'} = \mathrm{e}^{\overline{V}} \overline{\Delta}, \tag{5.7.22}$$

where

$$\overline{\Delta} \equiv \begin{pmatrix} & & \overset{j}{\downarrow} & & \\ 1 & & & & \\ & 1 & & & \\ & & \gamma+1 & & \\ & & & 1 & \\ & & & & \ddots \end{pmatrix} \leftarrow j \tag{5.7.23}$$

with

$$\gamma + 1 \equiv \exp\left(\frac{-2\beta J \sigma s_{jn}}{n} \right). \tag{5.7.24}$$

Using the expression (5.7.22) and the "Green's function" (5.7.19), we have

$$R = \frac{\det\left[\overline{I} + \mathrm{e}^{\overline{H}} \overline{\Delta} \right]}{\det\left[\overline{I} + \mathrm{e}^{\overline{H}} \right]} = \det\left[\overline{I} + \left(\overline{I} - \overline{G} \right) \left(\overline{\Delta} - \overline{I} \right) \right] \tag{5.7.25}$$

Since all the elements of the matrix $\overline{\Delta}-\overline{I}$ but one is vanishing, straightforward calculation gives the final result

$$R = 1 + \gamma \left(1 - \overline{G}_{jj}\right). \tag{5.7.26}$$

The probability that s_{jn} is flipped in a step of the simulation is obtained by $R_\uparrow R_\downarrow/(1 + R_\uparrow R_\downarrow)$. Note that, except in the half-filled case, the value R can be negative; we must replace R by $|R|$ as was done in Section 5.4.

We notice that it is convenient to keep values $\overline{G}$ in memory storage. After we update a spin s_{jn} we also have to update the values of $\overline{G}$: $\overline{G}\{s\} \longrightarrow \overline{G}' \equiv \overline{G}\{s\}'$. It takes much time to calculate $\overline{G}'$ from the first definition (5.7.19). We construct $\overline{G}'$ from $\overline{G}$ in less time as follows. Using the expression (5.7.22) again, we have

$$\overline{G}' = \left[\overline{I} + \left(\overline{G}^{-1} - \overline{I}\right)\overline{\Delta}\right]^{-1} = \left[\overline{I} + \left(\overline{I} - \overline{G}\right)\left(\overline{\Delta} - \overline{I}\right)\right]^{-1}\overline{G} \equiv \overline{C}\,\overline{G}. \tag{5.7.27}$$

The matrix $\overline{C}^{-1} \equiv \overline{I} + (\overline{I} - \overline{G})(\overline{\Delta} - \overline{I})$ is a sparse matrix. It is possible to invert $\overline{C}^{-1}$ to $\overline{C}$ analytically.

When we want to flip a spin on the $(n-1)$-th layer, we rewrite the matrix $\overline{G}$ in the form

$$\overline{G}'' \equiv \left(\overline{I} + \mathrm{e}^{\overline{H}''}\right)^{-1} = \left(\mathrm{e}^{\overline{K}_n}\mathrm{e}^{\overline{V}_n}\right)\overline{G}\left(\mathrm{e}^{-\overline{V}_n}\mathrm{e}^{-\overline{K}_n}\right) \tag{5.7.28}$$

where

$$\mathrm{e}^{\overline{H}''} \equiv \left(\mathrm{e}^{\overline{K}_n}\mathrm{e}^{\overline{V}_n}\right)\prod_{l=1}^{n-1}\left(\mathrm{e}^{\overline{K}_l}\mathrm{e}^{\overline{V}_l}\right). \tag{5.7.29}$$

Here we have to re-construct the matrices $\mathrm{e}^{\overline{K}_n}$ and $\mathrm{e}^{\overline{V}_n}$ from their definition.

To summarize, the algorithm goes as follows. First, choose an initial configuration $\{s\}$ and calculate $\overline{G}$, (5.7.19). Next, repeat the following many times.

(I) Repeat the following n times from $l = n$ to $l = 1$.

- **(1)** Repeat the following N times from $i = 1$ to $i = N$.
  - **(i)** In order to update s_{il}, calculate $P_{\text{flip}} \equiv R_\uparrow R_\downarrow/(1 + R_\uparrow R_\downarrow)$ using (5.7.26).
  - **(ii)** Compare P_{flip} and a random number P_{rnd}, and decide whether to flip the spin or not.
  - **(iii)** If you decide to flip it, update the matrix $\overline{G}$ using (5.7.27).
- **(2)** Reconstruct the matrix $\overline{G}$ using (5.7.28).

(II) Measure a quantity $\tilde{Q}$, (5.7.17).

The computational time for one Monte Carlo step depends on the size of the system as $N^3 n$. This size dependence is a disadvantage of the method: compare it with the dependence for the world-line approach, namely, proportional to Nn. First, since the matrix $\overline{C}$ in (5.7.27) is sparse, we execute only several operations in the step (iii) to obtain an element of the new matrix $\overline{G}'$. The number of the elements is N^2. We repeat the step Nn times as well. Hence the computational time for the step (iii) is proportional to $N^3 n$. Next, since the matrix $\mathrm{e}^{\overline{K}}\mathrm{e}^{\overline{V}}$ is not so sparse, the number of operations to be executed in the step (2), or in (5.7.28), is proportional to N^3. We repeat the step n times. Hence the computational time for the step (2) is also proportional to $N^3 n$.

There is no restriction on measurable quantities in the present method. In the world-line approach, on the other hand, there are some quantities that it is hard to measure, as is mentioned at the end of Appendix 5.C.

In addition it is known by experience that difficulty of the negative-sign problem is reduced using the method, which is expected from the above discussion.

At low temperatures, besides the negative-sign problem, we had another problem, namely the numerical instabilities. In the calculation of the matrix $e^{\overline{H}}$ in (5.7.14), we have to multiply many exponential operators. At low temperatures, each operator has a wide spectrum. In the multiplications of the operators, we have to add a very small number to a very large number. The addition tends to result in the numerical error.

This problem has been overcome by repeating orthogonalization [Sorella 89, White 89]. We execute the Gram-Schmidt orthogonalization of the exponential operators; thus we can sum up the small-number contributions separating them from the large-number contributions.

The auxiliary-field approach has been successfully applied to the half-filled Hubbard model [Hirsch 83c, Hirsch 85a, Gubernatis 85, Hirsch 87, Hirsch 89a], to the attractive-interaction Hubbard model [Hirsch 85b]. In both cases the negative-sign problem does not appear.

The approach has been applied even to the non-half-filled Hubbard model [Sorella 88, White 89, Imada 89]. The argument on the temperature dependence of the negative-sign problem, (5.4.18), has been developed in the studies on the model [Loh 90, Hamann 90, Sorella 91].

The method is now extended to an algorithm [Zhang 91a, Zhang 91b, Zhang 92] applicable to the t-J model [Kohn 64, Brinkman 70, Chao 77, Hirsch 85a, Anderson 87, Baskaran 87, Zhang 88].

5.8 Ground-state algorithms

We have introduced Monte Carlo algorithms for studies on finite-temperature properties. In the present section we introduce algorithms for studies on ground-state properties.

The study of ground-state phase transitions driven by quantum fluctuation is now one of the most interesting problems in condensed-matter physics. Critical points are defined in a parameter space of the relevant model, at which an energy gap from the ground state vanishes in the thermodynamic limit. At these critical points, correlation functions of the system show power-law behavior instead of exponential decay, and the correlation length diverges.

In investigating ground-state phase transitions using quantum Monte Carlo methods, however, there arises a problem, namely, the difficulty of taking the zero-temperature limit. We investigate the relevant system first at finite temperatures, and take the zero-temperature limit to extract the ground-state property. This can be performed practically at temperatures low enough to satisfy the inequality $T \ll \Delta E$. Here ΔE denotes the energy gap just above the ground state. Near phase boundaries the energy gap is narrow, and hence it is difficult to satisfy the condition $T \ll \Delta E$.

Moreover, when we treat frustrated spin systems or fermion systems, the negative-sign problem becomes quite serious at low temperatures.

Some attempts to circumvent the problems have been proposed [Kalos 74, Kuti 82, Blankenbecler 83, Sugiyama 86]. They are more or less based on the following formula:

$$\mathrm{e}^{-\beta\mathcal{H}}\,|\psi\rangle \longrightarrow \mathrm{e}^{-\beta E_{\mathrm{g}}}\,|\psi_{\mathrm{g}}\rangle \qquad \text{as} \quad \beta\to\infty, \tag{5.8.1}$$

where $|\psi_{\mathrm{g}}\rangle$ is the ground-state vector, E_{g} is the ground-state energy, and $|\psi\rangle$ is a trial vector which is not orthogonal to $|\psi_{\mathrm{g}}\rangle$. If the trial vector is orthogonal to the first excited state, the extraction of the ground state may be performed even at rather high temperatures (though the variable $T=1/\beta$ loses its meaning as the temperature). A quantity in the ground state is given by

$$\langle Q\rangle_{\mathrm{g}} \equiv \langle\psi_{\mathrm{g}}\,|Q|\,\psi_{\mathrm{g}}\rangle = \lim_{\beta\to\infty}\langle\!\langle Q\rangle\!\rangle_{\beta} \tag{5.8.2}$$

with

$$\langle\!\langle Q\rangle\!\rangle_{\beta} \equiv \frac{\left\langle\psi\left|\mathrm{e}^{-\beta\mathcal{H}}Q\mathrm{e}^{-\beta\mathcal{H}}\right|\psi\right\rangle}{\left\langle\psi\left|\mathrm{e}^{-2\beta\mathcal{H}}\right|\psi\right\rangle}. \tag{5.8.3}$$

In some methods the limit procedure $\beta\to\infty$ itself is simulated, by interpreting multiplications of a transfer matrix as a Markov process, We describe these methods in Section 5.9. In the present section we fix the parameter β to estimate quantities by a simulation. Analyzing the data we evaluate the quantities in the ground state. We describe application of the world-line approach (Section 5.3) and the auxiliary-field approach (Section 5.7) to the calculation of (5.8.2). (The former is the main subject of Chapter 3.)

First we describe the application of the the world-line approach [Hatano 93b]. Following the standard procedure [Suzuki 77b, Suzuki 86b, Suzuki 87b], we first decompose the density matrix as follows;

$$\mathrm{e}^{-\beta\mathcal{H}} = \left(\mathrm{e}^{-\beta A/(2n)}\mathrm{e}^{-\beta B/n}\mathrm{e}^{-\beta A/(2n)}\right)^n + O\left(\frac{\beta^3}{n^2}\right) \tag{5.8.4}$$

with

$$\mathcal{H} = A + B. \tag{5.8.5}$$

We should keep the Trotter number n smaller than β to eliminate the correction term $O(\beta^3/n^2)$. Application of the decomposition to (5.8.3) yields

$$\left\langle\psi\left|\mathrm{e}^{-2\beta\mathcal{H}}\right|\psi\right\rangle = \lim_{n\to\infty}\left\langle\psi\left|\mathrm{e}^{-\beta A/(2n)}\mathrm{e}^{-\beta B/n}\left(\mathrm{e}^{-\beta A/n}\mathrm{e}^{-\beta B/n}\right)^{2n-1}\mathrm{e}^{-\beta A/(2n)}\right|\psi\right\rangle. \tag{5.8.6}$$

Next we prepare an orthonormal set of bases which diagonalize the operators $\{\sigma_i^z\}$. We insert the resolution of the unit operator $\hat{1}$ between each pair of exponential operators in (5.8.4). At the same time we expand the trial function with respect to the bases as

$$|\psi\rangle = \sum F(\{\sigma\})\,|\{\sigma\}\rangle\,. \tag{5.8.7}$$

Thus we interpret the quantity (5.8.6) as the partition function of an Ising-spin system of the checkerboard type [Hirsch 82]. The partition function is given by [Hatano 93b]

$$Z_n \equiv \sum F(\{\sigma\}_0)W(\{\sigma\}_0,\{\sigma\}_1,\ldots,\{\sigma\}_{4n+1})F(\{\sigma\}_{4n+1}). \tag{5.8.8}$$

where

$$
\begin{aligned}
& W(\{\sigma\}_0, \{\sigma\}_1, \{\sigma\}_2, \ldots, \{\sigma\}_{4n+1}) \\
& \equiv \left\langle \{\sigma\}_0 \left| \mathrm{e}^{-\beta A/(2n)} \right| \{\sigma\}_1 \right\rangle \left\langle \{\sigma\}_1 \left| \mathrm{e}^{-\beta B/n} \right| \{\sigma\}_2 \right\rangle \\
& \quad \cdots \times \left\langle \{\sigma\}_{4n-1} \left| \mathrm{e}^{-\beta B/n} \right| \{\sigma\}_{4n} \right\rangle \left\langle \{\sigma\}_{4n} \left| \mathrm{e}^{-\beta A/(2n)} \right| \{\sigma\}_{4n+1} \right\rangle . \qquad (5.8.9)
\end{aligned}
$$

On the other hand, in the finite-temperature algorithm described in Section 5.3, we transform the partition function of the quantum system into that of the corresponding Ising system, (5.3.8). This system differs from the system (5.8.8) in boundary conditions. In the finite-temperature algorithm we require the periodic-boundary conditions $\{\sigma\}_{2n} = \{\sigma\}_0$. In the formulation (5.8.8) we require constrained-boundary conditions on the spins $\{\sigma\}_0$ and $\{\sigma\}_{4n+1}$; a spin configuration $\{\sigma\}_0$ appears with a rate determined by the Boltzmann factor $W(\{\sigma\}_0)$ times the extra factor $F(\{\sigma\}_0)$.

When we perform the importance sampling of (5.8.8), we have to flip the spins $\{\sigma\}_0$ and $\{\sigma\}_{4n+1}$,

$$\{\sigma\} \longrightarrow \{\sigma\}', \qquad (5.8.10)$$

according to the ratio

$$R = R_1 R_2, \qquad (5.8.11)$$

where

$$R_1 \equiv \frac{W(\{\sigma\}_0')}{W(\{\sigma\}_0)} \qquad (5.8.12)$$

and

$$R_2 \equiv \frac{F(\{\sigma\}_0')}{F(\{\sigma\}_0)}. \qquad (5.8.13)$$

Since the interactions of the Ising system are of short range, the factor R_1 can be calculated easily. The factor R_2 can also be calculated for a wide class of trial functions [Hatano 93b]. The other spins are flipped only according to the factor R_1.

The same procedure as (5.8.4)-(5.8.9) yields [Hatano 93b]

$$\langle\langle Q \rangle\rangle_\beta \simeq \frac{1}{Z_n} \sum_{\{\sigma\}} \tilde{Q} f W f, \qquad (5.8.14)$$

where

$$\tilde{Q}(\{\sigma\}_{2n}, \{\sigma\}_{2n+1}) \equiv \frac{\left\langle \{\sigma\}_{2n} \left| \mathrm{e}^{-\beta A/(2n)} Q \mathrm{e}^{-\beta A/(2n)} \right| \{\sigma\}_{2n+1} \right\rangle}{\left\langle \{\sigma\}_{2n} \left| \mathrm{e}^{-\beta A/n} \right| \{\sigma\}_{2n+1} \right\rangle}. \qquad (5.8.15)$$

Measurement of $\tilde{Q}$ thereby gives a Monte Carlo estimate of $\langle\langle Q \rangle\rangle_\beta$.

Next we describe the application of the auxiliary-field approach to the calculation of (5.8.3). We utilize the Suzuki-Trotter approximation

$$\mathrm{e}^{-\beta \mathcal{H}} \simeq \left(\mathrm{e}^{-\beta V/2n} \mathrm{e}^{-\beta K/n} \mathrm{e}^{-\beta V/2n} \right)^n = \mathrm{e}^{-\beta V/2n} \left(\mathrm{e}^{-\beta K/n} \mathrm{e}^{-\beta V/n} \right)^{n-1} \mathrm{e}^{-\beta K/n} \mathrm{e}^{-\beta V/2n} \qquad (5.8.16)$$

combined with the Stratonovich-Hubbard transformation (5.7.6).

At the same time we define the trial function as a direct product of one-particle states [Sugiyama 86, Sorella 88, Sorella 89, White 89, Imada 89, Von der Linden 90]:

$$|\psi\rangle \equiv \bigotimes_{m=1}^{M} \left(\sum_{k=1}^{N} F_{km} |k\rangle \right), \tag{5.8.17}$$

where

$$|k\rangle \equiv c_k^\dagger |0\rangle, \tag{5.8.18}$$

and M is the number of the fermions.

We thus obtain an expression of (5.8.3) in a form similar to (5.7.8), that is,

$$\left\langle \psi \left| \mathrm{e}^{-2\beta\mathcal{H}} \right| \psi \right\rangle \simeq A^{-1} \sum_{\{s\}} W_\uparrow\{s\} W_\downarrow\{s\} \tag{5.8.19}$$

with

$$W_\sigma\{s\} \equiv \left\langle \psi \left| \mathrm{e}^{-\beta\tilde{V}_\sigma\{s\}_0/2n} \left[\prod_{l=1}^{2n-1} \left(\mathrm{e}^{-\beta K_\sigma/n} \mathrm{e}^{-\beta\tilde{V}_\sigma\{s\}_l/n} \right) \right] \mathrm{e}^{-\beta K_\sigma/n} \mathrm{e}^{-\beta\tilde{V}_\sigma\{s\}_{2n}/2n} \right| \psi \right\rangle \tag{5.8.20}$$

and

$$A \equiv 2^{N(2n+1)} \mathrm{e}^{\beta UN/2}. \tag{5.8.21}$$

Employing the equality (5.7.13) we further reduce the expression (5.8.20) to

$$W_\sigma\{s\} = \left\langle \psi \left| \mathrm{e}^{c_i^\dagger \overline{H}_{ij} c_j} \right| \psi \right\rangle, \tag{5.8.22}$$

where the $N \times N$ matrix $\overline{H}$ is defined by

$$\mathrm{e}^{\overline{V}/2} \left[\prod_{l=1}^{2n-1} \left(\mathrm{e}^{\overline{K}} \mathrm{e}^{\overline{V}} \right) \right] \mathrm{e}^{\overline{K}} \mathrm{e}^{\overline{V}/2} = \mathrm{e}^{\overline{H}}. \tag{5.8.23}$$

As is shown in (5.E.17), the application of the operator $\exp(c_i^\dagger \overline{H}_{ij} c_j)$ to a direct product of one-particle states, (5.8.17), yields [Imada 89]

$$W_\sigma\{s\} = \bigotimes_{m_1=1}^{M} \bigotimes_{m_2=1}^{M} \left(\langle k| \, {}^{\mathrm{t}}F_{m_1 k} \right) \left(\left(\mathrm{e}^{\overline{H}} F \right)_{l m_2} |l\rangle \right) = \det \left[{}^{\mathrm{t}}F \mathrm{e}^{\overline{H}} F \right], \tag{5.8.24}$$

instead of (5.7.15). (The summation over k and l is assumed here.) The product ${}^{\mathrm{t}}F\overline{H}F$ is an $M \times M$ matrix.

A quantity Q can be measured with the formula (5.7.16). The equal-time Green's function is, instead of (5.7.18), given by the following $N \times N$ matrix [Imada 89]:

$$\overline{G} = F \left({}^{\mathrm{t}}F \mathrm{e}^{\overline{H}} F \right)^{-1} {}^{\mathrm{t}}F \mathrm{e}^{\overline{H}}. \tag{5.8.25}$$

We obtain the flip ratio of Boltzmann weights, (5.7.20), in the form

$$R = 1 + (\gamma + 1)\overline{G}_{jj}, \tag{5.8.26}$$

instead of (5.7.26).

Thus we can use the algorithm given below (5.7.29) as it is.

As is discussed at the beginning of the present section, if we optimize the trial vector, we may achieve the zero-temperature limit even at rather high temperatures [Furukawa 91b, Hatano 93b]. This property is useful in studies on ground-state phase transitions (Chapter 3 [Hatano 93b]), in which the energy gap becomes narrow. It is also useful in studies on the ground state of frustrated spin systems and fermion systems [Furukawa 91b], in which the negative-sign problem appears at low temperatures.

5.9 Diffusion Monte Carlo method

In this section we review the diffusion Monte Carlo method, which has been proposed under the names of the projector Monte Carlo method and the Green's-function Monte Carlo method.

The aim of the Green's-function Monte Carlo method [Kalos 62, Kalos 79, Schmidt 84, Schmidt 92, De Raedt 92] and the projector Monte Carlo method [Kuti 82, Blankenbecler 83] is to study on ground-state properties of quantum systems. The former was proposed at first for studies on quantum gases and liquids in continuous space; the latter was proposed for quantum lattice problems. There is no big difference between them. The method is generalized to the thermofield quantum Monte Carlo method [Suzuki 85c, Suzuki 86a, Suzuki 86c, Suzuki 87a], by which we can study on thermodynamic properties.

The starting point is the power method, which is also utilized in the previous section. The ground state emerges after successive applications of a matrix to a test vector:

$$|\psi_{\rm g}\rangle = \lim_{n\to\infty} T^n |\psi\rangle \,, \tag{5.9.1}$$

where the test vector is an appropriate superposition of the base kets:

$$|\psi\rangle \equiv \sum_{\{\sigma\}} F(\{\sigma\}) \, |\{\sigma\}\rangle \,. \tag{5.9.2}$$

A quantity Q at the ground state is estimated as

$$\langle Q \rangle_{\rm g} \equiv \langle \psi_{\rm g} | Q | \psi_{\rm g} \rangle = \lim_{n\to\infty} \frac{\left\langle \psi \left| {}^{\rm t}T^n Q T^n \right| \psi \right\rangle}{\left\langle \psi \left| {}^{\rm t}T^n T^n \right| \psi \right\rangle}. \tag{5.9.3}$$

In the Green's-function Monte Carlo method the matrix T is defined by

$$T \equiv I - \Delta\tau \mathcal{H} \tag{5.9.4}$$

with $\Delta\tau < 1/n$, while in the projector Monte Carlo method

$$T \equiv {\rm e}^{-\Delta\tau A} {\rm e}^{-\Delta\tau B} \tag{5.9.5}$$

is used in association with the decomposition of the Hamiltonian $\mathcal{H} = A + B$. These definitions are equivalent up to the first power of $\Delta\tau$.

Although the starting point is quite similar to the ground-state algorithm described in the previous section, the sampling method is considerably different. In the diffusion Monte Carlo method the limit procedure $n \to \infty$ itself is simulated, by interpreting multiplications of the matrix as a Markov process.

Let us review the simulation of a diffusion process. Consider a Markovian diffusion process of a walker on a chain. We define a stochastic matrix L, whose elements $L(i,j)$ is the probability that a walker hops from the j-th site to the i-th site in a time interval $\Delta\tau$: the matrix is hence a non-negative matrix. Because the total probability must be unity, all the elements in a column of the matrix add to one:

$$\sum_i L(i,j) = 1 \qquad \text{for all } j. \tag{5.9.6}$$

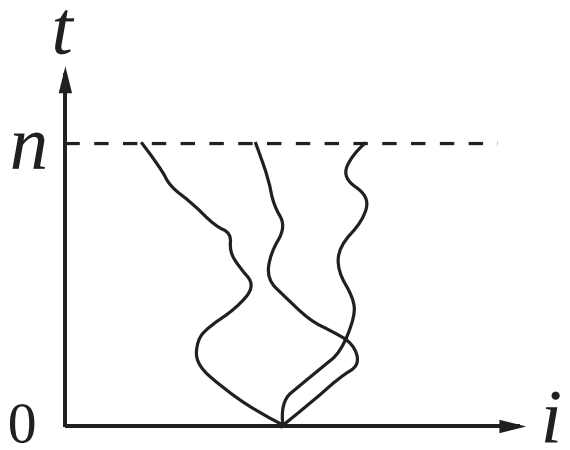

Figure 5.10 The diffusion process of random walkers.

The successive applications of the matrix to an initial distribution $P_{\rm init}(j)$ yield a unique stationary distribution:

$$P_{\rm stat} = \lim_{n\to\infty} L^n P_{\rm init}. \tag{5.9.7}$$

A Monte Carlo simulation of the diffusion process is carried out as follows; see Fig. 5.10. First, generate a random number $i(0)$ according to the initial distribution $P_{\rm init}(i(0))$, and place a walker on the site $i(0)$. Second, generate a random number $i(1)$ according the distribution $L(i(1), i(0))$, and move the walker to the site $i(1)$. Repeat the movement n times, and record the final position of the walker, $i(n)$, as a sample. This is the whole sequence of a trial. After we repeat the trials M times, we obtain a Monte Carlo estimate of the stationary distribution of walkers in the form

$$P_{\rm stat}(j) \simeq \frac{1}{M}\sum_{m=1}^{M} \delta(j, i_m(n)) \tag{5.9.8}$$

where $i_m(n)$ is the state where the m-th walker finally reaches. (In practical use many walkers are simulated simultaneously.)

The diffusion Monte Carlo method is based on the similarity between (5.9.1) and (5.9.7). We simulate the diffusion of a walker in the Hilbert space, moving the walker from a state $\{\sigma\}$ to another state $\{\sigma\}'$. In the case of (5.9.1), however, the matrix T is not stochastic, that is, the condition (5.9.6) does not hold. We decompose the matrix T into a stochastic matrix D and a weight w:

$$T(\{\sigma\}', \{\sigma\}) = w(\{\sigma\}')D(\{\sigma\}', \{\sigma\}), \tag{5.9.9}$$

where D satisfies the condition (5.9.6). Simulating the diffusion, we accumulate a weight of every state $\{\sigma\}(t)$ along the diffusion path:

$$W(\Gamma) \equiv \prod_{\Gamma} w(\{\sigma(t)\}), \tag{5.9.10}$$

where Γ specifies a sequence of n states through which the initial state $\{\sigma(0)\}$ migrates:

$$\Gamma \equiv \{\{\sigma(0)\}, \{\sigma(1)\}, \{\sigma(2)\}, \ldots, \{\sigma(n)\}\}. \tag{5.9.11}$$

After M trials we obtain a set of final bases $\{|\{\sigma(n)\}_m\rangle\}$ $(m = 1, 2, \ldots, M)$ and a set of the weights of them $\{W(\Gamma_m)\}$. An estimate of the ground-state wave function is given by

$$|\psi_{\rm g}\rangle \simeq \frac{1}{M}\sum_{m=1}^{M} W(\Gamma_m)\,|\{\sigma(n)\}_m\rangle\,. \tag{5.9.12}$$

Substitution of (5.9.12) to (5.9.3) gives the average of a quantity.

Hetherington pointed out [Hetherington 84] that a problem may appear when the number n is large. Since the matrix T is not a stochastic matrix, the random walkers do not generally reproduce the ground-state distribution; in other words, the formula (5.9.12) is not correct. As n increases, the distribution of the random walkers systematically deviates further from the ground-sate distribution; see [Hetherington 84] for a concrete example.

There appears a dilemma. Because of the above difficulty, we have to terminate the simulation at a small number n. When n is too small, on the other hand, the convergence to the ground state is insufficient.

In order to improve the situation we introduce a guidance function $f_{\rm G}$, and modify the process as follows [Kalos 74]:

$$\begin{aligned} |\widetilde{\{\sigma\}}\rangle &\equiv f_{\rm G}(\{\sigma\})\,|\{\sigma\}\rangle \\ \text{and} \qquad \widetilde{T}(\{\sigma\}', \{\sigma\}) &\equiv \frac{f_{\rm G}(\{\sigma\}')}{f_{\rm G}(\{\sigma\})} T(\{\sigma\}', \{\sigma\}). \end{aligned} \tag{5.9.13}$$

It is known from some examples that the systematic error is reduced when the guidance function is similar to the ground-state function. When not even a rough estimate of the ground-state function is known, we cannot help choosing the guidance function on an assumption. There is no general way to know the systematic error in that case.

Advantages of the diffusion Monte Carlo method over the world-line approach are pointed out as follows: (i) Samples $\{\{\sigma(n)\}_m\}$ are independent of each other, while in the world-line approach a sequence of samples auto-correlates. (ii) Once a state $\{\sigma(l)\}$ is generated, memory of the previous state $\{\sigma(l-1)\}$ can be discarded.

On the other hand, overcome of the disadvantage concerning the systematic error is desirable.

When we apply the method to frustrated spin systems or fermion systems, the negative-sign problem appears. Some of elements of the matrix T for these models are negative, and hence some of w in (5.9.9) are negative. Cancellation occurs in the summation of (5.9.12).

In order to circumvent the cancellation, the fixed-node approximation has been devised [Ceperley 80, Vitiello 91]. (i) We assume location of the nodal surfaces where the sign of the ground-state wave function changes, and divide the whole Hilbert space into several regions. (ii) We carry out the diffusion of states within each region individually. It is known [Moskowitz 82] that the ground-state energy estimated by the approximation gives an upper bound of the true ground-state energy. (iii) We should optimize the assumed location of the nodal surfaces.

The approximation may be convenient as a variational approach. There is, however, no general way to know how far the upper bound is from the true ground-state energy.

An application of the Green's-function Monte Carlo method to quantum lattice problems has begun quite recently. The one-dimensional $S = 1$ Heisenberg antiferromagnet [Parkinson 85a, Nightingale 86, Takahashi 89] and the two-dimensional Heisenberg antiferromagnet [Barnes 88a, Barnes 88b, Barnes 89, Gross 89, Carlson 89, Trivedi 89, Trivedi 90, Runge 92] have been studies by the method. The two-dimensional Hubbard model is also studied [An 91] with the use of the fixed-node approximation.

5.10 Handscomb's method

In this section we review Handscomb's method. The method is quite different from the methods described above. Here we sample expansion terms of high-temperature expansion, performing a Monte Carlo simulation.

Consider the ferromagnetic Heisenberg model in a magnetic field:

$$\mathcal{H} = \mathcal{H}_1 + \mathcal{H}_0, \tag{5.10.1}$$

where

$$\mathcal{H}_1 \equiv -\frac{J}{2}\sum_{\langle i,j\rangle} \boldsymbol{\sigma}_i \cdot \boldsymbol{\sigma}_j \qquad \text{and} \qquad \mathcal{H}_0 \equiv -H\sum_i \sigma_i^z. \tag{5.10.2}$$

The summand of $\mathcal{H}_1$ can be rewritten in the form

$$\boldsymbol{\sigma}_i \cdot \boldsymbol{\sigma}_j = 2P_b - 1, \tag{5.10.3}$$

where b denotes the nearest-neighbor bond $\langle i, j\rangle$. The operator P_b is the exchange operator, which causes a permutation between states on the sites i and j; for example, $P_b\,|\uparrow\downarrow\rangle = |\downarrow\uparrow\rangle$. Leaving out a constant term $JN/2$, we can express $\mathcal{H}_1$ as

$$\mathcal{H}_1 = -J\sum_b P_b. \tag{5.10.4}$$

Since the two terms commute with each other,

$$[\mathcal{H}_1, \mathcal{H}_0] = 0, \tag{5.10.5}$$

the statistical average of a quantity Q is expressed as follows:

$$\langle Q\rangle_{\mathrm{q}} \equiv \frac{1}{Z_{\mathrm{q}}}\mathrm{Tr}\, Q\mathrm{e}^{-\beta\mathcal{H}_1}\mathrm{e}^{-\beta\mathcal{H}_0} \qquad \text{with} \qquad Z_{\mathrm{q}} \equiv \mathrm{Tr}\,\mathrm{e}^{-\beta\mathcal{H}_1}\mathrm{e}^{-\beta\mathcal{H}_0}. \tag{5.10.6}$$

Expanding the term $\mathrm{e}^{-\beta\mathcal{H}_1}$, we have the following high-temperature expansion of the model:

$$Z_{\mathrm{q}} = \sum_{n=0}^{\infty}\frac{(\beta J)^n}{n!}\mathrm{Tr}\,\Big(\sum P_b\Big)^n\,\mathrm{e}^{-\beta\mathcal{H}_0}. \tag{5.10.7}$$

The summand is further expanded in the form

$$\mathrm{Tr}\,\Big(\sum P_b\Big)^n\,\mathrm{e}^{-\beta\mathcal{H}_0} = \sum_{C_n} W(C_n), \tag{5.10.8}$$

where

$$W(C_n) \equiv \mathrm{Tr}\, P_{b_1}P_{b_2}\cdots P_{b_n}\mathrm{e}^{-\beta\mathcal{H}_0}. \tag{5.10.9}$$

Here C_n denotes a sequence of nearest-neighbor bonds:

$$C_n \equiv \{b_1, b_2, \ldots, b_n\}\,. \tag{5.10.10}$$

The average of a quantity (5.10.6) is given by

$$\langle Q \rangle_{\mathrm{q}} = \frac{\displaystyle\sum_n \sum_{C_n} \tilde{Q}(C_n) W(C_n)}{\displaystyle\sum_n \sum_{C_n} W(C_n)}, \tag{5.10.11}$$

where

$$\tilde{Q}(C_n) \equiv \frac{1}{W(C_n)} \mathrm{Tr}\, Q P_{b_1} P_{b_2} \cdots P_{b_n} \mathrm{e}^{-\beta \mathcal{H}_0}. \tag{5.10.12}$$

Handscomb proposed replacing the summations $\sum_n$ and $\sum_{C_n}$ by a Monte Carlo summation [Handscomb 62, Handscomb 64, Lyklema 82, Lyklema 83, Lyklema 84, Chen 91]. We successively generate sequences C_n using the importance-sampling technique, and measure the quantity $\tilde{Q}$ every time. We define the following Monte Carlo "flips":

$$\text{(i)}\quad \text{Addition},\quad C_n \longrightarrow C'_{n+1} = C_n + b_{n+1}, \tag{5.10.13}$$

$$\text{(ii)}\quad \text{Deletion},\quad C_n = b_1 + C'_{n-1} \longrightarrow C'_{n-1}, \tag{5.10.14}$$

$$\text{(iii)}\quad \text{Rotation},\quad C_n = b_1 + C''_{n-1} \longrightarrow C'_n = C''_n + b_1. \tag{5.10.15}$$

Here the addition of a bond is defined by

$$\{b_1, b_2\} + b_3 = \{b_1, b_2, b_3\}\,. \tag{5.10.16}$$

Note that the order of the bonds in the notation is relevant.

It is essential for applicability of the method that the ratio of the weight $W(C_{n+1})/W(C_n)$ and the measured quantity $\tilde{Q}$ are calculated quickly. As for the isotropic Heisenberg model, we can obtain them analytically. When we can decompose a sequence C_n into k strings each of which connects a_i sites ($i = 1, 2, \ldots, k$), the weight of the sequence is given by [Handscomb 64, Lyklema 82, Lyklema 84]

$$W(C_n) = \prod_{i=1}^{k} 2 \cosh a_i \beta H. \tag{5.10.17}$$

In a vanishing field $H = 0$ the formula reduces to a simple factor; we can estimate the ratio $W(C_{n+1})/W(C_n)$ easily.

An advantage of the present method is that we directly evaluate the quantum-statistical average, contrary to the methods based on the Suzuki-Trotter decomposition. In the latter method we introduce the Trotter number n and analyze the data to obtain the quantum limit $n \to \infty$. In the present method no extrapolation procedures are necessary.

The method has been applied to the ferromagnetic Heisenberg model [Lyklema 83, Lyklema 84], and to the exchange interaction models with higher S [Chen 88]. The latter model is defined by summation of exchange operators for an arbitrary S, which is generally a polynomial of $\boldsymbol{S}_i \cdot \boldsymbol{S}_j$ [Chen 72].

In the antiferromagnetic case $J < 0$, however, the expansion (5.10.7) is an alternating series because a sign comes from the coefficient $(\beta J)^n$ for odd integers n. Numerical evaluation of a summation over an alternating series is generally difficult because of cancellation on a large scale. Another series expansion has been proposed to improve the situation using the expression [Lee 84b, Manousakis 88, Gomez-Santos 89]

$$-\boldsymbol{\sigma}_i \cdot \boldsymbol{\sigma}_j = 2(h_b^2 - h_b) - 1, \tag{5.10.18}$$

instead of the expression (5.10.3). Here the operator h_b is given by

$$h_b \equiv \sigma_i^+ \sigma_j^- + \sigma_i^- \sigma_j^+ . \tag{5.10.19}$$

(Hereafter we leave out the constant term in (5.10.18).) The partition function is expanded in the form

$$Z = \sum_{n=0}^{\infty} \frac{(\beta|J|)^n}{n!} \sum_{C_n} (-1)^{n_1} \mathrm{Tr}\ (O_{b_1} O_{b_2} \cdots O_{b_n}) , \tag{5.10.20}$$

where the operator O_b is either h_b or h_b^2. The set $\{O_{b_1}, \ldots, O_{b_n}\}$ contains n_1 pieces of h_b and n_2 pieces of h_b^2 with $n_1 + n_2 = n$. The summand does not vanish only when the operators h_b form a closed circle on the lattice. Hence in case of bipartite lattices the number n_1 is even, and the summand is always positive.

The method, applied to the antiferromagnetic Heisenberg model on a square lattice, has yielded results [Manousakis 88, Manousakis 89] which can be compared to the results by the world-line Monte Carlo method [Ding 90a, Makivic 91, Ding 91]; see Ref. [Manousakis 91] for a review.

Applicability of the present method strongly depends on the computational time necessary to evaluate $W(C_n)$. In the Heisenberg model, evaluation is easy because of the symmetry of the model. As for other models it may not be the case; we may have to further expand the weight W to obtain a tractable expression [Sandvik 91, Sandvik 92].

Kadowaki and Ueda [Kadowaki 86, Kadowaki 87, Kadowaki 89] have performed simulations by the simple-sampling method in order to evaluate expansion coefficients themselves. Since less than ten coefficients have been estimated, they have had to employ a kind of Padé approximation. Though a systematic error may be hidden in the results, their estimates seems to agree with other results.

5.11 Decoupled-cell method

In this section we mention the decoupled-cell method. This method is rather different from the methods mentioned so far.

As is explained in Section 5.1, it is difficult to apply naively the classical Metropolis algorithm to quantum-mechanical systems, because it is difficult to calculate the ratio of the Boltzmann factors. In the decoupled-cell method the Boltzmann factor of finite-size cells approximate the Boltzmann factor of the whole system.

Consider a flip trial of a spin on the i-th site, that is,

$$\sigma_i \longrightarrow -\sigma_i; \tag{5.11.1}$$

we leave other spins as they are. When we naively adopt the Metropolis algorithm, we have to calculate the ratio

$$R = \frac{\left\langle -\sigma_i \left| \mathrm{e}^{-\beta\mathcal{H}} \right| -\sigma_i \right\rangle}{\left\langle \sigma_i \left| \mathrm{e}^{-\beta\mathcal{H}} \right| \sigma_i \right\rangle}. \tag{5.11.2}$$

Since it is difficult to calculate the ratio as was described in Section 5.1, we employ the following approximation [Homma 84, Homma 86a]:

$$R \sim \frac{\left\langle -\sigma_i \left| \mathrm{e}^{-\beta\mathcal{H}_i^{(\nu)}} \right| -\sigma_i \right\rangle}{\left\langle \sigma_i \left| \mathrm{e}^{-\beta\mathcal{H}_i^{(\nu)}} \right| \sigma_i \right\rangle}, \tag{5.11.3}$$

where $\mathcal{H}_i^{(\nu)}$ denotes the Hamiltonian of a cell whose origin is the i-th site and whose radius is ν. Here the cell should be small enough to be easily diagonalized. Then we perform a simulation using the approximate ratio (5.11.3). Physical quantities are measured in a suitable spin representation; when we employ the x-direction as the quantization axis, we obtain the transverse magnetization and transverse correlations [Horiki 89].

In the approximation (5.11.3) we neglect quantum-mechanical coherence between the inside and the outside of the cell $\mathcal{H}^{(\nu)}$. This neglect may be justified when the coherence length is smaller than ν. Hence, at least at high temperatures, we expect that the method works [Matsuda 88].

An advantage of the present method over the Suzuki-Trotter approach is the disappearance of the negative-sign problem. Since we only use diagonal elements of the cell density matrix in (5.11.3), the ratio $r(\sigma)$ is necessarily positive. Thus the method looks applicable even to frustrated spin systems at low temperatures [Homma 86b, Zeng 90]. At low temperatures, however, the coherence effect appears distinctly, and may exceed the size of the decoupled cell. In this case the applicability of the method is questionable. In fact we observe a systematic error in the results for the one-dimensional XY model [Homma 86a].

The error decreases when we treat larger cells. Concerning the convergence in the limit $\nu \to \infty$ at low temperatures, only an empirical discussion is available so far [Zeng 90]. In contrast, the convergence in the infinite-Trotter-number limit in the case of the Suzuki-Trotter approach is well known as was mentioned in Section 5.2. Scaling of the cell size ν with the temperature should be discussed in future.

5.12 Dynamics and the maximum-entropy method

In this section we describe a method of obtaining information on dynamics. There has been no efficient Monte Carlo algorithm for direct measurement of functions which describes dynamic properties; for example, the real-time Green's function. Obtaining Monte Carlo data of thermodynamic quantities, we have to carry out analytic continuation from the imaginary time $i\tau$ to the real time t. However, the analytic continuation based on noisy numerical data is difficult in general.

Recently the maximum-entropy method developed in the field of the information theory was applied to the present problem [Silver 90a, Silver 90b, Gubernatis 91]. We

describe the method later, assuming that Monte Carlo data of thermodynamic quantities are available.

Let us review the relation between the real-time Green's function and the imaginary-time Matsubara Green's function (see [Abrikosov 61] for reference). We show that the analytic continuation is essentially equivalent to the inverse Laplace transformation.

The linear response of a system at finite temperatures to a time-dependent external field is described by the real-time Green's function [Kubo 57]

$$G(t) \equiv -i \left\langle \mathrm{T} \left[c(t) c^\dagger \right] \right\rangle, \tag{5.12.1}$$

where T denotes the time-ordering operator, and $c(t)$ denotes the Heisenberg representation of the operator c,

$$c(t) \equiv \mathrm{e}^{i\mathcal{H}t} c \mathrm{e}^{-i\mathcal{H}t}. \tag{5.12.2}$$

Note that the symbol $\langle \cdots \rangle$ denotes the thermal average as it did above. Hence the Green's function also depends on the temperature, though we have left out the argument β.

Hereafter we concentrate on the fermion systems; then the retarded Green's function,

$$G^{\mathrm{R}}(t) = \begin{cases} i \left\langle \left\{ c(t), c^\dagger \right\} \right\rangle & \text{for} \quad t > 0, \\ 0 & \text{for} \quad t < 0, \end{cases} \tag{5.12.3}$$

and the advanced Green's function,

$$G^{\mathrm{A}}(t) = \begin{cases} 0 & \text{for} \quad t > 0, \\ -i \left\langle \left\{ c(t), c^\dagger \right\} \right\rangle & \text{for} \quad t < 0, \end{cases} \tag{5.12.4}$$

are related with the real-time Green's function as follows;

$$G^{\mathrm{R}}(\omega) = \mathrm{Re}\, G(\omega) + i \mathrm{Im}\, G(\omega) \coth \frac{\beta\omega}{2} \tag{5.12.5}$$

$$G^{\mathrm{A}}(\omega) = \mathrm{Re}\, G(\omega) - i \mathrm{Im}\, G(\omega) \coth \frac{\beta\omega}{2}. \tag{5.12.6}$$

Here the functions $G(\omega)$ are the Fourier components of the corresponding functions $G(t)$. The retarded Green's function $G^{\mathrm{R}}(\omega)$ is analytic in the upper half plane of the variable ω, while the advanced Green's function $G^{\mathrm{A}}(\omega)$ is in the lower half plane.

The Matsubara Green's function, on the other hand, is defined by

$$\mathcal{G}(\tau) \equiv \left\langle c(\tau) c^\dagger \right\rangle \tag{5.12.7}$$

with

$$c(\tau) \equiv \mathrm{e}^{\tau\mathcal{H}} c \mathrm{e}^{-\tau\mathcal{H}}. \tag{5.12.8}$$

The function is defined in the domain $[-\beta, \beta]$. This function can be estimated by means of Monte Carlo simulations. The Fourier component of the function is given on the discrete points of the Matsubara frequencies, that is,

$$\omega_n \equiv \frac{(2n+1)\pi}{\beta} \tag{5.12.9}$$

for fermions.

The Monte Carlo data of the Matsubara Green's function give information about the real-time Green's function on the imaginary axis. The Fourier components are related with the real-time Green's functions in the following form;

$$\mathcal{G}(\omega_n) = \begin{cases} G^{\rm R}(i\omega_n) & \text{for} \quad \omega_n > 0, \\ G^{\rm A}(i\omega_n) & \text{for} \quad \omega_n < 0. \end{cases} \tag{5.12.10}$$

The problem is how to carry out the analytic continuation to the real axis.

The analytic continuation is essentially equivalent to the inverse Laplace transformation. With the use of the relation (5.12.10), the Matsubara Green's function in terms of τ is given by

$$\begin{aligned} \mathcal{G}(\tau) &= \frac{1}{\beta} \sum_{n=-\infty}^{\infty} {\rm e}^{-i\omega_n \tau} \mathcal{G}(\omega_n) \\ &= \frac{1}{\beta} \sum_{n=-\infty}^{-1} {\rm e}^{-i\omega_n \tau} G^{\rm A}(i\omega_n) + \frac{1}{\beta} \sum_{n=0}^{\infty} {\rm e}^{-i\omega_n \tau} G^{\rm R}(i\omega_n) \\ &= \int_{-\infty}^{\infty} \frac{d\omega}{2\pi i} \frac{{\rm e}^{-\tau\omega}}{1+{\rm e}^{-\beta\omega}} \left(G^{\rm R}(\omega + i0) - G^{\rm A}(\omega - i0) \right). \end{aligned} \tag{5.12.11}$$

We define the spectral density in the Lehmann representation,

$$\rho(\omega) \equiv \frac{1}{2\pi i} \left(G^{\rm R}(\omega + i0) - G^{\rm A}(\omega - i0) \right), \tag{5.12.12}$$

which gives the imaginary part of the real-time Green's function. We arrive at the relation similar to the Laplace transformation,

$$\mathcal{G}(\tau) = \int_{-\infty}^{\infty} \frac{{\rm e}^{-\tau\omega}}{1+{\rm e}^{-\beta\omega}} \rho(\omega) d\omega. \tag{5.12.13}$$

The analytic continuation is equivalent to the inverse transformation of (5.12.13). Since the real part and imaginary part of the Green's function are related, the spectral density (5.12.12) contains information about the entire Green's function.

Now the problem is how to obtain a set of data of the spectral density $\{\rho_i\} \equiv \{\rho(\omega_i)\}$ from a set of noisy data of the Matsubara Green's function $\{\mathcal{G}_{\rm data}(\tau_j) \pm \sigma_j\}$. A naive method of the inverse transformation of (5.12.13) may be the least-squares method. We determine the set $\{\rho_i\}$ so that the set $\{\mathcal{G}_{\rm fit}(\tau)\}$ given by

$$\mathcal{G}_{\rm fit}(\tau) \equiv \sum_i \frac{{\rm e}^{-\tau\omega_i}}{1+{\rm e}^{-\beta\omega_i}} \rho(\omega_i) \Delta\omega \tag{5.12.14}$$

may minimize the value

$$\chi^2 \equiv \sum_j \frac{\left(\mathcal{G}_{\rm data}(\tau_j) - \mathcal{G}_{\rm fit}(\tau_j) \right)^2}{\sigma_j^2}. \tag{5.12.15}$$

The least-squares method, however, does not work in general. The naive application of the least-squares method yields a result which generally does not satisfy physical conditions. We have knowledge about the spectral density $\rho(\omega)$ prior to the data analysis; that is, the positivity

$$\rho(\omega) \geq 0 \qquad \text{for all} \quad \omega, \tag{5.12.16}$$

and the sum rule

$$\int_{-\infty}^{\infty} \rho(\omega) d\omega = 1. \tag{5.12.17}$$

If the result does not satisfy these conditions, it might be nonsense in the physical point of view.

Data-analysis problems of this type frequently appear in many fields of science. The maximum-entropy method is one of the standard methods for the problems; see [Skilling 89a] for a review. A common feature of the difficulty in these problems is the competition between measured data and prior knowledge; when we insist on the measured data, we might obtain a result contradicting the prior knowledge, and vice versa. By the maximum-entropy method we control the competition.

The maximum-entropy method is based on Bayse's theorem, which is the law of conditional probabilities. The joint likelihood of the data $\{\mathcal{G}_{\rm data}\}$ and the image $\{\rho\}$, $P[\text{data}, \text{image}]$ is decomposed as

$$P[\text{data}, \text{image}] = P[\text{data}|\text{image}] \times P[\text{image}] = P[\text{image}|\text{data}] \times P[\text{data}], \tag{5.12.18}$$

where $P[X|Y]$ denotes the likelihood of X under the condition that Y is given. We have to maximize $P[\text{image}|\text{data}]$ in order to obtain the most likely image under the condition that the data is given. The maximum of $P[\text{image}|\text{data}]$ is achieved when $P[\text{data}|\text{image}]$ and $P[\text{image}]$ are maximized as well as $P[\text{data}]$ is minimized.

The likelihood of the data $P[\text{data}]$ is expressed by the statistical errors of the data, which is assumed to be given and fixed.

The conditional probability $P[\text{data}|\text{image}]$ may be defined by

$$P[\text{data}|\text{image}] \propto \mathrm{e}^{-\chi^2/2}, \tag{5.12.19}$$

where χ^2 is given in (5.12.15). Here we have assumed that likelihood of each data point $\mathcal{G}_{\rm data}(\tau_j)$ is given by the Gaussian factor,

$$\frac{1}{\sqrt{2\pi}\sigma_j} \exp\left[-\frac{\left(\mathcal{G}_{\rm data}(\tau_j) - \mathcal{G}_{\rm fit}(\tau_j)\right)^2}{2\sigma_j^2}\right] \tag{5.12.20}$$

and that the measurements of data are mutually independent.

The quantity $P[\text{image}]$ indicates how an image is likely in comparison with the positivity and the sum rule of $\{\rho\}$. In order to define this quantity we somehow make a proposal $\{m_i\}$ of the image $\{\rho(\omega_i)\}$; the proposal is called a "default model". The default model should be chosen so as to satisfy the prior knowledge;

$$m_i \geq 0 \tag{5.12.21}$$

and

$$\sum_i m_i \Delta\omega = 1. \tag{5.12.22}$$

The difference between a presumed image and the default model may be measured with the Shannon entropy,

$$S[\rho] = \sum_i \left[\rho(\omega_i) - m_i - \rho(\omega_i) \ln\left(\frac{\rho(\omega_i)}{m_i}\right)\right] \Delta\omega. \tag{5.12.23}$$

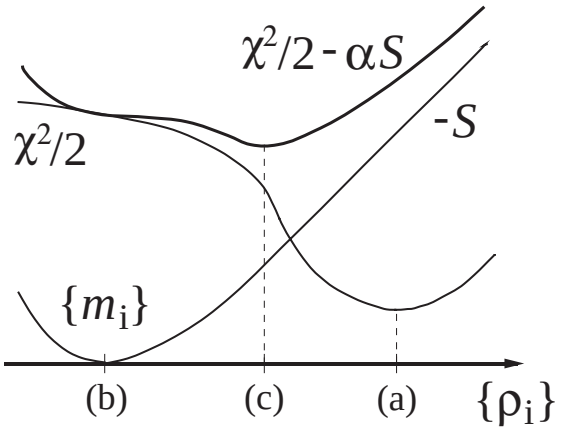

Figure 5.11 The value χ^2, (5.12.15), and the entropy S, (5.12.23). The points (a), (b) and (c) on the abscissa correspond to the maximum of S, the minimum of $\chi^2/2$ and the minimum of (5.12.25), respectively.

It is shown [Skilling 89b] that the only consistent measure of the quantity P[image] for a positive and additive image is

$$P[\text{image}] = \mathrm{e}^{\alpha S}, \tag{5.12.24}$$

where α is a parameter.

The maximization of P[image|data] is, therefore, equivalent to the maximization of P[data|image] $\times$ P[image], or minimization of

$$\frac{\chi^2}{2} - \alpha S, \tag{5.12.25}$$

and thus we arrive at a guess $\{\rho\}$. The maximum-entropy method thereby turns out to be a method of arranging a compromise between measured data and prior knowledge; see Fig. 5.11. The maximum of S (or the minimum of $-S$) corresponds to the guess of the default model $\rho(\omega_i) = m_i$, while the minimum of $\chi^2/2$ corresponds to the guess by the least-squares method.

An algorithm to determine the parameter α has been given as well as one to estimate appropriateness of a default model [Gubernatis 91].

Although estimation of possible systematic errors may not be easy, the method has been successfully applied to the Anderson model [Silver 90c, Jarrell 91b], dilute magnetic alloys [Jarrell 90, Jarrell 91a], one- and two-dimensional Heisenberg antiferromagnets [Deisz 90, Makivic 92a] and the one-dimensional t-J model [Deisz 92].

5.A Transfer-matrix calculations using the fractal decomposition**

In the present Appendix, transfer-matrix calculations were made to confirm the rapid convergence $n \to \infty$ of approximants of the fractal decomposition. We study the Trotter-number and temperature dependence of correction terms of approximants.

All the calculations in the present appendix were performed for the spin 1/2 antiferromagnetic XXZ model on the triangular lattice of size 4×2:

$$\mathcal{H} \equiv \sum_{\langle i,j \rangle} \left[-J_{xy}(\sigma_i^x \sigma_j^x + \sigma_i^y \sigma_j^y) - J_z \sigma_i^z \sigma_j^z \right] \tag{5.A.1}$$

**The content of this appendix was published in [Hatano 91b].

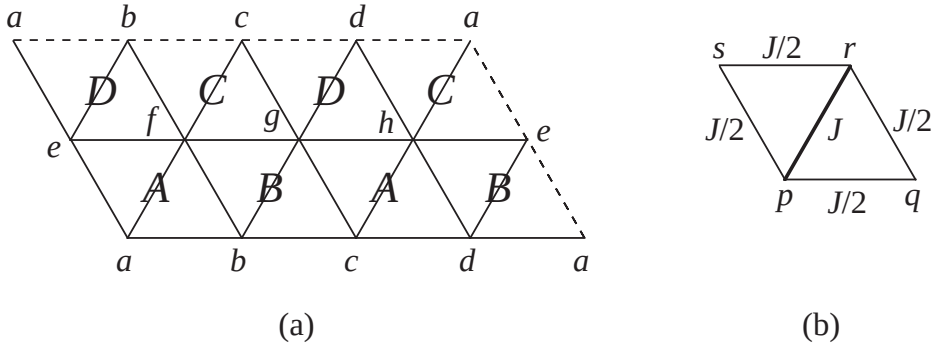

(a) (b)

Figure 5.12 (a) All the calculations were performed on the triangular lattice of size 4×2 with periodic boundary conditions. (b) A piece of the Hamiltonian into which the total Hamiltonian is decomposed.

where $\sum_{\langle i,j \rangle}$ denotes the summation over all the nearest neighbours on the lattice with periodic boundary conditions, as illustrated in Fig. 5.12(a).

Hereafter the following three cases of the parameters J_{xy} and J_z are examined; namely the Ising-like case ($J_{xy} = -1/4$, $J_z = -1$), the isotropic Heisenberg case ($J_{xy} = J_z = -1$), and the XY-like case ($J_{xy} = -1$, $J_z = -1/4$).

To apply the Suzuki-Trotter decomposition to the density matrix $\mathrm{e}^{-\beta\mathcal{H}}$, the total Hamiltonian (5.A.1) is decomposed into the following four parts [Takasu 86]:

$$\mathcal{H} = \mathcal{H}_A + \mathcal{H}_B + \mathcal{H}_C + \mathcal{H}_D, \tag{5.A.2}$$

where

$$\begin{aligned} \mathcal{H}_A &\equiv \mathcal{H}(a,b,f,e) + \mathcal{H}(c,d,h,g), \\ \mathcal{H}_B &\equiv \mathcal{H}(b,c,g,f) + \mathcal{H}(d,a,e,h), \\ \mathcal{H}_C &\equiv \mathcal{H}(f,g,c,b) + \mathcal{H}(h,e,a,d), \\ \text{and} \quad \mathcal{H}_D &\equiv \mathcal{H}(e,f,b,a) + \mathcal{H}(g,h,d,c), \end{aligned} \tag{5.A.3}$$

with

$$\begin{aligned} \mathcal{H}(p,q,r,s) \equiv \frac{1}{2} \sum_{\substack{\langle i,j \rangle = \langle p,q \rangle, \langle q,r \rangle, \\ \langle r,s \rangle, \langle s,p \rangle}} & \left[-J_{xy}(\sigma_i^x \sigma_j^x + \sigma_i^y \sigma_j^y) - J_z \sigma_i^z \sigma_j^z \right] \\ & + \left[-J_{xy}(\sigma_p^x \sigma_r^x + \sigma_p^y \sigma_r^y) - J_z \sigma_p^z \sigma_r^z \right], \end{aligned} \tag{5.A.4}$$

as illustrated in Fig. 5.12(b).

The following two kinds of the Suzuki-Trotter decomposition are used and compared in the present appendix; (a) the second-order decomposition [Suzuki 85d, Fye 86] with a Trotter number n_2,

$$\mathrm{e}^{-\beta\mathcal{H}} = \left[S_2\left(-\frac{\beta}{n_2} \right) \right]^{n_2} + O\left(\frac{\beta^3}{n_2^2} \right), \tag{5.A.5}$$

where

$$S_2(x) \equiv \mathrm{e}^{x\mathcal{H}_A/2} \mathrm{e}^{x\mathcal{H}_B/2} \mathrm{e}^{x\mathcal{H}_C/2} \mathrm{e}^{x\mathcal{H}_D} \mathrm{e}^{x\mathcal{H}_C/2} \mathrm{e}^{x\mathcal{H}_B/2} \mathrm{e}^{x\mathcal{H}_A/2} = \mathrm{e}^{x\mathcal{H}} + O(x^3), \tag{5.A.6}$$

and (b) the fourth-order decomposition [Suzuki 90, Suzuki 91] with a Trotter number n_4,

$$\mathrm{e}^{-\beta\mathcal{H}} = \left[S_4\left(-\frac{\beta}{n_4}\right)\right]^{n_4} + O\left(\frac{\beta^5}{n_4^4}\right), \tag{5.A.7}$$

where

$$S_4(x) \equiv S_2(p_2x)S_2(p_2x)S_2((1-4p_2)x)S_2(p_2x)S_2(p_2x) = \mathrm{e}^{x\mathcal{H}} + O(x^5), \tag{5.A.8}$$

with

$$4p_2^3 + (1-4p_2)^3 = 0, \quad \text{or} \quad p_2 = (4-\sqrt[3]{4})^{-1} \simeq 0.41449\cdots. \tag{5.A.9}$$

The parameter p_2 is chosen to cancel out the third-order corrections of the product of the five operators S_2 in (5.A.8). The fourth-order correction proves to vanish automatically [Suzuki 90, Suzuki 91]. Note that the propagator $S_4(-\beta)$ yield a *to-and-fro* path in the direction of the imaginary time $\tau = 0 \to \beta$, owing to the part $(1-4p_2) < 0$ in (5.A.8).

The approximate partition functions are defined by

$$Z_2(\beta) \equiv \mathrm{Tr}\ \left[S_2\left(-\frac{\beta}{n_2}\right)\right]^{n_2} \tag{5.A.10}$$

and

$$Z_4(\beta) \equiv \mathrm{Tr}\ \left[S_4\left(-\frac{\beta}{n_4}\right)\right]^{n_4}. \tag{5.A.11}$$

We calculated corrections to the approximants Z_2 and Z_4 in (5.A.10) and (5.A.11) as follows.

We express the transfer matrices with the orthonormal set of the bases $\{|\{\sigma\}_k\rangle\}$ which are the eigenstates of the operators $\{\sigma^z\}$ at the eight sites. The transfer matrices in this expression $\langle\{\sigma\}_k|\exp(-x\mathcal{H}_j)|\{\sigma\}_{k+1}\rangle$ are block-diagonalized into the subspaces of the total magnetization $M_z = 4, 3, 2, \ldots, -3, -4$. The maximal size of the blocks of the matrix is 70×70, and the multiplications of the blocks can be easily made on computers. Once the matrices S_2 and S_4 are calculated as in (5.A.6) and (5.A.8), then the Trotter number $n = 2^q$ can be achieved only by q times operations of matrix-product. Thus we calculated the approximate partition functions (5.A.10) and (5.A.11). On the other hand, the matrix of the original Hamiltonian $\langle\{\sigma\}|\mathcal{H}|\{\sigma'\}\rangle$ has the same size as the transfer matrix. Exact diagonalization of $\mathcal{H}$ can be made on computers. Hence we can obtain the true partition function. Corrections to the approximants Z_2 and Z_4 in (5.A.10) and (5.A.11) were thus calculated.

We compare these approximants with the number of the exponential operators fixed. For the second-order decomposition, the number of the operators is $L_2 = 6n_2$. In the case of the fourth-order decomposition (5.A.7) with the Trotter number $n = n_4$, the number is $L_4 = 30n_4$, because five operators of S_2 are combined into one operator of S_4 in (5.A.8). When these approximants are applied to quantum Monte Carlo simulations, the CPU-time for the simulations is proportional to the number of the exponential operators. From this point of view, comparisons between these two decompositions should be made under the condition $L_2 = L_4$, or $n_2 = 5n_4$. Hereafter the Trotter numbers n_2 and n_4 are chosen so as to satisfy this condition. We leave out the subscript of n_4, while we define $n_2 = 5n$ except where mentioned explicitly.

We discuss, in the following, the Trotter-number dependence of correction terms in high-temperature regions.

The partition functions and the energies of the system calculated with (5.A.5) and (5.A.7) at the temperature $T = 10.0$ are plotted in Fig. 5.13 in the Ising-like case, for example. The behaviour in the other two cases is quite similar to it.

Since the inverse temperature $\beta = 0.1$ (with $k_{\rm B} = 1$) is rather small, the data of the partition functions (Fig. 5.13(a)) can be fitted well to the following functions even for rather small Trotter numbers $n \simeq 1$:

$$\begin{aligned} Z_2(\beta) - Z_{\rm exact}(\beta) &\simeq \frac{A_2(\beta)}{n^2}, \\ \text{and} \quad Z_4(\beta) - Z_{\rm exact}(\beta) &\simeq \frac{A_4(\beta)}{n^4}, \end{aligned} \tag{5.A.12}$$

with some parameters A_2 and A_4. The data of the energies (Fig. 5.13(b)) show the same behaviour.

In every case, the correction to Z_4 in (5.A.12) is less than to Z_2 for $n \geq 1$. From this point of view, the fourth-order decomposition S_4 is more advantageous than the second-order decomposition S_2 in order to calculate physical quantities in this temperature region.

At lower temperatures, however, it occurs for small Trotter numbers that

$$|Z_2(\beta) - Z_{\rm exact}(\beta)| < |Z_4(\beta) - Z_{\rm exact}(\beta)|\,; \tag{5.A.13}$$

see Fig. 5.14 in the Ising-like case.

It is observed in most cases that the relation $|Z_2 - Z_{\rm exact}| > |Z_4 - Z_{\rm exact}|$ is satisfied only for $\beta/n \leq 1/4$ (In some cases, for $\beta/n \leq 1/8$, or $\beta/n \leq 1/2$). It is the situation as expected, because the correction term to the approximant S_4 is of higher order with respect to β than that to S_2; see (5.A.5) and (5.A.7).

It is supposed that the approximant S_4 is more advantageous than S_2 is, when the criterion [Suzuki 90, Suzuki 91]

$$O\left(\frac{\beta^5}{n_4^4}\right) \ll O\left(\frac{\beta^3}{n_2^2}\right) \quad \text{with} \quad n_2 = 5n_4, \qquad \text{or} \quad \frac{\beta}{n_4} \ll \frac{1}{5} \tag{5.A.14}$$

is satisfied. The above observation confirms this criterion.

In the following we discuss the temperature dependence of corrections in high-temperature regions.

At high temperatures $\beta/n \ll 1$, correction terms to the density matrix $\mathrm{e}^{-\beta\mathcal{H}}$ under a fixed Trotter number n can be written as follows:

$$\begin{aligned} \left[S_2\left(-\frac{\beta}{n}\right)\right]^n &= \mathrm{e}^{-\beta\mathcal{H}} + \frac{1}{n^2}\left(\beta^3 Q_3 + O(\beta^4)\right) + O\left(\frac{\beta^4}{n^3}\right), \\ \left[S_4\left(-\frac{\beta}{n}\right)\right]^n &= \mathrm{e}^{-\beta\mathcal{H}} + \frac{1}{n^4}\left(\beta^5 R_5 + O(\beta^6)\right) + O\left(\frac{\beta^6}{n^5}\right). \end{aligned} \tag{5.A.15}$$

It can be generally proved, however, that the *traces* of the lowest-order corrections in (5.A.15) always vanish, namely $\mathrm{Tr}\, Q_3 = \mathrm{Tr}\, R_5 \equiv 0$; see Appendix 5.B [Hatano 91a].

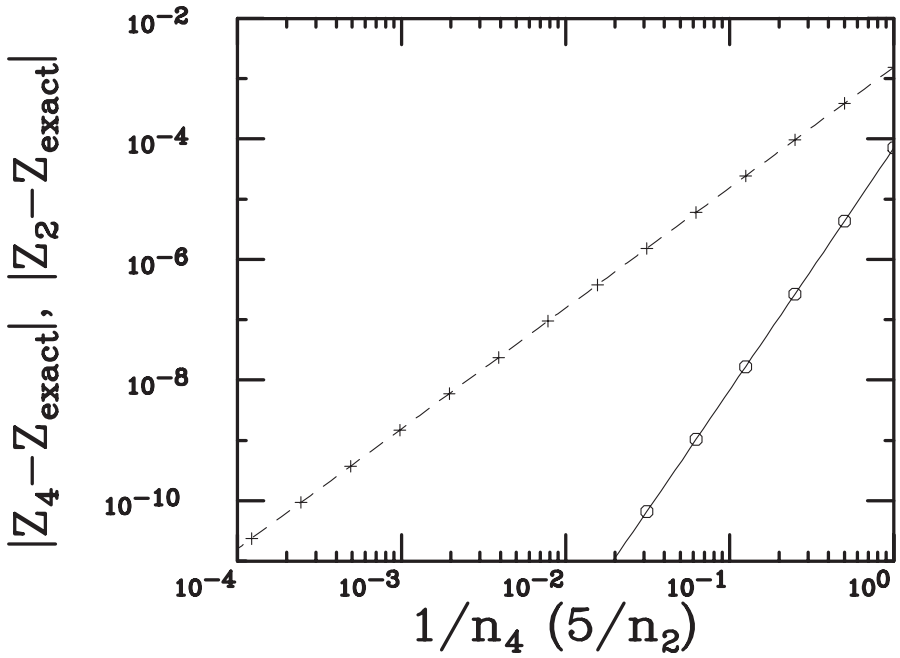

(a)

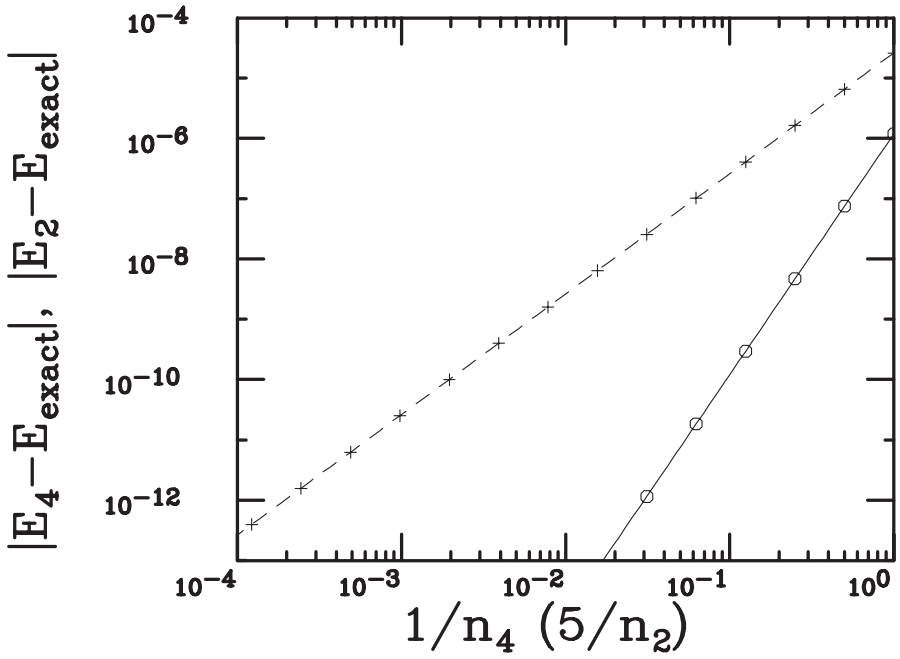

(b)

Figure 5.13 The Trotter-number dependence of corrections to (a) the partition functions and (b) the energies at the temperature $T = 10.0$ in the Ising-like case, calculated with the second-order decomposition (dashed lines) and the fourth-order decomposition (solid lines) respectively. These plots confirm the behaviour shown in (5.A.12).

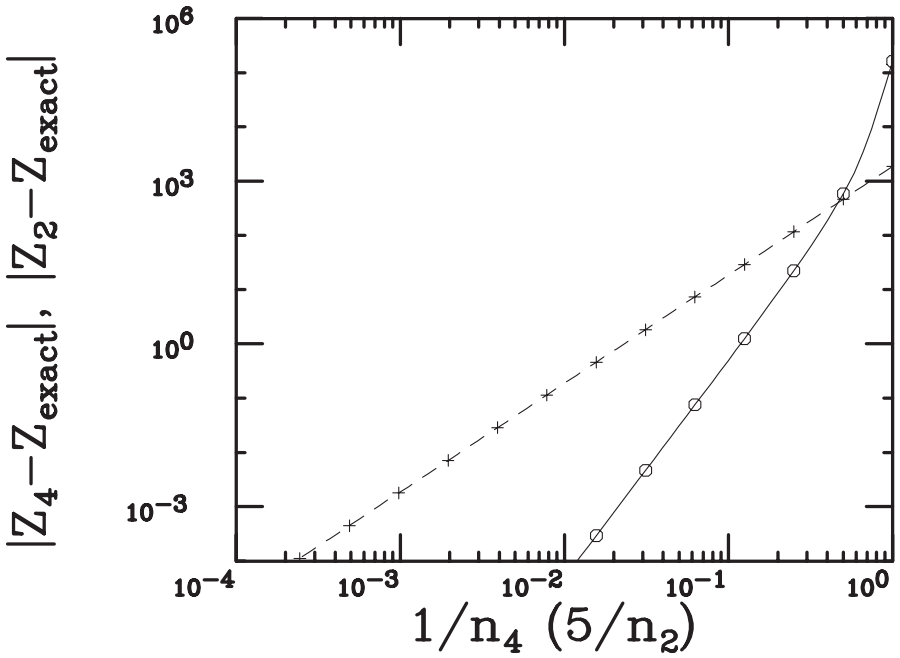

(a)

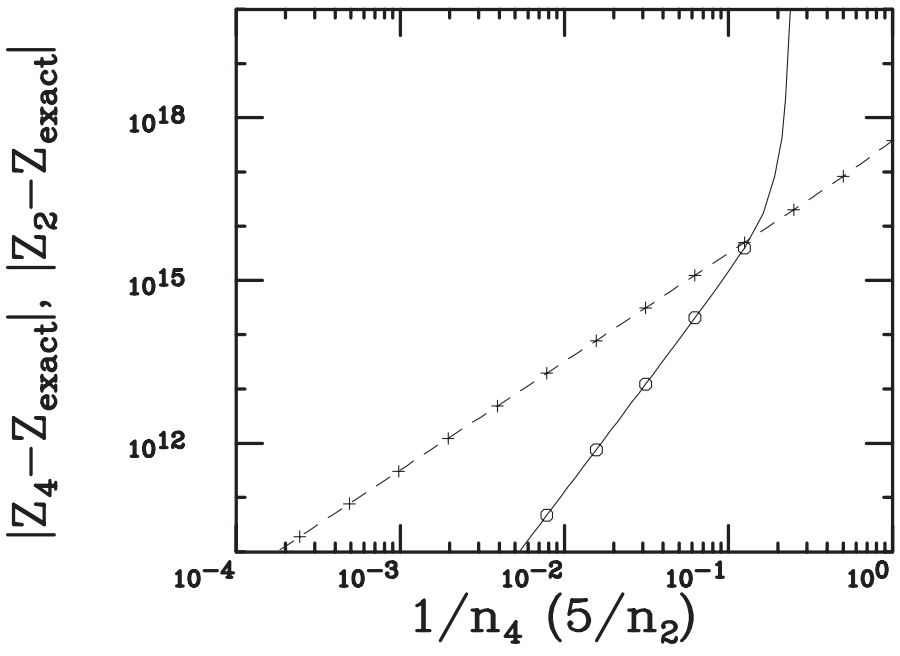

(b)

Figure 5.14 The Trotter-number dependence of corrections to the partition functions of the system at the temperatures (a) $T = 1.0$, (b) $T = 0.25$ in the Ising-like case, calculated with the second-order decomposition (dashed lines) and the fourth-order decomposition (solid lines) respectively. For a small Trotter-number, it occurs that $|Z_4 - Z_{\text{exact}}| > |Z_2 - Z_{\text{exact}}|$.

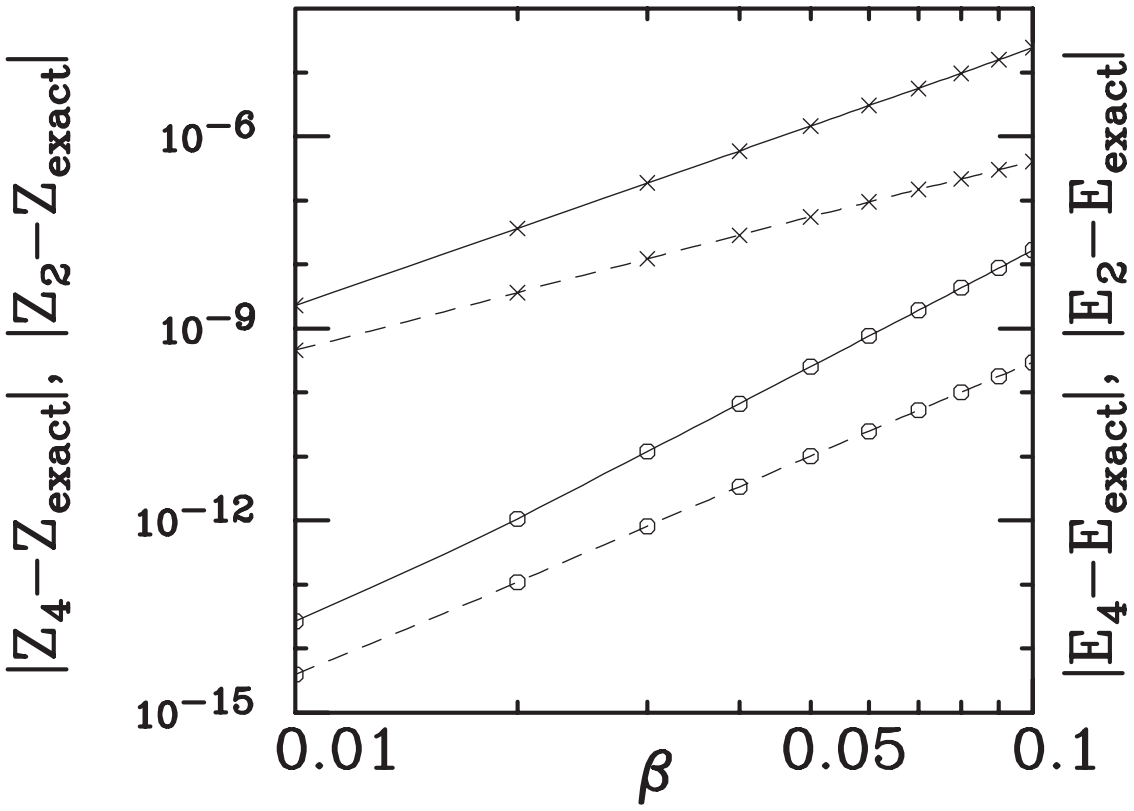

Figure 5.15 The inverse-temperature dependence in high-temperature regions of the partition functions (solid lines) and the energies (dashed lines) are calculated in the Ising-like case with the second-order decomposition (crosses) and the fourth-order decomposition (circles) respectively. The Trotter number is fixed at $n = 1024$. The plots confirm the behaviour shown in (5.A.16) and (5.A.17) respectively.

Then, as far as the partition functions are concerned, corrections come to be of higher order by one with respect to β as follows:

$$\begin{aligned} Z_2(\beta) &\equiv \mathrm{Tr}\left[S_2\left(-\frac{\beta}{n}\right)\right]^n \simeq Z_{\mathrm{exact}}(\beta) + \frac{B_2\beta^4}{n^2}, \\ Z_4(\beta) &\equiv \mathrm{Tr}\left[S_4\left(-\frac{\beta}{n}\right)\right]^n \simeq Z_{\mathrm{exact}}(\beta) + \frac{B_4\beta^6}{n^4}, \end{aligned} \tag{5.A.16}$$

for $\beta/n \ll 1$, with some constants B_2 and B_4. This behaviour is confirmed by the results, for example, in the Ising-like case plotted in Fig. 5.15. In high-temperature regions, correction to the partition function is suppressed by this effect.

Since Tr $(\mathcal{H}Q_3)$ and Tr $(\mathcal{H}R_5)$ are generally non-vanishing, corrections to the energies are fitted to the following functions:

$$E_2(\beta) - E_{\mathrm{exact}} \simeq C_2\frac{\beta^3}{n^2}, \quad \text{and} \quad E_4(\beta) - E_{\mathrm{exact}} \simeq C_4\frac{\beta^5}{n^4}, \tag{5.A.17}$$

with some constants C_2 and C_4; see Fig. 5.15, for example.

5.B Correction-term theorem concerning decompositions of exponential operators††

In this appendix we present some general results concerning the traces of the exponential operators and their approximants. We prove that the leading correction term to the Trotter-like approximations is traceless, and hence the correction to the trace of the exponential operator is of higher order by one.

In order to evaluate the exponential operator of the form $\mathrm{e}^{x\mathcal{H}}$, various approximants have been introduced [Weiss 62, Wilcox 67, Suzuki 76a, Suzuki 77a, Suzuki 90, Suzuki 91]. In particular, approximants of the following form are useful:

$$Q(x) \equiv \prod_{j=1}^{q} \exp\left(x^{k_j} A_j\right). \tag{5.B.1}$$

The arguments in the following can be applied to approximants of this general form, as well as the Suzuki-Trotter approximants.

Theorem 1 (Correction-Term Theorem) *Suppose that an exponential operator* $\mathrm{e}^{x\mathcal{H}}$ *is decomposed to a product of exponential operators as follows:*

$$Q(x) \equiv \prod_{j=1}^{q} \exp\left(x^{k_j} A_j\right) = \exp\left(x\mathcal{H} + \sum_{i=2}^{\infty} x^i \mathcal{R}_i\right). \tag{5.B.2}$$

For arbitrary decompositions of the above type with the condition

$$\sum_{j=1}^{q} x^{k_j} \, Tr \; A_j = x \, Tr \; \mathcal{H}, \tag{5.B.3}$$

all the traces of the correction terms vanish, i.e.,

$$Tr \; \mathcal{R}_i = 0, \quad for \quad i = 2, 3, 4, \ldots \tag{5.B.4}$$

Note 1. The fractal decompositions [Suzuki 90, Suzuki 91] described in Section 5.2,

$$\begin{aligned}
Q_1(x) &\equiv \mathrm{e}^{xA}\mathrm{e}^{xB} = \exp\left[x(A+B) + \sum_{i=2}^{\infty} x^i \mathcal{R}_i\right], && \text{(5.B.5)}\\
S_2(x) &\equiv \mathrm{e}^{xA/2}\mathrm{e}^{xB}\mathrm{e}^{xA/2} = \exp\left[x(A+B) + \sum_{i=3}^{\infty} x^i \mathcal{R}'_i\right], && \text{(5.B.6)}\\
S_4(x) &\equiv S_2(p_2 x) S_2(p_2 x) S_2((1-4p_2)x) S_2(p_2 x) S_2(p_2 x) \\
&= \exp\left[x(A+B) + \sum_{i=5}^{\infty} x^i \mathcal{R}''_i\right], && \text{(5.B.7)}\\
&\vdots
\end{aligned}$$

with the constant p_2 defined by

$$4p_2^3 + (1-4p_2)^3 = 0, \quad \text{or} \quad p_2 = (4 - \sqrt[3]{4})^{-1}, \tag{5.B.8}$$

††The content of this appendix was published in [Hatano 91a].

satisfy the condition (5.B.3). The Zassenhaus formula [Wilcox 67, Suzuki 77c]

$$\begin{aligned} f_m(x) &\equiv \exp(xA)\exp(xB)\exp\left(x^2C_2\right)\exp\left(x^3C_3\right)\cdots\exp\left(x^mC_m\right) \\ &= \exp\left[x(A+B)+\sum_{i=m+1}^{\infty}x^i\mathcal{R}_i'''\right] \end{aligned} \tag{5.B.9}$$

with the operators $\{C_k\}$ defined recursively by

$$\begin{aligned} C_2 &\equiv \frac{1}{2!}\frac{\partial^2}{\partial x^2}\left[\mathrm{e}^{-xB}\mathrm{e}^{-xA}\mathrm{e}^{x(A+B)}\right]\Big|_{x=0} = \frac{1}{2}[B,A], \\ C_3 &\equiv \frac{1}{3!}\frac{\partial^3}{\partial x^3}\left[\mathrm{e}^{-x^2C_2}\mathrm{e}^{-xB}\mathrm{e}^{-xA}\mathrm{e}^{x(A+B)}\right]\Big|_{x=0} = \frac{1}{3}[C_2,A+2B],\ldots, \end{aligned} \tag{5.B.10}$$

also satisfies the condition (5.B.3), since the traces of the commutation relations (5.B.10) vanish.

Note 2. As for the decomposition (5.B.5), the statement of this theorem is easily checked by the Baker-Campbell-Hausdorff formula [Weiss 62, Wilcox 67, Suzuki 77a], which takes the following form

$$\mathrm{e}^{xA}\mathrm{e}^{xB} = \exp\left[x(A+B)+\sum_{i=2}^{\infty}x^i\mathcal{R}_i\right] \tag{5.B.11}$$

with

$$\mathcal{R}_2 \equiv \frac{1}{2}[A,B], \quad \mathcal{R}_3 \equiv \frac{1}{6}[\mathcal{R}_2,B-A], \quad \mathcal{R}_4 \equiv \frac{1}{12}[[\mathcal{R}_2,A],B],\ldots, \tag{5.B.12}$$

since the traces of the commutation relations (5.B.12) vanish.

Note 3. If the decomposition $Q(x)$ satisfies the relation

$$Q(x)Q(-x) = Q(-x)Q(x) = I, \tag{5.B.13}$$

where I denotes the identity-operator, (e.g., the decompositions (5.B.6) and (5.B.7)), then all the correction terms of the even orders are the zero-operator, as well as the traces of them vanish, i.e.,

$$\mathcal{R}_i = O, \quad \text{for} \quad i = 2,4,6,\ldots \tag{5.B.14}$$

Direct substitution of (5.B.2) to (5.B.13) gives (5.B.14).

Proof. The following lemma is used.

Lemma 1 *For diagonalizable operators A and B, the following relation holds:*

$$Tr\ \log AB = Tr\ \log A + Tr\ \log B. \tag{5.B.15}$$

Proof of Lemma 1. This formula is essentially nothing but the decoupling of the determinant:

$$\begin{aligned} \mathrm{Tr}\ \log AB &= \log\det(AB) \\ &= \log(\det A\cdot\det B) = \log\det A + \log\det B \\ &= \mathrm{Tr}\ \log A + \mathrm{Tr}\ \log B. \quad \square \end{aligned} \tag{5.B.16}$$

Application of Lemma 1 yields

$$\begin{aligned} \mathrm{Tr}\ \log Q(x) &= \mathrm{Tr}\ \log \prod_{j=1}^{q} \exp\left(x^{k_j} A_j\right) \\ &= \sum_{j=1}^{q} \mathrm{Tr}\ \log \exp\left(x^{k_j} A_j\right) = \sum_{j=1}^{q} x^{k_j} \mathrm{Tr}\ A_j \\ &\overset{(5.B.3)}{=} x \mathrm{Tr}\ \mathcal{H}. \end{aligned} \tag{5.B.17}$$

On the other hand, the right-hand side of (5.B.2) gives

$$\mathrm{Tr}\ \log Q(x) = \mathrm{Tr}\ \left(x\mathcal{H} + \sum_{i=2}^{\infty} x^i \mathcal{R}_i\right). \tag{5.B.18}$$

Owing to (5.B.17) and (5.B.18), the following relation holds for an arbitrary real number x:

$$\sum_{i=2}^{\infty} x^i \mathrm{Tr}\ \mathcal{R}_i = 0. \tag{5.B.19}$$

This yields the statement (5.B.4). □

Corollary 2 *Suppose that an m-th order approximant $Q_m(x)$ defined by*

$$\mathrm{e}^{x\mathcal{H}} = Q_m(x) - x^{m+1} T_{m+1} + O(x^{m+2}), \qquad m \geq 1 \tag{5.B.20}$$

satisfies the condition (5.B.3). Then the trace of the lowest-order correction vanishes, i.e.,

$$Tr\ T_{m+1} = 0. \tag{5.B.21}$$

Note. The correction term of the order of x^{m+2} in (5.B.20) is

$$-\frac{x^{m+2}}{2}\{\mathcal{H}, T_{m+1}\}, \tag{5.B.22}$$

which yields

$$\mathrm{Tr}\ \mathrm{e}^{x\mathcal{H}} = \mathrm{Tr}\ Q_m(x) - x^{m+2} \mathrm{Tr}\ \mathcal{H} T_{m+1} + O(x^{m+3}). \tag{5.B.23}$$

The term $\mathrm{Tr}\ \mathcal{H}T_{m+1}$ is generally non-vanishing, except the case [Suzuki 85d, Fye 86] of the decomposition (5.B.5), in which

$$\mathrm{Tr}\ \mathcal{H}T_2 = \frac{1}{2}\mathrm{Tr}\ (A+B)[A,B] = 0. \tag{5.B.24}$$

Proof. The following lemma is used, which is almost self-evident.

Lemma 2 *Suppose the correction to an approximant is of the order of x^{m+1} for $m \geq 1$ as follows:*

$$Q_m(x) = \mathrm{e}^{x\mathcal{H}} + x^{m+1} T_{m+1} + O(x^{m+2}). \tag{5.B.25}$$

When these corrections are rewritten as

$$Q_m(x) = \exp\left[x\mathcal{H} + \sum_{i=2}^{\infty} x^q \mathcal{R}_i\right], \tag{5.B.26}$$

then the lowest-order corrections in the exponent $\{\mathcal{R}_i\}$ is the same as that of (5.B.25), i.e.,

$$\mathcal{R}_2 = \mathcal{R}_3 = \cdots = \mathcal{R}_m = O, \quad \mathcal{R}_{m+1} = T_{m+1}. \tag{5.B.27}$$

Lemma 2 together with Theorem 1 yields

$$\mathrm{Tr}\ T_{m+1} = \mathrm{Tr}\ \mathcal{R}_{m+1} = 0. \quad \square \tag{5.B.28}$$

Corollary 3 *We consider the following Suzuki-Trotter approximation [Suzuki 76a, Suzuki 77c] to the density matrix* $\mathrm{e}^{-\beta\mathcal{H}}$ *with the approximant* $Q_m(x)$ *(correct up to the order of* x^m*) as follows:*

$$\mathrm{e}^{-\beta\mathcal{H}} = \left[Q_m\left(-\frac{\beta}{n}\right)\right]^n - \frac{\beta^{m+1}}{n^m}T_{m+1} + O\left(\frac{\beta^{m+2}}{n^m}\right). \tag{5.B.29}$$

Then, the correction of the order of β^{m+1} *to the partition function* $Z \equiv Tr\ \mathrm{e}^{-\beta\mathcal{H}}$ *vanishes, i.e.,*

$$Tr\ T_{m+1} = 0. \tag{5.B.30}$$

Note. The lowest-order correction with respect to β is as follows [Hatano 91b]:

$$Z \equiv \mathrm{Tr}\ \mathrm{e}^{-\beta\mathcal{H}} = \mathrm{Tr}\ \left[Q_m\left(-\frac{\beta}{n}\right)\right]^n - \frac{\beta^{m+2}}{n^m}\mathrm{Tr}\ \mathcal{H}T_{m+1} + O(\beta^{m+3}). \tag{5.B.31}$$

Proof. The approximant, such as

$$Q_m(x) = \mathrm{e}^{x\mathcal{H}} + x^{m+1}T_{m+1} + O(x^{m+2}) = \exp\left(x\mathcal{H} + x^{m+1}T_{m+1} + O(x^{m+2})\right) \tag{5.B.32}$$

gives

$$Q_m\left(-\frac{\beta}{n}\right) = \exp\left[-\frac{\beta}{n}\mathcal{H} + \left(\frac{\beta}{n}\right)^{m+1} T_{m+1} + O\left(\left(\frac{\beta}{n}\right)^{m+2}\right)\right], \tag{5.B.33}$$

or

$$\begin{aligned}\left[Q_m\left(-\frac{\beta}{n}\right)\right]^n &= \exp\left[-\beta\mathcal{H} + \frac{\beta^{m+1}}{n^m}T_{m+1} + O\left(\frac{\beta^{m+2}}{n^{m+1}}\right)\right] \\ &= \mathrm{e}^{-\beta\mathcal{H}} + \frac{\beta^{m+1}}{n^m}T_{m+1} + O\left(\frac{\beta^{m+2}}{n^m}\right).\end{aligned} \tag{5.B.34}$$

Corollary 2 gives $\mathrm{Tr}\ T_{m+1} = 0$, or (5.B.30). $\square$

5.C Measurement formula in the world-line approach

In this section we present some formulae for measurement of physical quantities with Monte Carlo simulations to supplement Section 5.3. Here we concentrate on the model (5.3.1) and the decomposition (5.3.4)-(5.3.6) again.

A physical quantity is measured in the following way. When we perform a Monte Carlo simulation with the importance-sampling method according to the Boltzmann weight W, we obtain the thermal average of a quantity f in the form

$$\frac{\sum_{\{\sigma\}} Q\{\sigma\}W\{\sigma\}}{\sum_{\{\sigma\}} W\{\sigma\}} = \langle Q\rangle_{\mathrm{MCS}}\,. \tag{5.C.1}$$

Here $\langle f \rangle_{\rm MCS}$ denotes the average over the Monte Carlo steps. The problem here is how to express the quantum-statistical average

$$\langle Q \rangle_{\rm q} \equiv \frac{1}{Z_{\rm q}} \sum_{\{\sigma\}_0} \left\langle \{\sigma\}_0 \left| Q {\rm e}^{-\beta \mathcal{H}} \right| \{\sigma\}_0 \right\rangle \tag{5.C.2}$$

in the form (5.C.1). Following the same procedure as in (5.3.8), we have

$$\begin{aligned} \langle Q \rangle_{\rm q} &\simeq \langle Q \rangle_n \equiv \frac{1}{Z_n} \sum_{\{\sigma\}} \left\langle \{\sigma\}_0 \left| Q \left({\rm e}^{-\beta A/n} {\rm e}^{-\beta B/n} \right)^n \right| \{\sigma\}_0 \right\rangle & \text{(5.C.3)} \\ &= \frac{1}{Z_n} \sum_{\{\sigma\}} \left\langle \{\sigma\}_0 \left| Q {\rm e}^{-\beta A/n} \right| \{\sigma\}_1 \right\rangle \left\langle \{\sigma\}_1 \left| {\rm e}^{-\beta B/n} \right| \{\sigma\}_2 \right\rangle \\ &\qquad \cdots \left\langle \{\sigma\}_{2n-1} \left| {\rm e}^{-\beta B/n} \right| \{\sigma\}_0 \right\rangle . & \text{(5.C.4)} \end{aligned}$$

The following three cases are possible.

Case I: The operator Q is diagonal in the present representation, $\{|\{\sigma\}_l\rangle\}$. For the present model the z component of the magnetization $\langle \sum_i \sigma_i^z \rangle$ and the direct correlation $\langle \sigma_i^z \sigma_j^z \rangle$ are the quantities of this kind. In this case we write (5.C.4) in terms of (5.3.18) as

$$\langle Q \rangle_n = \frac{1}{Z_n} \sum_{\{\sigma\}} \tilde{Q}(\{\sigma\}_0) W\{\sigma\} = \left\langle \tilde{Q}(\{\sigma\}_0) \right\rangle_{\rm MCS} , \tag{5.C.5}$$

where

$$\tilde{Q}(\{\sigma\}_0) \equiv \langle \{\sigma\}_0 | Q | \{\sigma\}_0 \rangle . \tag{5.C.6}$$

The measurement of $\tilde{Q}$ in simulations thus yields an approximant of $\langle Q \rangle_{\rm q}$.

Moreover, the following formula is more practical than (5.C.5) when we perform Monte Carlo simulations. We can modify (5.C.3) as follows:

$$\begin{aligned} \langle Q \rangle_n &\equiv \frac{1}{Z_n} \sum_{\{\sigma\}} \langle \{\sigma\}_0 | \, Q \left({\rm e}^{-\beta A/n} {\rm e}^{-\beta B/n} \right)^n | \{\sigma\}_0 \rangle \\ &= \frac{1}{Z_n} \sum_{\{\sigma\}} \langle \{\sigma\}_0 | \left({\rm e}^{-\beta A/n} {\rm e}^{-\beta B/n} \right)^k Q \left({\rm e}^{-\beta A/n} {\rm e}^{-\beta B/n} \right)^{n-k} | \{\sigma\}_0 \rangle & \text{(5.C.7)} \\ &\simeq \frac{1}{Z_n} \sum_{\{\sigma\}} \langle \{\sigma\}_0 | \left({\rm e}^{-\beta A/n} {\rm e}^{-\beta B/n} \right)^k {\rm e}^{-\beta A/n} Q {\rm e}^{-\beta B/n} \\ &\qquad \times \left({\rm e}^{-\beta A/n} {\rm e}^{-\beta B/n} \right)^{n-k-1} | \{\sigma\}_0 \rangle & \text{(5.C.8)} \end{aligned}$$

for $k = 0, 1, \ldots, n-1$. Applying the same transformation as in (5.C.4) to (5.C.7) and (5.C.8), we have

$$\langle Q \rangle_n = \frac{1}{2n} \sum_{l=0}^{2n-1} \left\langle \tilde{Q}(\{\sigma\}_l) \right\rangle_{\rm MCS} . \tag{5.C.9}$$

The number of Monte Carlo samples here is greater than in (5.C.5), and hence we can expect improvement of statistical errors.

The total magnetization

$$M \equiv \sum_{i=0}^{N} \sigma_i^z \tag{5.C.10}$$

is given by

$$\langle M \rangle_n = \frac{1}{2n} \left\langle \tilde{M} \right\rangle_{\rm MCS}, \tag{5.C.11}$$

where

$$\tilde{M} \equiv \sum_{i=0}^{N} \sum_{l=0}^{2n-1} \sigma_{i,l}. \tag{5.C.12}$$

The longitudinal direct correlation is given by

$$\left\langle \sigma_i^z \sigma_j^z \right\rangle_n = \frac{1}{2n} \sum_{l=0}^{2n-1} \langle \sigma_{i,l} \sigma_{j,l} \rangle_{\rm MCS}. \tag{5.C.13}$$

Case II: A matrix element of the operator $Q\mathrm{e}^{-\beta A/n}$ vanishes when the corresponding element of the operator $\mathrm{e}^{-\beta A/n}$ vanishes, namely,

$$\left\langle \{\sigma\}_0 \left| Q\mathrm{e}^{-\beta A/n} \right| \{\sigma\}_1 \right\rangle = 0 \qquad \text{if} \quad \left\langle \{\sigma\}_0 \left| \mathrm{e}^{-\beta A/n} \right| \{\sigma\}_1 \right\rangle = 0. \tag{5.C.14}$$

The nearest-neighbor correlation $\langle \boldsymbol{\sigma}_i \cdot \boldsymbol{\sigma}_{i+1} \rangle$ is the quantity of this kind, provided i is an even number. In this case we write (5.C.3) in the form [Suzuki 77b, Hirsch 82]

$$\langle Q \rangle_n = \frac{1}{Z_n} \sum_{\{\sigma\}} \tilde{Q}(\{\sigma\}_0, \{\sigma\}_1) W\{\sigma\} = \left\langle \tilde{Q}(\{\sigma\}_0, \{\sigma\}_1) \right\rangle_{\rm MCS} \tag{5.C.15}$$

with

$$\tilde{Q}(\{\sigma\}_0, \{\sigma\}_1) \equiv \frac{\left\langle \{\sigma\}_0 \left| Q\mathrm{e}^{-\beta A/n} \right| \{\sigma\}_1 \right\rangle}{\langle \{\sigma\}_0 | \mathrm{e}^{-\beta A/n} | \{\sigma\}_1 \rangle}. \tag{5.C.16}$$

When we utilize the modification (5.C.7) and (5.C.8) again, we have

$$\langle Q \rangle_n = \frac{1}{n} \sum_{l=0}^{n-1} \left\langle \tilde{Q}'(\{\sigma\}_{2l}, \{\sigma\}_{2l+1}) \right\rangle_{\rm MCS} \tag{5.C.17}$$

with

$$\tilde{Q}'(\{\sigma\}_l, \{\sigma\}_{l+1}) \equiv \frac{1}{2} \frac{\left\langle \{\sigma\}_0 \left| \left(Q\mathrm{e}^{-\beta A/n} + \mathrm{e}^{-\beta A/n} Q \right) \right| \{\sigma\}_1 \right\rangle}{\left\langle \{\sigma\}_0 \left| \mathrm{e}^{-\beta A/n} \right| \{\sigma\}_1 \right\rangle}. \tag{5.C.18}$$

The nearest-neighbor correlation $\langle \boldsymbol{\sigma}_i \cdot \boldsymbol{\sigma}_{i+1} \rangle$, with i being an odd number, satisfies the condition (5.C.14) when we replace A by B. In this case the reformulation is trivial, namely,

$$\langle Q \rangle_n = \left\langle \tilde{Q}(\{\sigma\}_1, \{\sigma\}_2) \right\rangle_{\rm MCS} \tag{5.C.19}$$

with

$$\tilde{Q}(\{\sigma\}_1, \{\sigma\}_2) \equiv \frac{\left\langle \{\sigma\}_1 \left| Q\mathrm{e}^{-\beta B/n} \right| \{\sigma\}_2 \right\rangle}{\langle \{\sigma\}_1 | \mathrm{e}^{-\beta B/n} | \{\sigma\}_2 \rangle}. \tag{5.C.20}$$

We can modify this formula as in (5.C.17)-(5.C.18).

Measurement of the internal energy of (5.3.1) is thereby possible; the part A of (5.3.6) can be measured with (5.C.15) (or (5.C.17)) while the part B with (5.C.19). Thus we have [Suzuki 77b]

$$E \equiv \langle \mathcal{H} \rangle_{\rm q} \simeq \langle \mathcal{H} \rangle_n = \frac{1}{n} \sum_{i,l} \left\langle \tilde{\mathcal{H}}(i,l) \right\rangle_{\rm MCS}, \tag{5.C.21}$$

where

$$\begin{aligned} \tilde{\mathcal{H}}(i,l) &\equiv -\frac{\langle \sigma_{i,l}, \sigma_{i+1,l} \,|\hat{\boldsymbol{\sigma}}_i \cdot \hat{\boldsymbol{\sigma}}_{i+1} \exp(\beta \hat{\boldsymbol{\sigma}}_i \cdot \hat{\boldsymbol{\sigma}}_{i+1}/n)|\, \sigma_{i,l+1}, \sigma_{i+1,l+1} \rangle}{\langle \sigma_{i,l}, \sigma_{i+1,l} \,|\exp(\beta \hat{\boldsymbol{\sigma}}_i \cdot \hat{\boldsymbol{\sigma}}_{i+1}/n)|\, \sigma_{i,l+1}, \sigma_{i+1,l+1} \rangle} \\ &= -\begin{pmatrix} 1 & & & \\ & b' & c' & \\ & c' & b' & \\ & & & 1 \end{pmatrix} \end{aligned} \tag{5.C.22}$$

with

$$b' \equiv -1 + 2\tanh(2\beta/n) \qquad \text{and} \qquad c' \equiv -1 + 2\coth(2\beta/n). \tag{5.C.23}$$

The summation in (5.C.21) runs over all the Nn four-body interactions: $i = 0, 1, \ldots, N$ and $l = 0, 1, \ldots, 2n-1$ with $i + l =$even.

Case III: Otherwise. For example, the correlation $\left\langle \sigma_i^x \sigma_j^x \right\rangle$ of the model (5.3.1) with $|i - j| \geq 2$. Since (5.C.16) is not well defined in this case, we have to devise some other formulations to measure the quantities. Measurement of some quantities becomes possible only after a further modification which results in increase of the computational time [Hirsch 82].

A response function is given by summation of canonical correlations. Unlike the three cases above, Kubo's canonical correlation

$$\langle Q; R \rangle_{\rm q} \equiv \frac{1}{\beta} \int_0^\beta \left\langle Q \mathrm{e}^{-\tau \mathcal{H}} R \mathrm{e}^{-(\beta-\tau)\mathcal{H}} \right\rangle d\tau. \tag{5.C.24}$$

does not take the form (5.C.2); it is necessary to devise another formula. We utilize the approximant

$$\langle Q; R \rangle_{\rm q} \simeq \frac{1}{nZ_n} \sum_{k=0}^{n-1} \sum_{\{\sigma\}_0} \langle \{\sigma\}_0 | \, Q \left(\mathrm{e}^{-\beta A/n} \mathrm{e}^{-\beta B/n} \right)^k R \left(\mathrm{e}^{-\beta A/n} \mathrm{e}^{-\beta B/n} \right)^{n-k} |\{\sigma\}_0 \rangle \,. \tag{5.C.25}$$

When Q and R are diagonal operators, we have

$$\begin{aligned} \langle Q; R \rangle_n &= \frac{1}{n} \sum_{l=0}^{n-1} \left\langle \tilde{Q}(\{\sigma\}_0) \tilde{R}(\{\sigma\}_{2l}) \right\rangle_{\rm MCS} \\ &= \frac{1}{4n^2} \sum_{k=0}^{2n-1} \sum_{l=0}^{2n-1} \left\langle \tilde{Q}(\{\sigma\}_k) \tilde{R}(\{\sigma\}_l) \right\rangle_{\rm MCS}. \end{aligned} \tag{5.C.26}$$

When Q and R are not diagonal but satisfy (5.C.14), the formula is more complicated than above:

$$\langle Q; R \rangle_n = \frac{1}{n} \left(\widetilde{QR}(\{\sigma\}_0, \{\sigma\}_1) + \sum_{l=1}^{n-1} \left\langle \tilde{Q}(\{\sigma\}_0, \{\sigma\}_1) \tilde{R}(\{\sigma\}_{2l}, \{\sigma\}_{2l+1}) \right\rangle_{\rm MCS} \right)$$

$$= \frac{1}{n^2}\left(\sum_{l=0}^{n-1}\widetilde{QR}(\{\sigma\}_{2l},\{\sigma\}_{2l+1}) + \sum_{k=0}^{n-1}\sum_{\substack{l=0\\k\neq l}}^{n-1}\left\langle\tilde{Q}(\{\sigma\}_{2k},\{\sigma\}_{2k+1})\tilde{R}(\{\sigma\}_{2l},\{\sigma\}_{2l+1})\right\rangle_{\rm MCS}\right), \tag{5.C.27}$$

where

$$\widetilde{QR}(\{\sigma\}_0,\{\sigma\}_1) \equiv \frac{\left\langle\{\sigma\}_0\left|QR\mathrm{e}^{-\beta A/n}\right|\{\sigma\}_1\right\rangle}{\left\langle\{\sigma\}_0\left|\mathrm{e}^{-\beta A/n}\right|\{\sigma\}_1\right\rangle}. \tag{5.C.28}$$

Here $\widetilde{QR}$ is necessary unlike the case (5.C.26); we have to distinguish $\widetilde{QR}$ from $\tilde{Q}\tilde{R}$.

The susceptibility with respect to the magnetic field along the z axis

$$\chi \equiv \frac{\beta}{N\beta}\frac{\partial^2\log Z_{\rm q}(H)}{\partial H^2} = \frac{1}{N}\sum_{i,j}\left(\left\langle\sigma_i^z;\sigma_j^z\right\rangle_{\rm q} - \langle\sigma_i^z\rangle_{\rm q}\left\langle\sigma_j^z\right\rangle_{\rm q}\right). \tag{5.C.29}$$

is obtained from (5.C.26) in the form [Suzuki 77b]

$$\chi \simeq \frac{\beta}{4n^2N}\left(\left\langle\tilde{M}^2\right\rangle_{\rm MCS} - \left\langle\tilde{M}\right\rangle_{\rm MCS}^2\right), \tag{5.C.30}$$

where $\tilde{M}$ is defined by (5.C.12).

Since the Hamiltonian is not a diagonal operator, a formula for the specific heat

$$C \equiv \frac{1}{N}\frac{\partial E}{\partial T} = -\frac{\beta^2}{N}\frac{\partial E}{\partial\beta} \tag{5.C.31}$$

is more complicated than the one for the susceptibility. The formula (5.C.27) yields [Suzuki 77b]

$$C \simeq \frac{\beta^2}{n^2N}\left\{\left\langle\left(\sum_{i,l}\tilde{\mathcal{H}}\right)^2\right\rangle_{\rm MCS} - \left\langle\sum_{i,l}\tilde{\mathcal{H}}\right\rangle_{\rm MCS}^2 + \left\langle\sum_{i,l}\left(\widetilde{\mathcal{H}^2} - \tilde{\mathcal{H}}^2\right)\right\rangle_{\rm MCS}\right\}. \tag{5.C.32}$$

Here $\tilde{\mathcal{H}}$ is given by (5.C.22), while $\widetilde{\mathcal{H}^2}$ is defined by (5.C.28), or

$$\begin{aligned}\widetilde{\mathcal{H}^2}(i,l) &\equiv \frac{\left\langle\sigma_{i,l},\sigma_{i+1,l}\left|(\hat{\boldsymbol{\sigma}}_i\cdot\hat{\boldsymbol{\sigma}}_{i+1})^2\exp(\beta\hat{\boldsymbol{\sigma}}_i\cdot\hat{\boldsymbol{\sigma}}_{i+1}/n)\right|\sigma_{i,l+1},\sigma_{i+1,l+1}\right\rangle}{\left\langle\sigma_{i,l},\sigma_{i+1,l}\left|\exp(\beta\hat{\boldsymbol{\sigma}}_i\cdot\hat{\boldsymbol{\sigma}}_{i+1}/n)\right|\sigma_{i,l+1},\sigma_{i+1,l+1}\right\rangle} \\ &= \begin{pmatrix} 1 & & & \\ & b'' & c'' & \\ & c'' & b'' & \\ & & & 1 \end{pmatrix}\end{aligned} \tag{5.C.33}$$

with

$$b'' \equiv 5 - 4\tanh(2\beta/n) \qquad \text{and} \qquad c'' \equiv 5 - 4\coth(2\beta/n). \tag{5.C.34}$$

Note that the third term in (5.C.32) is necessary unlike the case of (5.C.30).

5.D Negative-sign problem in the auxiliary-field approach

In this appendix we discuss a case where the negative-sign problem of the auxiliary-field approach disappears.

First, we prove that the weight $W_\uparrow W_\downarrow$ in (5.7.8) is non-negative for all the auxiliary-field configurations $\{s\}$, provided that $\mu = 0$ and the lattice is bipartite [Hirsch 83c, Hirsch 85a]. We introduce particle-hole transformation as follows:

$$\begin{array}{lcllcllll} d_{i\sigma} & \equiv & c^\dagger_{i-\sigma} & \text{and} & d^\dagger_{i\sigma} & \equiv & c_{i-\sigma} & \text{for} & i \in \text{sublattice } A, \\ d_{i\sigma} & \equiv & -c^\dagger_{i-\sigma} & \text{and} & d^\dagger_{i\sigma} & \equiv & -c_{i-\sigma} & \text{for} & i \in \text{sublattice } B. \end{array} \tag{5.D.1}$$

Since this is a unitary transformation, the integration measure of the trace operation Tr does not change. In terms of the hole operators d, the kinetic energy (5.7.3) is transformed to

$$K_\sigma \equiv -t \sum_{\langle i,j \rangle} \left(c^\dagger_{i\sigma} c_{j\sigma} + c^\dagger_{j\sigma} c_{i\sigma} \right) = -t \sum_{\langle i,j \rangle} \left(d^\dagger_{i-\sigma} d_{j-\sigma} + d^\dagger_{j-\sigma} d_{i-\sigma} \right) = K_{-\sigma}. \tag{5.D.2}$$

Since the number operator is changed into

$$n_{i\sigma} = c^\dagger_{i\sigma} c_{i\sigma} = d_{i\sigma} d^\dagger_{i\sigma} = 1 - d^\dagger_{i-\sigma} d_{i-\sigma}, \tag{5.D.3}$$

the potential energy (5.7.10) with $\mu = 0$ is transformed to

$$\begin{aligned} -\beta \tilde{V}_\sigma / n &= \sum_i 2a\sigma s_{il} n_{i\sigma} = \sum_i 2a(-\sigma) s_{il} (d^\dagger_{i-\sigma} d_{i-\sigma} - 1) \\ &= -\beta \tilde{V}_{-\sigma} / n + 2a\sigma \sum_i s_{il}. \end{aligned} \tag{5.D.4}$$

The weight (5.7.9) is thereby transformed to

$$W_\sigma = W_{-\sigma} \mathrm{e}^{2a\sigma h}, \tag{5.D.5}$$

where

$$h \equiv \sum_{i,l} s_{il}. \tag{5.D.6}$$

Therefore the product of the weights is non-negative:

$$W_\uparrow W_\downarrow = (W_\downarrow)^2 \, \mathrm{e}^{2a\sigma h} \geq 0. \tag{5.D.7}$$

Next, we show that the case $\mu = 0$ corresponds to the half-filled band. Besides the number operator is transformed in the form (5.D.3), the Boltzmann weight has the particle-hole symmetry (5.D.5) in the case $\mu = 0$. Therefore, concerning the average of the number operator, the following equality holds:

$$\langle n_{i\sigma} \rangle = 1 - \left\langle d^\dagger_{i-\sigma} d_{i-\sigma} \right\rangle = 1 - \langle n_{i-\sigma} \rangle . \tag{5.D.8}$$

In addition the model has the inversion symmetry $\langle n_{i\sigma} \rangle = \langle n_{i-\sigma} \rangle$. Thereby we have

$$\langle n_{i\sigma} \rangle = \langle n_{i-\sigma} \rangle = \frac{1}{2} \qquad \text{for} \quad \mu = 0, \tag{5.D.9}$$

or the electrons fill half of the conduction band.

In the half-filled-band case the Hubbard model becomes the antiferromagnetic Heisenberg model in the limit $U \to \infty$ [Cleveland 76]. The disappearance of the negative-sign problem in the present case coincides with the fact that, in the case of the antiferromagnetic Heisenberg model on a bipartite lattice, the negative-sign problem does not appear even in the world-line approach (see the argument below (5.4.6)). Even if we treat the model by the auxiliary-field approach, the problem remains in the case of a frustrated lattice.

5.E Equalities used in the auxiliary-field approach

In this appendix we prove several equalities used in the formulation of the auxiliary-field approach, namely, (5.7.13), (5.7.15), (5.7.19) [Blankenbecler 81, Hirsch 85a, De Raedt 92], and (5.8.24) [Imada 89]. A measurement formula for the Matsubara Green's function is also shown. [Blankenbecler 81, Hirsch 85a].

First, we prove the operator identity

$$\exp(c_i^\dagger \overline{B}_{ij} c_j) \exp(c_i^\dagger \overline{A}_{ij} c_j) = \exp(c_i^\dagger \overline{L}_{ij} c_j), \tag{5.E.1}$$

where $\overline{L}$ is defined by

$$\mathrm{e}^{\overline{B}} \mathrm{e}^{\overline{A}} = \mathrm{e}^{\overline{L}}. \tag{5.E.2}$$

Summation over repeated indices is assumed here.

Let us operate the operator

$$\exp(c_i^\dagger \overline{A}_{ij} c_j) \tag{5.E.3}$$

to a one-particle state

$$|\psi\rangle \equiv \sum_k F_k |k\rangle , \tag{5.E.4}$$

where

$$|k\rangle \equiv c_k^\dagger |0\rangle \tag{5.E.5}$$

with $|0\rangle$ denoting the vacuum state. We define a $N \times N$ unitary matrix $\overline{P}$ to diagonalize the matrix $\overline{A}$:

$$\overline{P}^\dagger \overline{A}\, \overline{P} = \overline{D} \equiv \begin{pmatrix} \lambda_1 & & & \\ & \lambda_2 & & \\ & & \ddots & \\ & & & \lambda_N \end{pmatrix}. \tag{5.E.6}$$

Using this matrix we define a unitary transformation of fermion operators:

$$a_\mu \equiv \overline{P}^\dagger_{\mu i} c_i \quad \text{and} \quad a_\mu^\dagger \equiv c_i^\dagger \overline{P}_{i\mu}. \tag{5.E.7}$$

Then the operator (5.E.3) is rewritten in the form

$$\exp(c_i^\dagger \overline{A}_{ij} c_j) = \exp\left(\sum_{\mu=1}^N \lambda_\mu a_\mu^\dagger a_\mu \right) = \prod_{\mu=1}^N \exp\left(\lambda_\mu a_\mu^\dagger a_\mu \right). \tag{5.E.8}$$

The state (5.E.4), on the other hand, is rewritten in the form

$$|\psi\rangle = \sum_{k,\nu} \overline{P}^{\dagger}_{\nu k} F_k \, |\nu\rangle\!\rangle \,, \tag{5.E.9}$$

where

$$|\nu\rangle\!\rangle \equiv a^{\dagger}_{\nu} \, |0\rangle \,. \tag{5.E.10}$$

Operation of (5.E.8) to (5.E.9) yields

$$\exp(c^{\dagger}_i \overline{A}_{ij} c_j) \, |\psi\rangle = \sum_{k,\nu} \mathrm{e}^{\lambda_\nu} \overline{P}^{\dagger}_{\nu k} F_k \, |\nu\rangle \,. \tag{5.E.11}$$

When we go back to the c-operator representation, we have

$$\exp(c^{\dagger}_i \overline{A}_{ij} c_j) \, |\psi\rangle = \sum_{k,l,\nu} \overline{P}_{l\nu} \mathrm{e}^{\lambda_\nu} \overline{P}^{\dagger}_{\nu k} F_k \, |l\rangle = \sum_{k,l} \left(\mathrm{e}^{\overline{A}}\right)_{lk} F_k \, |l\rangle \,. \tag{5.E.12}$$

When we apply the other operator $\exp(c^{\dagger}_i \overline{B}_{ij} c_j)$ successively to the state (5.E.12), calculation goes in the same way, and hence

$$\exp(c^{\dagger}_i \overline{B}_{ij} c_j) \exp(c^{\dagger}_i \overline{A}_{ij} c_j) \, |\psi\rangle = \sum_{k,g} \left(\mathrm{e}^{\overline{L}}\right)_{gk} F_k \, |g\rangle \,. \tag{5.E.13}$$

with

$$\left(\mathrm{e}^{\overline{L}}\right)_{gk} = \sum_{l} \left(\mathrm{e}^{\overline{B}}\right)_{gl} \left(\mathrm{e}^{\overline{A}}\right)_{lk} . \tag{5.E.14}$$

The argument above can be extended to cases of many-particle states,

$$\sum_{i_1, i_2, \ldots} F(i_1, i_2, \ldots) \, |i_1, i_2, \cdots\rangle \,. \tag{5.E.15}$$

Thus we have the operator identity (5.E.1). Successive applications of (5.E.1) give (5.7.13).

The direct product of one-particle states, in particular, can be treated easily. When we apply the operator $\exp(c^{\dagger}_i A_{ij} c_j)$ to the state

$$|\psi\rangle \equiv \bigotimes_{m=1}^{M} \left(\sum_{k=1}^{N} F_{km} \, |k\rangle \right) , \tag{5.E.16}$$

the result is

$$\exp(c^{\dagger}_i A_{ij} c_j) \, |\psi\rangle = \bigotimes_{m=1}^{M} \left(\sum_{k,l} \left(\mathrm{e}^{\overline{A}}\right)_{lk} F_{km} \, |l\rangle \right) . \tag{5.E.17}$$

This manipulation can be expressed by the multiplication of the $N \times N$ matrix $\mathrm{e}^{\overline{A}}$ and the $N \times M$ matrix F. This gives (5.8.24).

Next, we prove the equality

$$\mathrm{Tr} \, \exp(c^{\dagger}_i \overline{A}_{ij} c_j) = \det \left[\overline{I} + \mathrm{e}^{\overline{A}} \right] . \tag{5.E.18}$$

This is directly derived from (5.E.8). Since the unitary transformation (5.E.7) does not change the integration measure of the trace operation Tr , the left-hand side of (5.E.18) is transformed as

$$\mathrm{Tr}\ \exp(c_i^\dagger \overline{A}_{ij} c_j) = \prod_{\mu=1}^{N} \mathrm{Tr}\ \exp\left(\lambda_\mu a_\mu^\dagger a_\mu\right) = \prod_{\mu=1}^{N} \left(1 + \mathrm{e}^{\lambda_\mu}\right) = \det\left[\overline{I} + \mathrm{e}^{\overline{D}}\right]. \tag{5.E.19}$$

Substituting the equality $\mathrm{e}^{\overline{D}} = \overline{P}^\dagger \mathrm{e}^{\overline{A}} \overline{P}$ to (5.E.19), we have (5.E.18), or (5.7.15).

Derivation of the equality

$$\overline{G}_{kl} \equiv \frac{\mathrm{Tr}\, c_k c_l^\dagger \exp(c_i^\dagger \overline{A}_{ij} c_j)}{\mathrm{Tr}\ \exp(c_i^\dagger \overline{A}_{ij} c_j)} = \left(\overline{I} + \mathrm{e}^{\overline{A}}\right)^{-1}_{kl} \tag{5.E.20}$$

is similar to (5.E.19), that is,

$$\begin{aligned} \frac{\mathrm{Tr}\, c_k c_l^\dagger \exp(c_i^\dagger \overline{A}_{ij} c_j)}{\mathrm{Tr}\ \exp(c_i^\dagger \overline{A}_{ij} c_j)} &= \sum_{\nu,\eta} \overline{P}_{k\nu} \delta_{\nu\eta} \overline{P}^\dagger_{\eta l} \frac{\mathrm{Tr}\, a_\nu a_\nu^\dagger \mathrm{e}^{\lambda_\nu a_\nu^\dagger a_\nu} \prod_{\mu(\neq\nu)} \exp\left(\lambda_\mu a_\mu^\dagger a_\mu\right)}{\prod_\mu \mathrm{Tr}\ \exp\left(\lambda_\mu a_\mu^\dagger a_\mu\right)} \\ &= \sum_{\nu} \overline{P}_{k\nu} \left(1 + \mathrm{e}^{\lambda_\nu}\right)^{-1} \overline{P}^\dagger_{\nu l} = \left(\overline{I} + \mathrm{e}^{\overline{A}}\right)^{-1}_{kl}. \end{aligned} \tag{5.E.21}$$

This result gives (5.7.19).

A measurement formula for the Matsubara Green's function follows from the equality

$$\frac{\mathrm{Tr}\, c_k \exp(c_i^\dagger \overline{B}_{ij} c_j) c_m^\dagger \exp(-c_i^\dagger \overline{B}_{ij} c_j) \exp(c_i^\dagger \overline{A}_{ij} c_j)}{\mathrm{Tr}\ \exp(c_i^\dagger \overline{A}_{ij} c_j)} = \left(\left(\overline{I} + \mathrm{e}^{\overline{A}}\right)^{-1} \mathrm{e}^{\overline{B}}\right)_{km}. \tag{5.E.22}$$

Substitution of the equality

$$\exp(c_i^\dagger \overline{B}_{ij} c_j) c_m^\dagger \exp(-c_i^\dagger \overline{B}_{ij} c_j) = \sum_l c_l^\dagger \left(\mathrm{e}^{\overline{B}}\right)_{lm} \tag{5.E.23}$$

combined with (5.E.20) yields (5.E.22). The proof of (5.E.23) is quite similar to the procedure (5.E.3)-(5.E.12).

The Matsubara Green's function $\langle c_k(\tau) c_l^\dagger \rangle_{\mathrm{q}}$, where

$$c_k(\tau) \equiv \mathrm{e}^{\tau \mathcal{H}} c_k \mathrm{e}^{-\tau \mathcal{H}}, \tag{5.E.24}$$

is given by measurement of [Blankenbecler 81, Hirsch 85a]

$$\overline{\mathcal{G}}_{kl} \equiv \frac{1}{W} \mathrm{Tr}\, c_k \mathrm{e}^{c_i^\dagger \overline{H}'_{ij} c_j} c_l^\dagger \mathrm{e}^{-c_i^\dagger \overline{H}'_{ij} c_j} \mathrm{e}^{c_i^\dagger \overline{H}_{ij} c_j}, \tag{5.E.25}$$

where $\overline{H}'$ is defined by

$$\prod_{l=1}^{m} \left(\mathrm{e}^{\overline{K}} \mathrm{e}^{\overline{V}}\right) = \mathrm{e}^{\overline{H}'} \tag{5.E.26}$$

with $m = \tau/\beta$. Using (5.E.22) we have the formula

$$\overline{\mathcal{G}} = \left(\overline{I} + \mathrm{e}^{\overline{H}}\right)^{-1} \mathrm{e}^{\overline{H}'} = \overline{G} \mathrm{e}^{\overline{H}'}. \tag{5.E.27}$$

Bibliography ⟨ with Citation index ⟩

[Abrikosov 61] A. A. Abrikosov, L. P. Gorkov and I. E. Dzyaloshinski, translated by R. A. Silverman, *Methods of Quantum Field Theory in Statistical Physics*, the Dover edition (Dover Publications, New York, 1975). ⟨85⟩

[Affleck 88] I. Affleck, T. Kennedy, E. H. Lieb, and H. Tasaki, Valence bond ground states in isotropic quantum antiferromagnets, Commun. Math. Phys. **115** (1988) 477-528. ⟨4, 17, 18⟩

[Affleck 89] I. Affleck, Quantum spin chains and the Haldane gap, J. Phys.: Condens. Matter. **1** (1989) 3047-3072. ⟨4, 17, 65⟩

[An 91] G. An and J. M. van Leeuwen, Fixed-node Monte Carlo study of the two-dimensional Hubbard model, Phys. Rev. B **44** (1991) 9410-9417. ⟨81⟩

[Anderson 87] P. W. Anderson, The resonating valence bond state in La_2CuO_4 and superconductivity, Science **235** (1987) 1196-1198. ⟨74⟩

[Barma 78] M. Barma and B. S. Shastry, Classical equivalence of one-dimensional quantum-mechanical systems, Phys. Rev. B **18** (1978) 3351-3359. ⟨56⟩

[Barnes 88a] T. Barnes and G. J. Daniell, Numerical solution of spin systems and the $S = 1/2$ Heisenberg antiferromagnet using guided random walks, Phys. Rev. **37** (1988) 3637-3651. ⟨81⟩

[Barnes 88b] T. Barnes and E. S. Swanson, Two-dimensional Heisenberg antiferromagnet: A numerical study, Phys. Rev. B **37** (1988) 9405-9409. ⟨81⟩

[Barnes 89] T. Barnes, D. Kotchan and E. S. Swanson, Evidence for a phase transition in the zero-temperature anisotropic two-dimensional Heisenberg antiferromagnet, Phys. Rev. B **39** (1989) 4357-4362. ⟨81⟩

[Baskaran 87] G. Baskaran, Z. Zou and P. W. Anderson, The resonating valence bond state and high-T_c superconductivity — A mean field theory, Solid State Commun. **63** (1987) 973-976. ⟨74⟩

[Batrouni 90] G. G. Batrouni and R. T. Scalettar, Anomalous decouplings and the fermion sign problem, Phys. Rev. B **42** (1990) 2282-2289. ⟨34⟩

[Bethe 31] H. A. Bethe, Zur Theorie der Metalle. I. Eigenwerte und Eigenfunktionen der Linearen Atomkette, Z. Phys. **71** (1931) 205-226. ⟨3⟩

[Betsuyaku 84] H. Betsuyaku, Study of one-dimensional XY-model by the transfer-matrix method, Phys. Rev. Lett. **53** (1984) 629-632. ⟨63⟩

[Betsuyaku 85] H. Betsuyaku, Study of one-dimensional quantum spin systems by the transfer-matrix method, Prog. Theor. Phys. **73** (1985) 319-331. ⟨5, 64⟩

[Betsuyaku 86a] H. Betsuyaku, Cluster transfer-matrix method for one-dimensional quantum spin systems, Prog. Theor. Phys. **75**

(1986) 774-789. ⟨7, 58, 67⟩

[Betsuyaku 86b] H. Betsuyaku and T. Yokota, Study of one-dimensional quantum spin systems by the transfer-matrix method. II — $S = 1$ case —, Prog. Theor. Phys. **75** (1986) 808-827. ⟨65⟩

[Binder 79] K. Binder, ed., *Monte Carlo Methods in Statistical Physics*, Topics in Current Physics **7** (Springer, Berlin, 1979); 2nd edition (Springer, Berlin, 1986). ⟨47⟩

[Binder 84] K. Binder, ed., *Application of the Monte Carlo Method in Statistical Physics*, Topics in Current Physics **36** (Springer, Berlin, 1984); 2nd edition (Springer, Berlin, 1987). ⟨47⟩

[Binder 92] K. Binder, ed., *The Monte Carlo Methods in Condensed Matter Physics*, Topics in Applied Physics **71** (Springer, Berlin, 1992). ⟨47⟩

[Blankenbecler 81] R. Blankenbecler, D. J. Scalapino and R. L. Sugar, Monte Carlo calculations of coupled boson-fermion systems. I, Phys. Rev. D **24** (1981) 2278-2286. ⟨70, 71, 72, 104, 106⟩

[Blankenbecler 83] R. Blankenbecler and R. L. Sugar, Projector Monte Carlo method, Phys. Rev. D **27** (1983) 1304-1311. ⟨15, 16, 75, 78⟩

[Brinkman 70] W. F. Brinkman and T. M. Rice, Application of Gutzwiller's variational method to the metal-insulator transition, Phys. Rev. B **2** (1970) 4302-4304. ⟨74⟩

[Buyers 86] W. J. L. Buyers, R. M. Morra, R. L. Armstrong, M. J. Hogan, P. Gerlach and K. Hirakawa, Experimental evidence for the Haldane gap in a spin-1, nearly isotropic, antiferromagnetic chain, Phys. Rev. Lett. **56** (1986) 371-374. ⟨3⟩

[Carlson 89] J. Carlson, Ground-state and low-lying excitation of the Heisenberg antiferromagnet, Phys. Rev. B **40** (1989) 846-849 (RC). ⟨81⟩

[Ceperley 80] D. M. Ceperley and B. J. Alder, Ground state of the electron gas by a stochastic method, Phys. Rev. Lett. **45** (1980) 566-569. ⟨62, 81⟩

[Chandra 88] P. Chandra and B. Doucot, Possible spin-liquid state at large S for the frustrated square Heisenberg lattice, Phys. Rev. B **38** (1988) 9335-9338 (RC). ⟨28⟩

[Chao 77] K. A. Chao, J. Spałek and A. M. Oleś, Kinetic exchange interaction in a narrow S-band, J. Phys. C: Solid State Phys. **10** (1977) L271-L276. ⟨74⟩

[Chen 72] H. H. Chen and R. L. Joseph, Exchange interaction model of ferromagnetism, J. Math. Phys. **13** (1972) 725-739. ⟨83⟩

[Chen 88] Y. C. Chen, H. H. Chen and F. Lee, Quantum Monte Carlo study of the one-dimensional exchange interaction model, Phys. Lett. A **130** (1988) 257-130. ⟨83⟩

[Chen 91] Y. C. Chen, H. H. Chen and F. Lee, Quantum Monte Carlo study of the spin-1/2 Heisenberg model, Phys. Rev. B **43** (1991) 11082-11087. ⟨82⟩

[Chen 92] S. Chen, A. M. Ferrenberg and D. P. Landau, Randomness-

induced second-order transition in the two-dimensional eight-state Potts model: A monte Carlo study, Phys. Rev. Lett. **69** (1992) 1213-1215. ⟨35⟩

[Cleveland 76] C. L. Cleveland and R. Medina A., Obtaining a Heisenberg Hamiltonian from the Hubbard model, Am. J. Phys. **44** (1976) 44-46. ⟨104⟩

[Cullen 83] J. J. Cullen and D. P. Landau, Monte Carlo studies of one-dimensional quantum Heisenberg and XY models, Phys. Rev. B **27** (1983) 297-313. ⟨58⟩

[Dagotto 89a] E. Dagotto and A. Moreo, Exact diagonalization study of the frustrated Heisenberg model, Phys. Rev. B **39** (1989) 4744-4747 (RC). ⟨28⟩

[Dagotto 89b] E. Dagotto and A. Moreo, Phase diagram of the frustrated spin-1/2 Heisenberg antiferromagnet in two dimensions, Phys. Rev. Lett. **63** (1989) 2148-2151. ⟨28⟩

[De Raedt 81] H. De Raedt and A. Lagendijk, Monte Carlo calculation of the thermodynamic properties of a quantum model: A one-dimensional fermion lattice model, Phys. Rev. Lett. **46** (1981) 77-80. ⟨58⟩

[De Raedt 84a] H. De Raedt, B. De Raedt, J. Fives and A. Lagendijk, Monte Carlo study of the two-dimensional spin-1/2 XY model, Phys. Lett. **104** (1984) 430-434. ⟨58⟩

[De Raedt 84b] H. De Raedt, B. De Raedt and A. Lagendijk, Thermodynamics of the two-dimensional spin-1/2 XY model, Z. Phys. B – Condensed Matter **57** (1984) 209-220. ⟨58⟩

[De Raedt 92] H. De Raedt and W. von der Linden, Quantum lattice problems, in *The Monte Carlo Methods in Condensed Matter Physics*, ed. by K. Binder, Topics in Applied Physics **71** (Springer, Berlin, 1992) 249-284. [Note that "the projector Monte Carlo method" of their terminology corresponds to the ground-state algorithm of the auxiliary-field approach described in Section 5.8, not to the projector Monte Carlo method described in Section 5.9.] ⟨71, 78, 104⟩

[Deisz 90] J. Deisz, M. Jarrell and D. L. Cox, $S(Q,\omega)$ for the $S = 1/2$ and $S = 1$ one-dimensional Heisenberg antiferromagnet: A quantum Monte Carlo study, Phys. Rev. B **42** (1990) 4869-4872 (RC). ⟨88⟩

[Deisz 92] J. Deisz, K.-H. Luk, M. Jarrell and D. L. Cox, Spin and charge dynamics for the one-dimensional t-J model, Phys. Rev. B **46** (1992) 3410-3419. ⟨88⟩

[Delica 91] T. Delica, K. Kopinga, H. Leschke and K. K. Mon, Thermal properties of chains of antiferromagnetically coupled spins with $s = 1$: Numerical evidence of the Haldane gap at nonzero temperature, Europhys. Lett. **15** (1991) 55-61. ⟨7, 65⟩

[Den Nijs 89] M. den Nijs and K. Rommelse, Preroughening transitions in crystal surfaces and valence-bond phases in quantum spins

chains, Phys. Rev. B **40** (1989) 4709-4734. ⟨18⟩

[Ding 90a] H.-Q. Ding and M. S. Makivić, Spin correlations of 2D quantum antiferromagnet at low temperatures and a direct comparison with neutron-scattering experiments, Phys. Rev. Lett. **64** (1990) 1449-1452. ⟨58, 83⟩

[Ding 90b] H.-Q. Ding and M. S. Makivić, Kosterlitz-Thouless transition in the two-dimensional quantum XY model, Phys. Rev. B **42** (1990) 6827-6830 (RC). ⟨58⟩

[Ding 91] H.-Q. Ding, 2D quantum antiferromagnet at low temperatures, Phys. Lett. A **159** (1991) 355-357. ⟨58, 83⟩

[Ding 92] H.-Q. Ding, Phase transition and thermodynamics of quantum XY model in two dimensions, Phys. Rev. B **45** (1992) 230-242. ⟨58⟩

[Fahy 90] S. B. Fahy and D. R. Hamann, Positive-projection Monte Carlo simulation: A new variational approach to strongly interacting fermion systems, Phys. Rev. Lett. **65** (1990) 3437-3440. ⟨62⟩

[Fahy 91] S. Fahy and D. R. Hamann, Diffusive behavior of states in the Hubbard-Stratonovich transformation, Phys. Rev. B **43** (1991) 765-779. ⟨62⟩

[Ferrenberg 88] A. M. Ferrenberg and R. H. Swendsen, New Monte Carlo technique for studying phase transition, Phys. Rev. Lett. **61** (1988) 2635-2638. ⟨35⟩

[Ferrenberg 89] A. M. Ferrenberg and R. H. Swendsen, Optimized Monte Carlo data analysis, Phys. Rev. Lett. **63** (1989) 1195-1198. ⟨35⟩

[Ferrenberg 91] A. M. Ferrenberg and D. P. Landau, Critical behavior of the three-dimensional Ising model: A high-resolution Monte Carlo study, Phys. Rev. B **44** (1991) 5081-5091. ⟨35⟩

[Feynman 65] R. P. Feynman and A. R. Hibbs, *Quantum Mechanics and Path Integrals* (McGraw-Hill, New York, 1965). ⟨50⟩

[Figueirido 89] F. Figueirido, A. Karlhede, S. Kivelson, S. Sondhi, M. Rocek and D. S. Rokhsar, Exact diagonalization of finite frustrated spin-1/2 Heisenberg models, Phys. Rev. B **41** (1989) 4619-4632. ⟨28⟩

[Fisher 64] M. E. Fisher, Magnetism in one-dimensional systems — The Heisenberg model for infinite spin, Am. J. Phys. **32** (1964) 343-346. ⟨9⟩

[Fradkin 91] E. Fradkin, *Field Theories of Condensed Matter Systems*, Frontiers in Physics **82** (Addison-Wesley, California, 1991). ⟨70⟩

[Fujiki 86] S. Fujiki and D. D. Betts, On long range chiral order of the $s = 1/2$ XY and Heisenberg antiferromagnets on the triangular lattice, Prog. Theor. Phys. Supple. **87** (1986) 268-272. ⟨29⟩

[Fujiki 87a] S. Fujiki and D. D. Betts, Zero-temperature properties of quantum spin models on the triangular lattice II: The $s = 1/2$ XY antiferromagnet, Can. J. Phys. **65** (1987) 76-81. ⟨29⟩

[Fujiki 87b] S. Fujiki, Zero-temperature properties of quantum spin models on the triangular lattice III: The $s = 1/2$ Heisenberg antiferro-

magnet, Can. J. Phys. **65** (1987) 489-491. ⟨29⟩

[Fujiki 91] S. Fujiki and D. D. Betts, High temperature series expansion of the fluctuation of the vector chirality for the spin-1/2 XY antiferromagnet on the triangular lattice, J. Phys. Soc. Jpn. **60** (1991) 435-440. ⟨29⟩

[Furukawa 91a] N. Furukawa and M. Imada, Minus sign problem in the Monte Carlo simulation of lattice fermion systems, J. Phys. Soc. Jpn. B **60** (1991) 810-824. ⟨62, 63⟩

[Furukawa 91b] N. Furukawa and M. Imada, Optimization of initial state vector in the ground state algorithm of lattice Fermion simulations, J. Phys. Soc. Jpn. B **60** (1991) 3669-3674. ⟨78⟩

[Fye 86] R. M. Fye, New results on Trotter-like approximation, Phys. Rev. B **33** (1986) 6271-6280. ⟨39, 90, 97⟩

[Gelfand 89] M. P. Gelfand, R. R. P. Singh and D. A. Huse, Zero-temperature ordering in two-dimensional frustrated quantum Heisenberg antiferromagnets, Phys. Rev. B **40** (1989) 10801-10809. ⟨28⟩

[Gomez-Santos 89] G. Gomez-Santos, J. D. Joannopoulos and J. W. Negele, Monte Carlo study of the quantum spin-1/2 Heisenberg antiferromagnet on the square lattice, Phys. Rev. B **39** (1989) 4435-4443. ⟨83⟩

[Griffiths 72] R. B. Griffiths, Rigorous results and theorems, in *Phase Transitions and Critical Phenomena, Vol. 1, Exact Results*, ed. by C. Domb and M. S. Green (Academic Press, London, 1972) 7-109. ⟨28⟩

[Gross 89] M. Gross, E. Sánchez-Velasco and E. Siggia, Ground-state properties of the two-dimensional antiferromagnetic Heisenberg model, Phys. Rev. **39** (1989) 2484-2493. ⟨81⟩

[Gubernatis 85] J. E. Gubernatis, D. J. Scalapino, R. L. Sugar and W. D. Toussaint, Two-dimensional spin-polarized fermion lattice gases, Phys. Rev. B **32** (1985) 103-116. ⟨74⟩

[Gubernatis 91] J. E. Gubernatis, M. Jarrell, R. N. Silver and D. S. Sivia, Quantum Monte Carlo simulations and maximum entropy: Dynamics from imaginary-time data, Phys. Rev. B **44** (1991) 6011-6029. ⟨85, 88⟩

[Haldane 83a] F. D. M. Haldane, Nonlinear field theory of large-spin Heisenberg antiferromagnets: Semiclassically quantized solitons of the one-dimensional easy-axis Néel state, Phys. Rev. Lett. **50** (1983) 1153-1156. ⟨1, 3, 4, 17, 18, 65⟩

[Haldane 83b] F. D. M. Haldane, Continuum dynamics of the 1-D Heisenberg antiferromagnet: Identification with the $O(3)$ nonlinear sigma model, Phys. Lett. A **93** (1983) 464-468. ⟨1, 3, 4, 17, 18, 65⟩

[Hamann 90] D. R. Hamann and S. B. Fahy, Energy measurement in auxiliary-field many-electron calculations, Phys. Rev. B **41** (1990) 11352-11363. ⟨32, 62, 74⟩

[Handscomb 62] D. C. Handscomb, The Monte Carlo method in quantum statistical mechanics, Proc. Camb. Phil. Soc. **58** (1962) 594-598.

⟨82⟩

[Handscomb 64] D. C. Handscomb, A Monte Carlo method applied to the Heisenberg ferromagnet, Proc. Camb. Phil. Soc. **60** (1964) 115-122. ⟨82⟩

[Hatano 91a] N. Hatano and M. Suzuki, Correction-term theorem concerning decompositions of exponential operators, Phys. Lett. A **153** (1991) 191-194. ⟨94⟩

[Hatano 91b] N. Hatano and M. Suzuki, Transfer-matrix calculation of the spin 1/2 antiferromagnetic XXZ model on the 4×2 triangular lattice using the fractal decomposition, Prog. Theor. Phys. (1991) 481-491. ⟨32, 39, 45, 51, 61, 89, 98⟩

[Hatano 92] N. Hatano and M. Suzuki, Representation basis in quantum Monte Carlo calculations and the negative-sign problem, Phys. Lett. A **163** (1992) 246-249. ⟨27, 42, 61⟩

[Hatano 93a] N. Hatano and M. Suzuki, Correlation length of the $S = 2$ antiferromagnetic Heisenberg chain, J. Phys. Soc. Jpn. **62** (1993) 1346-1353. ⟨3, 68⟩

[Hatano 93b] N. Hatano and M. Suzuki, Ground-state quantum Monte Carlo method applied to alternating-bond spin chains, J. Phys. Soc. Jpn. **62** (1993) 847-850. ⟨15, 75, 76, 78⟩

[Hatano 93c] N. Hatano and M. Suzuki, Quantum Monte Carlo and related methods — Recent developments —, to be published in *Quantum Monte Carlo Methods in Condensed Matter Physics*, ed. by M. Suzuki (World Scientific, Singapore, 1993). ⟨47⟩

[Hatsugai 92] Y. Hatsugai, String correlation of quantum antiferromagnetic spin chains with $S = 1$ and 2, J. Phys. Soc. Jpn. **61** (1992) 3856-3860. ⟨4⟩

[Hetherington 84] J. H. Hetherington, Observations on the statistical iteration of matrices, Phys. Rev. A **30** (1984) 2713-2719. ⟨16, 80⟩

[Hida 92a] K. Hida, Crossover between the Haldane-gap phase and the dimer phase in the spin-1/2 alternating Heisenberg chain, Phys. Rev. B **45** (1992) 2207-2212. ⟨2, 16, 17, 22⟩

[Hida 92b] K. Hida, Ground-state phase diagram of the spin-1/2 ferromagnetic-antiferromagnetic alternating Heisenberg chain with anisotropy, Phys. Rev. B **46** (1992) 8268-8275. ⟨2, 17⟩

[Hida 92c] K. Hida and S. Takada, String order parameters in the Haldane gap phase of the spin-1/2 alternating Heisenberg chain — Numerical diagonalization and variational study — J. Phys. Soc. Jpn. **61** (1992) 1879-1881. ⟨19⟩

[Hirsch 81] J. E. Hirsch, D. J. Scalapino, R. L. Sugar and R. Blankenbecler, Efficient Monte Carlo procedure for systems with fermions, Phys. Rev. Lett. **47** (1981) 1628-1631. ⟨20, 22, 56, 57, 58⟩

[Hirsch 82] J. E. Hirsch, R. L. Sugar, D. J. Scalapino and R. Blankenbecler, Monte Carlo simulations of one-dimensional fermion systems, Phys. Rev. B **26** (1982) 5033-5055. ⟨20, 22, 31, 32, 56, 58, 60, 61, 76, 100, 101⟩

[Hirsch 83a] J. E. Hirsch and D. J. Scalapino, $2p_{\rm F}$ and $4p_{\rm F}$ instabilities in a one-quarter-filled-band Hubbard model, Phys. Rev. B **27** (1983) 7169-7185. ⟨58⟩

[Hirsch 83b] J. E. Hirsch, Discrete Hubbard-Stratonovich transformation for fermion lattice models, Phys. Rev. B **28** (1983) 4059-4061 (RC). ⟨16, 69⟩

[Hirsch 83c] J. E. Hirsch, Monte Carlo study of the two-dimensional Hubbard model, Phys. Rev. Lett. **51** (1983) 1900-1903. ⟨34, 69, 71, 74, 103⟩

[Hirsch 84a] J. E. Hirsch and D. J. Scalapino, $2p_{\rm F}$ and $4p_{\rm F}$ instabilities in the one-dimensional Hubbard model, Phys. Rev. B **29** (1984) 5554-5561. ⟨58⟩

[Hirsch 84b] J. E. Hirsch, Charge-density-wave to spin-density-wave transition in the extended Hubbard model, Phys. Rev. Lett. **53** (1984) 2327-2330. ⟨58⟩

[Hirsch 85a] J. E. Hirsch, Two-dimensional Hubbard model: Numerical simulation study, Phys. Rev. B **31** (1985) 4403-4419. ⟨34, 69, 71, 72, 74, 103, 104, 106⟩

[Hirsch 85b] J. E. Hirsch, Attractive interaction and pairing in Fermion systems with strong on-site repulsion, Phys. Rev. Lett. **54** (1985) 1317-1320. ⟨74⟩

[Hirsch 86] J. E. Hirsch, Connection between world-line and determinantal functional-integral formulations of the Hubbard model, Phys. Rev. B **34** (1986) 3216-3220. ⟨70⟩

[Hirsch 87] J. E. Hirsch, Simulations of the three-dimensional Hubbard model: Half-filled band sector, Phys. Rev. **35** (1987) 1851-1859. ⟨74⟩

[Hirsch 89a] J. E. Hirsch and S. Tang, Antiferromagnetism in the two-dimensional Hubbard model, Phys. Rev. Lett. **62** (1989) 591-594. ⟨74⟩

[Hirsch 89b] J. E. Hirsch and S. Tang, Two-dimensional Heisenberg antiferromagnet with next-nearest neighbor coupling, Phys. Rev. B **39** (1989) 2887-2889. ⟨28⟩

[Homma 84] S. Homma, H. Matsuda and N. Ogita, Monte Carlo simulation for quantum spin systems, Prog. Theor. Phys. **72** (1984) 1245-1247 (L). ⟨84⟩

[Homma 86a] S. Homma, H. Matsuda and N. Ogita, Decoupled cell method Monte Carlo simulation for quantum spin systems, Prog. Theor. Phys. **75** (1986) 1058-1065. ⟨84⟩

[Homma 86b] S. Homma, K. Sano, H. Matsuda and N. Ogita, Decoupled cell Monte Carlo method for quantum spin systems on linear chain and on triangular lattice, Prog. Theor. Phys. **87** (1986) 127-138. ⟨84⟩

[Horiki 89] T. Horiki, S. Homma, H. Matsuda and N. Ogita, Short-range spin pair correlation in the one-dimensional quantum XXZ model, Prog. Theor. Phys. **82** (1989) 507-513. ⟨84⟩

[Hu 92] C.-K. Hu, Histogram Monte Carlo renormalization group method for phase transition models without critical slowing down, Phys. Rev. Lett. **69** (1992) 2739-2742. ⟨35⟩

[Hubbard 59] J. Hubbard, Calculation of partition function, Phys. Rev. Lett. **3** (1959) 77-78. ⟨16, 69⟩

[Hubbard 63] J. Hubbard, Electrons correlations in narrow energy bands, Proc. Roy. Soc. A **276** (1963) 238-257. ⟨48⟩

[Imada 89] M. Imada and Y. Hatsugai, Numerical studies on the Hubbard model and the t-J model in one- and two- dimensions, J. Phys. Soc. Jpn. **58** (1989) 3752-3780. ⟨74, 77, 104⟩

[Inoue 88] M. Inoue and M. Suzuki, The ST-transformation approach to analytic solutions of quantum systems. II — Transfer-matrix and Pfaffian methods —, Prog. Theor. Phys. **79** (1988) 645-664. ⟨6, 66⟩

[Jarrell 90] M. Jarrell, D. S. Sivia and B. Patton, Gap states in dilute-magnetic-alloy superconductors: A quantum Monte Carlo study, Phys. Rev. B **42** (1990) 4804-4807 (RC). ⟨88⟩

[Jarrell 91a] M. Jarrell, J. Gubernatis, R. N. Silver and D. S. Sivia, Transport coefficients of dilute magnetic alloys: A quantum Monte Carlo study, Phys. Rev. B **43** (1991) 1206-1209 (BR). ⟨88⟩

[Jarrell 91b] M. Jarrell, J. E. Gubernatis and R. N. Silver, Dynamic susceptibility of the Anderson model: A quantum Monte Carlo study, Phys. Rev. B **44** (1991) 5347-5350 (RC). ⟨88⟩

[Kadowaki 86] S. Kadowaki and A. Ueda, A direct evaluation method of the partition function of quantum spin systems, Prog. Theor. Phys. **75** (1986) 451-454 (L). ⟨83⟩

[Kadowaki 87] S. Kadowaki and A. Ueda, A new Monte Carlo approach to quantum spin systems, Prog. Theor. Phys. **78** (1987) 224-236. ⟨83⟩

[Kadowaki 89] S. Kadowaki and A. Ueda, A new Monte Carlo approach to quantum spin systems. II — Two dimensional systems —, Prog. Theor. Phys. **82** (1989) 493-506. ⟨83⟩

[Kalos 62] M. H. Kalos, Monte Carlo calculations of the ground state of three- and four-body nuclei, Phys. Rev. **128** (1962) 1791-1795. ⟨78⟩

[Kalos 74] M. H. Kalos, D. Levesque and L. Verlet, Helium at zero temperature with hard-sphere and other forces, Phys. Rev. A **9** (1974) 2178-2195. ⟨15, 16, 75, 80⟩

[Kalos 79] M. H. Kalos, ed., *Monte Carlo Methods in Quantum Problems*, NATO ASI Series C **125** (Reidel, Dordrecht, 1984). ⟨78⟩

[Kawashima 89] N. Kawashima and M. Suzuki, Chiral phase transition of planar antiferromagnets analyzed by the super-effective-field theory, J. Phys. Soc. Jpn. **58** (1989) 3123-3130. ⟨29⟩

[Kohmoto 92] M. Kohmoto and H. Tasaki, Hidden $Z_2 \times Z_2$ symmetry breaking and the Haldane phase in the $S = 1/2$ quantum spin chain with bond alternation, Phys. Rev. B **46** (1992) 3486-3495. ⟨18⟩

[Kohn 64] W. Kohn, Theory of the insulating state, Phys. Rev. **133** (1964) A171-A181. ⟨74⟩

[Kolb 83] M. Kolb, R. Botet, and R. Jullien, Comparison of ground state properties for odd half-integer and integer spin antiferromagnetic Heisenberg chains, J. Phys. A: Math. Gen. **16** (1983) L673-L677. ⟨1, 3, 18⟩

[Koma 87] T. Koma, Thermal Bethe-ansatz method for the one-dimensional Heisenberg model, Prog. Theor. Phys. **78** (1987) 1213-1218 (L). ⟨6, 65, 66⟩

[Koma 89] T. Koma, Thermal Bethe-ansatz method for the spin-1/2 XXZ Heisenberg chain, Prog. Theor. Phys. **81** (1989) 783-809. ⟨6, 12, 65, 66⟩

[Koma 90] T. Koma, An extension of the thermal Bethe ansatz — One-dimensional Hubbard model —, Prog. Theor. Phys. **83** (1990) 655-659. ⟨66⟩

[Koma 93] T. Koma, A new Monte Carlo power method for the eigenvalue problem of transfer matrices, J. Stat. Phys. **71** (1993) 269-297. ⟨4, 8, 67⟩

[Kubo 57] R. Kubo, Statistical-mechanical theory of irreversible processes. I. General theory and simple applications to magnetic and conduction problems, J. Phys. Soc. Jpn. **12** (1957) 570-586. ⟨85⟩

[Kubo 86] K. Kubo and S. Takada, Critical properties of $S = 1$ XXZ chain, J. Phys. Soc. Jpn. **55** (1986) 438-441 (L). ⟨7, 18, 65⟩

[Kubo 92] K. Kubo, Spin correlations in the $S = 1$ XXZ chain, Phys. Rev. B **46** (1992) 866-873. ⟨4, 7, 18, 65⟩

[Kuti 82] J. Kuti, Stochastic method for the numerical study of lattice fermions, Phys. Rev. Lett. **49** (1982) 183-186. ⟨15, 16, 75, 78⟩

[Lee 84a] D. H. Lee, J. D. Joannopoulos, J. W. Negele and D. P. Landau, Discrete-symmetry breaking and novel critical phenomena in an antiferromagnetic planar (XY) model in two dimensions, Phys. Rev. Lett. **52** (1984) 433-436. ⟨29⟩

[Lee 84b] D. H. Lee, J. D. Joannopoulos and J. W. Negele, Monte Carlo solution of antiferromagnetic quantum Heisenberg spin systems, Phys. Rev. B **30** (1984) 1599-1602 (RC). ⟨83⟩

[Lee 86] D. H. Lee, J. D. Joannopoulos, J. W. Negele and D. P. Landau, Symmetry analysis and Monte Carlo study of a frustrated antiferromagnetic planar (XY) model in two dimensions, Phys. Rev. B **33** (1986) 450-475. ⟨29⟩

[Liang 90] S. Liang, Monte Carlo calculations of the correlation functions for Heisenberg spin chains at $T = 0$, Phys. Rev. Lett. **64** (1990) 1597-1600. ⟨4⟩

[Loh 85a] E. Loh, Jr., D. J. Scalapino and P. M. Grant, Monte Carlo studies of the quantum XY model in two dimensions, Phys. Rev. B **31** (1985) 4712-4714 (RC). ⟨58⟩

[Loh 85b] E. Loh, Jr. and D. J. Scalapino, Monte Carlo simulations of the quantum XXZ model in two dimensions, Physica Scripta

32 (1985) 327-333. ⟨30, 58⟩

[Loh 90] E. Y. Loh Jr., J. E. Gubernatis, R. T. Scalettar, S. R. White, D. J. Scalapino and R. L. Sugar, Sign problem in the numerical simulation of many-electron systems, Phys. Rev. B **41** (1990) 9301-9307. ⟨32, 61, 74⟩

[Lyklema 82] J. W. Lyklema, Quantum-statistical Monte Carlo method for Heisenberg spins, Phys. Rev. Lett. **49** (1982) 88-90. ⟨82⟩

[Lyklema 83] J. W. Lyklema, Monte Carlo study of the one-dimensional quantum Heisenberg ferromagnet near $T = 0$, Phys. Rev. B **27** (1983) 3108-3110. ⟨82, 83⟩

[Lyklema 84] J. W. Lyklema, A quantum Monte Carlo method for the Heisenberg spin system, ed. by M. H. Kalos, NATO ASI Series C **125** (Reidel, Dordrecht, 1984) 145-155. ⟨82, 83⟩

[Makivic 91] M. S. Makivić and H.-Q. Ding, Two-dimensional spin-1/2 Heisenberg antiferromagnet: A quantum Monte Carlo study, Phys. Rev. B **43** (1991) 3562-3574. ⟨45, 58, 59, 83⟩

[Makivic 92a] M. Makivić and M. Jarrell, Low-temperature dynamics of the 2D spin-1/2 Heisenberg antiferromagnet: A quantum Monte Carlo study, Phys. Rev. Lett. **68** (1992) 1770-1773. ⟨88⟩

[Makivic 92b] M. S. Makivić, Low-temperature phase of the two-dimensional quantum XY model, Phys. Rev. B **46** (1992) 3167-3170 (RC). ⟨58⟩

[Manousakis 88] E. Manousakis and R. Salvador, Long-range correlations in the two-dimensional spin-1/2 antiferromagnetic Heisenberg model: A quantum Monte Carlo study, Phys. Rev. Lett. **60** (1988) 840-843. ⟨83⟩

[Manousakis 89] E. Manousakis and R. Salvador, Monte Carlo study of the two-dimensional spin-1/2 quantum Heisenberg model: Spin correlation in La_2CuO_4, Phys. Rev. B **39** (1989) 575-585. ⟨83⟩

[Manousakis 91] E. Manousakis, The spin-1/2 Heisenberg antiferromagnet on a square lattice and its application to the cuprous oxides, Rev. Mod. Phys. **63** (1991) 1-62. ⟨28, 83⟩

[Masui 92] S. Masui and D. D. Betts, Evidence for a chiral phase in the quantum XY model on the triangular lattice, preprint. ⟨29⟩

[Matsubara 88] F. Matsubara and S. Inawashiro, Solid State Commun. **67** (1988) 229-232. ⟨29⟩

[Matsuda 88] H. Matsuda, K. Ishii, S. Homma and N. Ogita, Theoretical basis of the decoupled cell Monte Carlo simulation for quantum systems, Prog. Theor. Phys. **80** (1988) 583-587 (L). ⟨84⟩

[Mermin 66] N. D. Mermin and H. Wagner, Absence of ferromagnetism or antiferromagnetism in one- or two-dimensional isotropic Heisenberg models, Phys. Rev. Lett. **17** (1966) 1133-1136. ⟨28⟩

[Metropolis 53] N. C. Metropolis, A. W. Rosenbluth, M. N. Rosenbluth, A. H. Teller and E. Teller, Equation of state calculation by fast computing machines, J. Chem. Phys. **21** (1953) 1087-1092. ⟨48, 56⟩

[Mila 91] F. Mila, D. Poilblanc and C. Bruder, Spin dynamics in a frustrated magnet with short-range order, Phys. Rev. B **43** (1991) 7891-7898. ⟨28⟩

[Miyashita 84] S. Miyashita and H. Shiba, Nature of the phase transition of the two-dimensional antiferromagnetic plane rotator model on the triangular lattice, J. Phys. Soc. Jpn. **53** (1984) 1145-1154. ⟨29⟩

[Miyashita 86] S. Miyashita, The ground state and thermodynamic properties of generalized Heisenberg models on the triangular lattice, Prog. Theor. Phys. Supple. **87** (1986) 112-126. ⟨29⟩

[Miyashita 88] S. Miyashita, Thermodynamic properties of spin 1/2 antiferromagnetic Heisenberg model on the square lattice, J. Phys. Soc. Jpn. **57** (1988) 1934-1946. ⟨58⟩

[Momoi 92a] T. Momoi and M. Suzuki, Vector chiral order in the quantum XXZ antiferromagnet on a triangular lattice analyzed with the super-effective-field theory, J. Phys. Soc. Jpn. **61** (1992) 3277-3286. ⟨29⟩

[Momoi 92b] T. Momoi and M. Suzuki, Ground-state properties and phase diagram of the quantum XXZ antiferromagnet on a triangular lattice, J. Phys. Soc. Jpn. **61** (1992) 3732-3744. ⟨29⟩

[Morgenstern 89] I. Morgenstern, Quantum-Monte-Carlo simulations for fermionic systems, Z. Phys. B – Condensed Matter **77** (1989) 267-273. ⟨32, 61⟩

[Moskowitz 82] J. W. Moskowitz, K. E. Schmidt, M. A. Lee and M. H. Kalos, A new look at correlation energy in atomic and molecular systems. II. The application of the Green's function Monte Carlo method to LiH, J. Chem. Phys. **77** (1982) 349-355. ⟨62, 81⟩

[Muller-Krumbhaar 73] H. Müller-Krumbhaar and K. Binder, Dynamic properties of the Monte Carlo method in statistical mechanics, J. Stat. Phys. **8** (1973) 1-24. ⟨32, 61⟩

[Munger 91] E. P. Münger and M. A. Novotny, Reweighting in Monte Carlo and Monte Carlo renormalization-group studies, Phys. Rev. B **43** (1991) 5773-5783. ⟨35⟩

[Nakamura 92a] T. Nakamura, N. Hatano and H. Nishimori, Reweighting method for quantum Monte Carlo simulations with the negative-sign problem, J. Phys. Soc. Jpn. **61** (1992) 3494-3502. ⟨34, 35, 37, 45, 62⟩

[Nakamura 92b] T. Nakamura, N. Hatano and H. Nishimori, Negative-sign problem in quantum Monte Carlo and the reweighting method, in *Computer Aided Innovation of New Materials II*, ed. by M. Doyama, J. Kihara, M. Tanaka and R. Yamamoto (Elsevier, Amsterdam, 1993) 379-382. ⟨34, 35, 37, 45, 62⟩

[Nakamura 92c] T. Nakamura, N. Hatano and H. Nishimori, in preparation. ⟨37, 38, 62, 63⟩

[Nightingale 86] M. P. Nightingale and H. W. J. Blöte, Gap of the linear spin-1 Heisenberg antiferromagnet: A Monte Carlo calculation, Phys.

Rev. B **33** (1986) 659-661. ⟨4, 81⟩

[Nishimori 88] H. Nishimori and H. Nakanishi, Ground state of quantum spin systems on the triangular lattice, J. Phys. Soc. Jpn. **57** (1988) 626-638. ⟨29⟩

[Nishimori 90] H. Nishimori and Y. Saika, Modified spin wave theory of the two-dimensional frustrated Heisenberg model, J. Phys. Soc. Jpn. **59** (1990) 4454-4461. ⟨28⟩

[Nomura 89a] K. Nomura, Spin correlation function of the $S = 1$ antiferromagnetic Heisenberg chain by the large-cluster-decomposition Monte Carlo method, Phys. Rev. B **40** (1989) 2421-2425. ⟨4, 58⟩

[Nomura 89b] K. Nomura, Spin-correlation functions of the $S = 1$ Heisenberg-Ising chain by the large-cluster-decomposition Monte Carlo method, Phys. Rev. B **40** (1989) 9142-9146. ⟨18, 58⟩

[Oguchi 90] T. Oguchi and H. Kitatani, Spin wave theory for a frustrated antiferromagnetic Heisenberg model on a square lattice, J. Phys. Soc. Jpn. **59** (1990) 3322-3330. ⟨28⟩

[Okabe 87] Y. Okabe and M. Kikuchi, Cluster-spin quantum Monte Carlo study of one-dimensional Heisenberg model, J. Phys. Soc. Jpn. **56** (1987) 1963-1973. ⟨58⟩

[Parkinson 85a] J. B. Parkinson, J. C. Bonner, G. Müller, M. P. Nightingale and H. W. J. Blöte, Heisenberg spin chains: Quantum-classical crossover and the Haldane conjecture, J. Appl. Phys. **57** (1985) 3319-3321. ⟨81⟩

[Parkinson 85b] J. B. Parkinson and J. C. Bonner, Spin chains in a field: Crossover from quantum to classical behavior, Phys. Rev. B **32** (1985) 4703-4724. ⟨18⟩

[Reger 88] J. D. Reger and A. P. Young, Monte Carlo study of the spin-1/2 Heisenberg antiferromagnet on a square lattice, Phys. Rev. B **37** (1988) 5978-5981 (RC). ⟨58⟩

[Ruelle 69] D. Ruelle, *Statistical Mechanics: Rigorous Results*, The Mathematical Physics Monograph Series (Benjamin, New York, 1969). ⟨28⟩

[Runge 92] K. J. Runge, Quantum Monte Carlo calculation of the long-range order in the Heisenberg antiferromagnet, Phys. Rev. B **45** (1992) 7229-7236. ⟨81⟩

[Sakai 90a] T. Sakai and M. Takahashi, Energy gap of the $S = 1$ antiferromagnetic Heisenberg chain, Phys. Rev. B **42** (1990) 1090-1092. ⟨4⟩

[Sakai 90b] T. Sakai and M. Takahashi, Finite-size scaling study of $S = 1$ XXZ spin chain, J. Phys. Soc. Jpn. **59** (1990) 2688-2693. ⟨18⟩

[Salsburg 59] Z. W. Salsburg, J. D. Jacobson, W. Fickett and W. W. Wood, Application of the Monte Carlo method of the lattice-gas model. I. Two-dimensional triangular lattice, J. Chem. Phys. **30** (1959) 65-72. ⟨35⟩

[Sandvik 91] A. W. Sandvik and J. Kurkijärvi, Quantum Monte Carlo sim-

ulation method for spin systems, Phys. Rev. B **43** (1991) 5950-5961. ⟨83⟩

[Sandvik 92] A. W. Sandvik, A generalization of Handscomb's quantum Monte Carlo scheme — Application to the 1D Hubbard model, J. Phys. A: Math. Gen. **25** (1992) 3667-3682. ⟨83⟩

[Sano 91] K. Sano, I. Doi and K. Takano, The ground state and gapless excitations for a two-dimensional frustrated antiferromagnet, J. Phys. Soc. Jpn. **60** (1991) 3807-3817. ⟨28⟩

[Scalapino 81a] D. J. Scalapino and R. L. Sugar, Method for performing Monte Carlo calculations for systems with fermions, Phys. Rev. Lett. **46** (1981) 519-521. ⟨70⟩

[Scalapino 81b] D. J. Scalapino and R. L. Sugar, Monte Carlo calculations of coupled boson-fermion systems. II, Phys. Rev. B **24** (1981) 4295-4308. ⟨70⟩

[Schlottmann 85] P. Schlottmann, Critical behavior of the isotropic ferromagnetic quantum Heisenberg chain, Phys. Rev. Lett. **54** (1985) 2131-2134. ⟨54⟩

[Schmidt 84] K. E. Schmidt and M. H. Kalos, Few- and many-Fermion problems, in *Application of the Monte Carlo Method in Statistical Physics*, ed. by K. Binder, Topics in Current Physics **36** (Springer, Berlin, 1984) 125-143; 2nd edition (Springer, Berlin, 1987). ⟨78⟩

[Schmidt 92] K. E. Schmidt and D. M. Ceperley, Monte Carlo techniques for quantum fluids, solids and droplets, in *The Monte Carlo Methods in Condensed Matter Physics*, ed. by K. Binder, Topics in Applied Physics **71** (Springer, Berlin, 1992) 205-248. ⟨78⟩

[Silver 90a] R. N. Silver, D. S. Sivia and J. E. Gubernatis, Dynamical properties from quantum Monte Carlo by the maximum-entropy method, in *Quantum Simulations of Condensed Matter Phenomena*, ed. by J. D. Doll and J. E. Gubernatis, (World Scientific, Singapore, 1990) 340-354. ⟨85⟩

[Silver 90b] R. N. Silver, D. S. Sivia and J. E. Gubernatis, Maximum-entropy method for analytic continuation of quantum Monte Carlo data, Phys. Rev. B **41** (1990) 2380-2389. ⟨85⟩

[Silver 90c] R. N. Silver, J. E. Gubernatis, D. S. Sivia and M. Jarrell, Spectral densities of the symmetric Anderson model, Phys. Rev. Lett. **65** (1990) 496-499. ⟨88⟩

[Skilling 89a] J. Skilling, ed., *Maximum Entropy and Baysian Methods*, Fundamental Theories of Physics, (Kluwer Academic Publishers, Dordrecht, 1989). ⟨87⟩

[Skilling 89b] J. Skilling, Classic maximum entropy, in *Maximum Entropy and Baysian Methods*, ed. by J. Skilling, Fundamental Theories of Physics, (Kluwer Academic Publishers, Dordrecht, 1989) 45-52. ⟨88⟩

[Sorella 88] S. Sorella, E. Tosatti, S. Baroni, R. Car and M. Parrinello, Numerical simulation of the 1D and 2D Hubbard models: Fermi

liquid behavior and its breakdown, Int. J. Mod. Phys. B **1** (1988) 993-1003. ⟨74, 77⟩

[Sorella 89] S. Sorella, S. Baroni, R. Car and M. Parrinello, A novel technique for the simulation of interacting Fermion systems, Europhys. Lett. **8** (1989) 663-668. ⟨16, 74, 77⟩

[Sorella 91] S. Sorella, The Hubbard-Stratonovich transformation and the Hubbard model, Int. J. Mod. Phys. B **5** (1991) 937-976. ⟨74⟩

[Stratonovich 57] R. L. Stratonovich, On a method of calculating quantum distribution functions, Doklady Akad. Nauk SSSR **115** (1957) 1097-1100 [in Russian], Soviet Phys. Doklady **2** (1958) 416-419 [translated into English]. ⟨16, 69⟩

[Sugiyama 86] G. Sugiyama and S. E. Koonin, Auxiliary field Monte-Carlo for quantum many-body ground states, Annals of Physics **168** (1986) 1-26. ⟨15, 16, 75, 77⟩

[Suzuki 76a] M. Suzuki, Generalized Trotter's formula and systematic approximations of exponential operators and inner derivations with applications to many-body problems, Commun. Math. Phys. **51** (1976) 183-190. ⟨5, 29, 50, 94, 98⟩

[Suzuki 76b] M. Suzuki, Relationship between d-dimensional quantal spin systems and $(d+1)$-dimensional Ising systems — Equivalence, critical exponents and systematic approximations of the partition function and spin correlations —, Prog. Theor. Phys. **56** (1976) 1454-1469. ⟨5, 16, 19, 20, 24, 29, 55, 56⟩

[Suzuki 77a] M. Suzuki, Classical representation and scaling property of the Kondo, Hubbard and Anderson Hamiltonians, and quantal random systems, Prog. Theor. Phys. **58** (1977) 755-766. ⟨55, 94, 96⟩

[Suzuki 77b] M. Suzuki, S. Miyashita and A. Kuroda, Monte Carlo simulations of quantum spin systems. I, Prog. Theor. Phys. **58** (1977) 1377-1387. ⟨5, 16, 19, 20, 24, 29, 58, 75, 100, 101, 102⟩

[Suzuki 77c] M. Suzuki, On the convergence of exponential operators — The Zassenhaus formula, BCH formula and systematic approximations, Commun. Math. Phys. **57** (1977) 193-200. ⟨29, 50, 96, 98⟩

[Suzuki 85a] M. Suzuki, Transfer-matrix method and Monte Carlo simulation in quantum spin systems, Phys. Rev. B **31** (1985) 2957-2965. ⟨5, 6, 63, 64, 65⟩

[Suzuki 85b] M. Suzuki, Decomposition formulas of exponential operators and Lie exponentials with some applications to quantum mechanics and statistical physics, J. Math. Phys. **26** (1985) 601-612. ⟨50⟩

[Suzuki 85c] M. Suzuki, Thermo field Monte Carlo and transfer-matrix methods in quantum systems, Phys. Lett. A **111** (1985) 440-444. ⟨78⟩

[Suzuki 85d] M. Suzuki, General correction theorems on decomposition formulae of exponential operators and extrapolation methods for

quantum Monte Carlo simulations, Phys. Lett. A **113** (1985) 299-300. ⟨6, 39, 50, 90, 97⟩

[Suzuki 86a] M. Suzuki, Thermo field dynamics of quantum spin systems, J. Stat. Phys. **42** (1986) 1047-1070. ⟨78⟩

[Suzuki 86b] M. Suzuki, Quantum statistical Monte Carlo methods and applications to spin systems, J. Stat. Phys. **43** (1986) 883-909. ⟨55, 75⟩

[Suzuki 86c] M. Suzuki and H. Betsuyaku, Thermofield transfer-matrix method and its application to quantum spin systems, Phys. Rev. B **34** (1986) 1829-1834. ⟨78⟩

[Suzuki 87a] M. Suzuki, S. Miyashita and M. Takasu, Thermofield quantum Monte Carlo method and its applications to quantum spin systems, Phys. Rev. B **35** (1987) 3569-3575. ⟨78⟩

[Suzuki 87b] M. Suzuki, ed., *Quantum Monte Carlo Methods*, Solid-State Sciences **74** (Springer, Berlin, 1987). ⟨5, 19, 34, 45, 55, 75⟩

[Suzuki 87c] M. Suzuki and M. Inoue, The ST-transformation approach to analytic solutions of quantum systems. I — General formulations and basic limit theorems —, Prog. Theor. Phys. **78** (1987) 787-799. ⟨5, 6, 65, 66⟩

[Suzuki 90] M. Suzuki, Fractal decomposition of exponential operators with applications to many-body theories and Monte Carlo simulations, Phys. Lett. A **146** (1990) 319-323. ⟨40, 45, 50, 51, 52, 90, 91, 94, 95⟩

[Suzuki 91] M. Suzuki, General theory of fractal path integrals with applications to many-body theories and statistical physics, J. Math. Phys. **32** (1991) 400-407. ⟨40, 45, 51, 52, 90, 91, 94, 95⟩

[Suzuki 92a] M. Suzuki, General theory of higher-order decomposition of exponential operators and symplectic integrators, Phys. Lett. A **165** (1992) 387-395. ⟨54⟩

[Suzuki 92b] M. Suzuki, General nonsymmetric higher-order decomposition of exponential operators and symplectic integrators, J. Phys. Soc. Jpn. **61** (1992) 3015-3019 (L). ⟨54⟩

[Takada 86] S. Takada and K. Kubo, Critical properties of $S = 1/2$ XXZ chain, J. Phys. Soc. Jpn. **55** (1986) 1671-1685. ⟨54, 65⟩

[Takada 87] S. Takada, Critical properties of spin chains, in *Quantum Monte Carlo Methods*, Solid State Sciences **74**, ed. by M. Suzuki (Springer-Verlag, Berlin, 1987) 86-103. ⟨4⟩

[Takada 92] S. Takada, Nonlocal unitary transformation and string order in $S = 1/2$ Heisenberg chain with bond alternation, J. Phys. Soc. Jpn. **61** (1992) 428-432. ⟨19⟩

[Takahashi 85] M. Takahashi and M. Yamada, Spin-1/2 one-dimensional Heisenberg ferromagnet at low-temperature, J. Phys. Soc. Jpn. **54** (1985) 2808-2811 (L). ⟨54⟩

[Takahashi 88] M. Takahashi, Spin-correlation function of the $S = 1$ antiferromagnetic Heisenberg chain at $T = 0$, Phys. Rev. B **38** (1988) 5188-5191. ⟨4⟩

[Takahashi 89] M. Takahashi, Monte Carlo calculation of elementary excitation of spin chains, Phys. Rev. Lett. **62** (1989) 2313-2316. ⟨4, 81⟩

[Takahashi 91a] M. Takahashi, Correlation length and free energy of the $S = 1/2$ XYZ chain, Phys. Rev. B **43** (1991) 5788-5797; Erratum, Phys. Rev. B **44** (1991) 5397. ⟨12, 66⟩

[Takahashi 91b] M. Takahashi, Correlation length and free energy of the $S = 1/2$ XXZ chain in a magnetic field, Phys. Rev. B **44** (1991) 12382-12394. ⟨66⟩

[Takasu 86] M. Takasu, S. Miyashita and M. Suzuki, Monte Carlo simulation of quantum Heisenberg magnets on the triangular lattice, Prog. Theor. Phys. **75** (1986) 1254-1257 (L). ⟨31, 34, 39, 45, 60, 89⟩

[Takasu 87] M. Takasu, S. Miyashita and M. Suzuki, Thermodynamic properties of the spin-1/2 Heisenberg antiferromagnet on the triangular lattice, in *Quantum Monte Carlo Methods* ed. by M. Suzuki, Solid-State Sciences **74** (Springer, Berlin, 1987) 114-124. ⟨40⟩

[Teitel 83] S. Teitel and C. Jayaprakash, Phase transitions in frustrated two-dimensional XY models, Phys. Rev. B **27** (1983) 598-601 (RC). ⟨29⟩

[Torrie 74] G. M. Torrie and J. P. Valleau, Monte Carlo free energy estimates using non-Boltzmann sampling application to the subcritical Lennard-Jones fluid, Chem. Phys. Lett. **28** (1974) 578-581. ⟨35⟩

[Toulouse 77] G. Toulouse, Theory of the frustration effect in spin glasses: I, Commun. Phys. **2** (1977) 115-119. ⟨27⟩

[Trivedi 89] N. Trivedi and D. M. Ceperley, Green-function Monte Carlo study of quantum antiferromagnet, Phys. Rev. B **40** (1989) 2737-2740 (RC). ⟨81⟩

[Trivedi 90] N. Trivedi and D. M. Ceperley, Ground-state correlations of quantum antiferromagnets: A Green-function Monte Carlo study, Phys. Rev. B **41** (1990) 4552-4569. ⟨81⟩

[Trotter 59] H. F. Trotter, On the product of semi-groups of operators, Proc. Am. Math. Soc. **10** (1959) 545-551. ⟨29, 50⟩

[Tsunetsugu 91] H. Tsunetsugu, Temperature dependence of spin correlation length of half-filled one-dimensional Hubbard model, J. Phys. Soc. Jpn. **60** (1991) 1460-1463 (L). ⟨66⟩

[Tsuzuki 85] T. Tsuzuki, An improved transfer matrix method for quantum spin systems, Prog. Theor. Phys. **73** (1985) 1352-1368. ⟨7, 58, 67⟩

[Tsuzuki 86] T. Tsuzuki, An improved transfer matrix method for quantum spin systems. II — Isotropic Heisenberg chain with spin 1/2 —, Prog. Theor. Phys. **75** (1986) 225-242. ⟨7, 58, 67⟩

[Valleau 72] J. P. Valleau and D. N. Card, Monte Carlo estimation of the free energy by multistage sampling, J. Chem. Phys. **57** (1972)

5457-5462. ⟨35⟩

[Villain 77a] J. Villain, A magnetic analogue of stereoisomerism: Application to helimagnetism in two dimensions, J. Physique **38** (1977) 385-391. ⟨29⟩

[Villain 77b] J. Villain, Spin glass with non-random interactions, J. Phys. C: Solid State Phys. **10** (1977) 1717-1734. ⟨29⟩

[Villain 77c] J. Villain, Two-level systems in a spin-glass model: I. General formalism and two-dimensional model, J. Phys. C: Solid State Phys. **10** (1977) 4793-4802. ⟨29⟩

[Vitiello 91] S. A. Vitiello and P. A. Whitlock, Green's-function Monte Carlo algorithm for the solution of the Schrödinger equation with the shadow wave function, Phys. Rev. B **44** (1991) 7373-7377. ⟨81⟩

[Von der Linden 90] W. von der Linden, I. Morgenstern and H. de Raedt, Quantum Monte Carlo study of quasiparticles in the Hubbard model, Phys. Rev. B **41** (1990) 4669-4673. ⟨77⟩

[Weiss 62] G. H. Weiss and A. A. Maradudin, The Baker-Hausdorff formula and a problem in crystal physics, J. Math. Phys. **3** (1962) 771-777. ⟨94, 96⟩

[Wen 89] X. G. Wen, F. Wilczek and A. Zee, Chiral spin states and superconductivity, Phys. Rev. B **39** (1989) 11413-11423. ⟨28⟩

[White 89] S. R. White, D. J. Scalapino, R. L. Sugar, E. Y. Loh, J. E. Gubernatis and R. T. Scalettar, Numerical study of the two-dimensional Hubbard model, Phys. Rev. B **40** (1989) 506-516. ⟨74, 77⟩

[Wilcox 67] R. M. Wilcox, Exponential operators and parameter differentiation in quantum physics, J. Math. Phys. **8** (1967) 962-982. ⟨94, 96⟩

[Xu 90] J. H. Xu and C. S. Ting, Phase diagram of the frustrated square Heisenberg lattice based upon a modified spin-wave theory, Phys. Rev. B **42** (1990) 6861-6864 (RC). ⟨28⟩

[Yamada 90] M. Yamada, Thermal Bethe ansatz study of correlation length of spin-1/2 Heisenberg ferromagnetic chain, J. Phys. Soc. Jpn. **59** (1990) 848-856. ⟨66⟩

[Yamanaka 92] M. Yamanaka, Y. Hatsugai and M. Kohmoto, Phase diagram of the $S = 1/2$ quantum spin chain with bond alternation, preprint. ⟨18⟩

[Yokota 86] T. Yokota and H. Betsuyaku, Study of one-dimensional fermion model by the transfer-matrix method, Prog. Theor. Phys. **75** (1986) 46-58. ⟨64⟩

[Yoshida 90] H. Yoshida, Construction of higher order symplectic integrators, Phys. Lett. A **150** (1990) 262-268. ⟨51⟩

[Zeng 90] C. Zeng and V. Elser, Numerical studies of antiferromagnetism on a kagomé net, Phys. Rev. B **42** (1990) 8436-8444. ⟨84⟩

[Zhang 88] F. C. Zhang, C. Gros, T. M. Rice and H. Shiba, A renormalized Hamiltonian approach to a resonant valence bond wave-

function, Supercond. Sci. Technol. **1** (1988) 36-46. ⟨74⟩

[Zhang 91a] X. Y. Zhang, E. Abrahams and G. Kotliar, Quantum Monte Carlo algorithm for constrained Fermions: Application to the infinite-U Hubbard model, Phys. Rev. Lett. **66** (1991) 1236-1239. ⟨74⟩

[Zhang 91b] X. Y. Zhang, Quantum Monte Carlo algorithm for constrained Fermions, Mod. Phys. Lett. B **5** (1991) 1255-1265. ⟨74⟩

[Zhang 92] X. Y. Zhang, R. L. Sugar and R. T. Scalettar, Green's function updating for Monte Carlo simulation of constrained Fermions, Phys. Rev. B **45** (1992) 471-472 (BR). ⟨74⟩

Subject index